NUI MAYNOOTH

Ollscoil na hÉireann Má Nuad

The role of human DEAD-box protein DDX3X in the activation and function of Estrogen Receptor-alpha.

Jyotsna Pardeshi M.Sc. (Biotechnology)

February 2022

A thesis submitted to: Maynooth university, Ireland for the degree of Doctor of Philosophy

Department of Biology, Maynooth University, Ireland

Head of Department: Prof. Paul Moynagh

Supervisor: Dr. Martina Schröder

Table of Contents

Abstract

The human DEAD-box RNA helicase DDX3X was shown to be involved in innate immune signalling pathways mediated by IKKε and TBK1. Interestingly, both DDX3 and IKKε have independently been shown to act as breast cancer oncogenes. In breast cancer, DDX3 expression was shown to be upregulated and linked with tumourigenesis. IKKε was suggested to phosphorylate Estrogen receptor alpha (ERα) at Serine-167 and drive expression of ERα-responsive genes in an estrogen-independent manner, leading to cell proliferation and resistance to anti-estrogen treatment. The current study aimed to investigate whether DDX3 and IKKε also collaborate in the activation of ERα.

This work suggests that DDX3 and IKKε collaborate to mediate ERα phosphorylation and activation, akin to the mechanism that the MU Host-Pathogen Lab elucidated for IRF3 activation in innate immune signalling. DDX3 knockdown in breast cancer cell lines resulted in reduced ERα phosphorylation, reduced ERE-controlled reporter gene expression, decreased expression of ERα target genes, decreased cell proliferation. Vice versa, overexpression of DDX3 resulted in enhanced ERα phosphorylation and activity. This study provides evidence from co-immunoprecipitation and pulldown experiments that, DDX3 directly binds to ERα to regulate its activation and function. Present work further analyses the effect of DDX3 knockdown on the proteome of the T47D breast cancer cell line grown under estrogen-replete and -deplete conditions. DDX3 knockdown lead to decreased expression of three chaperones involved in regulating ERα activity, Hsp90, Hsp70 and FKBP52. DDX3 was previously also shown to activate β-catenin by regulating CK1ε in Wnt pathway activation, and β-catenin was linked to an increased ERα protein level. This work demonstrates that, CK1ε and β-catenin might also be contributing to activation of ERα. In conclusion, this work provides evidence for a novel molecular role of DDX3 in activation of ERα, highlighting the oncogenic effect of DDX3 in breast cancer and linking it to endocrine therapy resistance.

Acknowledgments

Firstly, and most importantly I would like to thank Dr Martina Schröder for her unending guidance, support, and help. I would not have gotten this far without you. I can't thank you enough for putting up with me and encouraging me for all these years!

I would like to thank Maynooth University for John Hume Scholarship for my degree, and the HEA-Covid-funding award for the duration of last few months. I would also like to thank Prof. Paul Moynagh for giving me the opportunity to do this PhD.
I greatly appreciate all the help and guidance provided by Dr Marion Butler and Dr Paul Dowling, from my advisor-assessor team.

I would also like to thank everyone in the Host-Pathogen Interaction lab, in the past and the present and everyone in the cell-signalling lab who were great lab-sharing partners. Without you guys I would have probably quit a long time ago.

Finally, I would like to thank my family for supporting me and cheering me up, through all these years. Mom, Dad and Ganesh, I wouldn't have done this without your constant support and inspiration. And my son Tanmay who always brought smiles and positivity to my day. Thank you!

😊

List of Tables

List of Figures

List of abbreviations

Abbreviation	Meaning
ABCA3	ATP Binding Cassette subfamily A member 3
AF	Activation Function
AIM2	Absent In Melanoma 2
AMP	Adenosine Mono-Phosphate
AP	Activating Protein
AP2	Activating protein 2
AP2α	Activator Protein 2α
AP2γ	Activator Protein 2γ
APC	Adenomatous Polyposis Coli
ATP	Adenosine Triphosphate
ATPase	Adenosine TriPhosphatase
BAFF	B-cell activating factor of the TNF family
BAFFR	B-cell activating factor of the TNF family receptor
BCL9	B-cell CLL/Lymphoma 9 protein
bHLH	basic Helix Loop Helix
BLIMP1	B-Lymphocyte-Induced Maturation Protein
BN	Blue Native
BN-PAGE	Blue Native Polyacrylamide Gel Electrophoresis
BSA	Bovine Serum Albumin
β-TrCP	β-Transducin repeat Containing Protein
CARD	Caspase Activation and Recruitment Domain
CBP	CREB (cAMP response element-binding protein)-binding protein
CD4	Cluster of Differentiation 4
CD40	Cluster of Differentiation 40
CD8	Cluster of Differentiation 8 15
c-jun	Protein that in humans is encoded by the JUN gene
CK1ε	The Casein kinase 1
CK1α	Casein kinase 1 alpha
CREB	cAMP Response Element Binding protein
CRM1	Chromosome Region Maintainance 1
DAI	DNA-dependent Activator of IFN regulatory factors
DBD	DNA Binding Domain
DC	Dendritic Cell DDX DEAD-box Helicase
DMEM	Dulbecco's Modified Eagle Medium
DMOG	Dimethyoxaloylgylicine
DMSO	Dimethyl sulfoxide

DNA	Deoxyribonucleic acid
dsDNA	Double-stranded Deoxyribonucleic acid
dsRNA	Double-stranded Ribonucleic acid
DTT	Dithiothreitol
Dvl	Dishevelled
E2	Estradiol (17β -Estradiol)
ECL	Enhanced Chemoluminescence
EDTA	Ethylenediaminetetraacetic acid
EGTA	Ethylene Glycol Tetraacetic Acid
ER	Estrogen Receptor
ERBF-1	Estrogen Receptor promoter B associated Factor 1
ERE	Estrogen Response Element
ERE-luc	The estrogen-responsive reporter luc plasmid
ERα	Estrogen Receptor Alpha
ERβ	Estrogen Receptor Beta
EZH2	Enhancer of Zeste Homolog2
FASP	Filter Aided Sample Preparation
FBS	fetal bovine serum
FCS	Foetal Calf Serum
FOXM1	Forkhead box M1
FOXO3a	Forkhead box protein 3a
GATA	GATA transcription factors
GATA3	GATA binding protein 3
GREB1	Growth Regulation by Estrogen in Breast Cancer 1
GST	Glutathione S-transferases
GSK3a/b	Glycogen synthase kinase 3 alpha and beta
GTP	Guanosine-5'-triphosphate 16
HAT	Histone Acetyl Transferase
HBS	HEPES Buffered Saline
HBV	Hepatitis B Virus
HCC	Hepatocellular Carcinoma
HCL	Hydrochloric Acid
HCV	Hepatitis C Virus HEK Human Embryonic Kidney (cells)
HDAC	Histone Deacetylase
HIF1α	hypoxia inducible factor
HIV	Human Immunodeficiency Virus
HMT	Histone Methyl Transferase
HREs	HIF-response elements
HRP	Horse Radish Peroxidase HSV Herpes Simplex Virus
HVEM	HSV Entry Mediator
IFN	Interferon
IGF1	Insulin-like Growth Factor 1
IKK	IκB Kinase
IPS-1	MAVS

IPTG	Isopropyl β-D-1-thiogalactopyranoside
IRAK	IL-1R associated kinases
IRF	Interferon Regulatory Factor 17
ISG	Interferon Stimulated Gene
IκB	Inhibitor of κB
JAK	Janus Kinase
LB	Luria Bertani
LBD	Ligand Binding Domain
LEF	Lymphocyte Enhancer Factor
LGP2	Laboratory of Genetics and Physiology 2
LIGHT	homologous to LT, inducible expression, competes with herpes simplex virus (HSV) glycoprotein D for HSV entry mediator (HVEM), a receptor expressed on T lymphocytes
LRRFIP1	Leucine-rich repeat flightless-interacting protein 1
LTβR	Lymphotoxin-β receptor
MAP	Mitogen Activated Protein
MAPK	Mitogen-Activated Protein Kinase
MAVS	Mitochondrial antiviral-signalling protein (IPS-1)
MDA5	Melanoma Differentiation-Associated protein 5
mDC	Myeloid Dendritic Cell
MHC	Major Histocompatobility Complex
MKK	Mitogen Activated Protein Kinase Kinase 18
mRNA	Messenger RNA
MyD88	Myeloid Differentiation gene 88
NEMO	NF-kappa-B essential modulator
NES	Nuclear Export Sequence
NF-kB	Nuclear Factor Kappa light chain enhancer of activated B cells
NHR	Nuclear Hormone Receptor
NIK	NF-κB Inducing Kinase
NK	Natural Killer
NLS	Nuclear Localization Signal
NMR	Nuclear Magnetic Resonance
NR	Nuclear Receptor
NSC	non-silencing control
NTP	Nucleoside triphosphate
PAMP	Pathogen Associated Molecular Pattern
PAMPs	pathogen-associated molecular patterns
pCAF	p300/CBP-Associated Factor
pDC	Plasmacytoid Dendritic Cell
PR	Progesterone Receptor
PRR	Pathogen Recognition Receptor
PRRs	patter recognition receptors
PTM	Post Translational Modifications
PVDF	Polyvinylidene fluoride
REN	Ring Expanded Nucleoside

RIG-I	Retinoic acid-Inducible Gene 1 RLH RIG-I Like Helicase 19
RNA	Ribonucleic acid
RRERev	Responsive Element
RTKs	Receptor Tyrosine Kinase
SARM	Sterile-α and Armadillo Motif containing protein
SDS	Sodium Dodecyl Sulfate
SDS-PAGE	SDS- Polyacrylamide Gel Electrophoresis
SERD	Selective Estrogen Receptor Down-regulator
SERM	Selective Estrogen Receptor Modulator
SeV	Sendai Virus
SFM	Serum Free Medium
SHP-1	Src homology region 2 domain-containing phosphatase-1
shRNA	Short Hairpin RNA
siRNA	Small Interfering RNA
SOC	Super Optimal Broth with Catabolite repression
SP-1	Stimulatory Protein 1.
ssDNA	Single-stranded Deoxyribonucleic acid
ssRNA	Single-stranded Ribonucleic acid
STAT	Signal Transducer and Activator of Transcription
STING	Stimulator of Interferon Genes
TAB1	TAK1 binding protein 1
TAB2	TAK1 binding protein 2 20
TAD	Transactivation Domain
TAK	TGF-β activated kinase
TB	Transformation Buffer
TBK1	TANK-Binding Kinase-1
TBS	Tris Buffered Saline
TBST	TBS Tween
TCF	T-cell factor
TCF4	Transcription Factor 4
TF	Transcription Factor
TIRAP	TIR domain containing Adaptor Protein (Mal)
TLR	Toll Like Receptor
TLE	transducing-like enhancer protein
TNF	Tumor Necrosis Factor
TNFα	Tumor Necrosis Factor alpha
TRAF	TNF Receptor Associated Factor
TRAM	TRIF-Related Adaptor Molecule
TRE	Telomeric Repeat Elongation
TRIF	TIR-domain-containing adaptor-inducing interferon-β

Chapter 1. Introduction

1.1 DExD/H-box helicases

Helicases are ATP-dependent enzymes that can unwind or remodel dsDNA or RNA and are categorized as DNA helicases and RNA helicases. There are also some helicases that can act as both DNA and RNA helicases (Linder and Jankowsky, 2011). Several super families of helicases have been identified, of these the SF1, SF2 and SF3 are the main superfamilies. The SF1 and SF2 families are characterized by similar conserved motifs but are distinct from one another(Fairman-Williams et al., 2010). The SF3 superfamily is comprised of viral DNA and RNA helicases that contain only three conserved motifs. The families are grouped based on highly conserved regions in their sequences which are shared by all the members of one family. The DEAD-box family of RNA helicases is characterized by 9 conserved motifs.

The DExD/H-box family of RNA helicases belongs to the large SF2 superfamily. This family was identified by (Linder and Jankowsky, 2011) systemic sequence analysis of proteins containing a purine NTP binding motif. These helicases have a conserved structural fold with two Rec-A like globular domains that are connected by a flexible linker. As previously stated, the DEAD-box family has 9 characteristic conserved motifs, which are the Q-motif, motif-1 (Walker motif- A), motif 1a, motif1b, motif II (Walker motif-B), motif III, motif, IV, motif V, and motif VI (Cordin et al., 2006). This family derives its name from motif II that contains the amino acid sequence D-E-A-D. These motifs contribute to ATP binding, ATP hydrolysis, RNA binding and RNA unwinding. The first Rec-A like domain contains motifs, I, Ia, Ib, II and III. The second Rec-A like domain contains motifs, IV, V, and VI that are involved in ATP hydrolysis and nucleic acid binding and RNA unwinding activity.

The SF2 superfamily helicases can adopt an open and a closed protein conformation. They exist in the open conformation when they are not bound to nucleic acid. The cleft between the two

recA-like domains hosts the ATP binding site, whereas nucleic acid binding sites are spread across both domains. The cleft between the two domains closes when ATP and a nucleic acid bind to the protein, leading to a 'closed conformation' that facilitates ATP binding and hydrolysis.

RNA unwinding activity of DEAD-box proteins is restricted to duplexes fewer than 10-12 base pairs. There is no unwinding polarity for DEAD box helicases, unlike other helicases (Linder and Jankowsky, 2011), because they do not unwind duplexes based on translocation on the RNAs. Instead, DEAD-box proteins load directly onto the duplex region, prying the strands apart in an ATP-dependent manner (Halls et al., 2007) (Yang et al., 2007). This is called local strand separation. Single stranded tails aid in loading the helicase protein onto the duplex. For most DEAD-box proteins, ATP binding is more important than ATP hydrolysis for strand separation (with the exception of bacterial dbpA that is more ATP hydrolysis dependent). In the absence of RNA and ATP the two Rec-A like domains move relatively freely with respect to each other (Jankowsky and Fairman, 2007).

Most DExD/H-box helicases also contain variable N- and C- terminal domains that confer functional specificity to these helicases. These regions can modulate enzymatic activity and contain additional RNA binding domains. They also provide docking site for protein-protein interactions (Fairman-Williams et al., 2010).In addition to nucleic acid unwinding, many DEAD-box proteins have additional functions independent of RNA unwinding and /or ATPase activity, such as their involvement in transcriptional regulation, innate immunity and viral replication (Fuller-Pace, 2006), (Schröder et al., 2008), (Soulat et al., 2008), (Fuller-Pace and Nicol, 2012).

1.2 DExD/H-box helicases in innate immunity

Some of the DExD/H-box family helicases (members of DEAD, DEAH, DExD, DExH helicase family) have been shown to be involved in innate immune responses to viruses (Fullam and Schröder, 2013). They are involved in sensing viral nucleic acids and/or downstream signalling events. Some of the helicases play dual roles in innate immune responses and on the other hand acting as essential host factors for replication of some viruses (Fullam and Schröder, 2013). Innate immune cells detect pathogens with the help of pattern recognition receptors (PRRs). PRRs can recognize pathogen-associated molecular patterns (PAMPs), conserved structures present in certain pathogens (Medzhitov et al., 1997). The endosomal Toll-like receptors (Thompson et al.), the RIG-like helicases (RLHs) that are part of the DExH family of RNA helicases, and cytoplasmic DNA receptors, are the main PRRs sensing viral nucleic acids (Thompson et al., 2011). Some other DExD/H-box helicases that are not part of the RIG-I family have recently been shown to be involved in the sensing of viral nucleic acids and/or downstream signalling pathways; they are DDX3, DDX60, DDX41, DDX1, DHX9 and DHX36 (Zhang et al., 2011), (Schröder et al., 2008), (Gu et al., 2013). The induction of type I interferons (IFN-α and IFN-β), cytokines with potent anti-viral activity, is a characteristic of anti-viral PRR signalling. Their anti-viral activity is largely mediated by interferon-stimulated genes (ISGs) that encode proteins with direct anti-viral effector functions. This requires activation of transcription factors, IRF3 and IRF7, (Sato et al., 2000) which are phosphorylated and activated by the IKK-related kinases TBK1 and IKKε (Fitzgerald et al., 2003) (Schröder et al., 2008).

Other than their conventional role in regulation of gene expression, DExD/H-box helicases have also been shown to play a role as signalling adaptor molecule, which is independent of their enzymatic RNA remodelling activity. Enzymatic activity is also not essential for nuclear export of human DDX3.

1.3 DDX3

DDX3, or DEAD-box helicase-3 is a multifaceted protein belonging to the DEAD-box RNA helicase family. It is an ATP-dependent RNA helicase, conserved in different organisms from yeast to human.

DDX3 has two different homologues DDX3X and DDX3Y. The DDX3X gene is located on the X-chromosome in the region Xp11.4 and encodes a 662-amino acid long polypeptide. The DDX3/ DDX3X gene escapes X-inactivation and is expressed in a wide range of tissues (Cotton et al., 2015). This study focuses on DDX3X exclusively and it will be referred as DDX3 in the remaining document.

DDX3Y, a homologue of the human DDX3X is located on the non-recombining, Yq11.21 region of Y-chromosome (Lahn and Page, 1997). There is recent evidence and uncertainty over the redundancy with DDX3Y for certain cellular functions. DDX3Y was shown to be expressed only in male germ line. This was disputed recently in the paper on the conditional DDX3X knockout mice, which shows that DDX3Y can partially compensate for DDX3X (Venkataramanan et al., 2020). This suggests that DDX3Y might be expressed in other tissues, including immune cells.

DDX3 is 662 amino acid long protein, expressed in different cells at different times (Kim et al 2010). DDX3 has the nine conserved motifs that are characteristic of the DEAD-box RNA helicase family and also contains a nuclear export signal (Ariumi, Tanner et al., 2003) (Figure 1.1).

DDX3 has been implicated in almost all aspects of RNA metabolism (RNA unwinding, splicing, import/export, transcription, translation and ribosome assembly (Schröder, 2010); (Geissler et al., 2012). Because it has been suggested to play roles in cell cycle control (Chang et al., 2006) (Choi and Lee, 2012), it has been indicated to play a major role in development and progression

of different cancers (Sun et al., 2011) (Liu et al., 2012a). Depending on the cancer type, it has been shown to have dual roles, acting as a tumour suppressor or an oncogene (Botlagunta et al., 2011).

In addition to this it is also an important factor for the host response to viral infection. DDX3 has been shown to have an unconventional role in anti-viral immune signalling and can also act as viral host factor (via its RNA remodeling function).

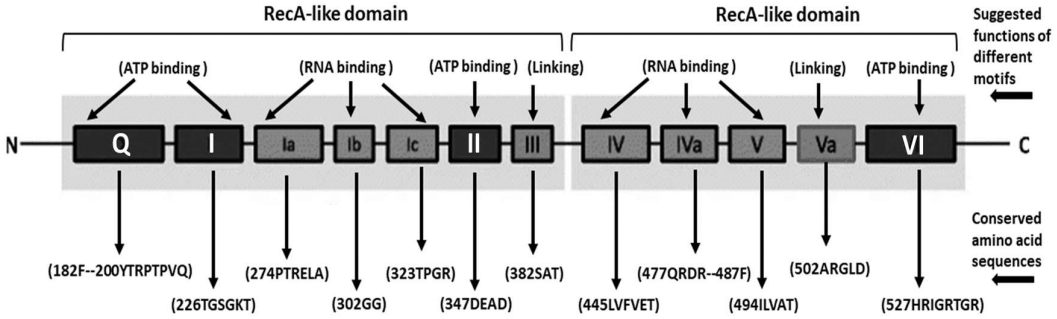

Figure 1.1: Schematic representation of DDX3 (human) and conserved motifs

The two RecA-like domains are highlighted in rectangles. The motifs include Q (182F--200YTRPTPVQ), I (226TGSGKT), Ia (274PTRELA), Ib (302GG), Ic (323TPGR), II (347DEAD), III (382SAT), IV (445LVFVET), Iva (477QRDR--487F), V (494ILVAT), Va (502ARGLD), VI (527HRIGRTGR). Conserved amino acid sequences are indicated in the brackets. The conserved motifs involved in ATP binding (Q,I, II,VI), RNA binding (Ia,Ib,Ic, IV,Iva,V) and linking (III, Va).

- Adapted from: DDX3, a potential target for cancer treatment (Guus Martinus Bol, Min Xie & Venu Raman 2015) (Bol et al., 2015)

1.4 DDX3 as an essential host factor for viral replication

Several viruses were shown to target and use DDX3 for their own benefit (Maggi, 2011). DDX3 is indispensable for translation initiation of HIV-1 mRNA and was shown be essential for replication of Human Immunodeficiency Virus 1 (Stunnenberg et al.) and Hepatitis C Virus (Ariumi et al.) (Ariumi et al 2007; Yedavalli et al 2004; Randall et al 2007). Several DEAD-box RNA helicases, including DDX3, have been shown to interact with HCV proteins and regulate HCV replication (Ariumi et al., 2007) (Yedavalli et al., 2004) (Schröder, 2010).

For HIV-1, DDX3 was first suggested to be required for the export of unspliced and partially spliced HIV-1 RNA out of the nucleus. (Yedavalli et al., 2004), showed that DDX3 could bind to HIV-1 rev protein and Chromosome Maintenance Region 1 Yedavalli et al. (2004) leading to export of partially spliced Rev Response Element (Merrell et al.)- containing RNAs out of the nucleus. CRM1 is known to export proteins that contain leucine rich Nuclear Export Signal (NES) as well as small nuclear RNAs (snRNA) and ribosomal RNA (rRNA). Importantly, HIV-1 replication was shown to be blocked by shRNA knockdown of DDX3. DDX3 knockdown inhibited the export of HIV-1 RNAs, suppressing replication of virus without affecting cell viability (Ishaq et al., 2008). DDX3's role in HIV-1 replication has led to development of DDX3 inhibitors that have potential for clinical therapeutic application in HIV-1 infection and beyond (Yedavalli et al., 2004, Radi et al., 2012); A ring expanded nucleoside analogue (REN) that inhibits ATP dependent functions of DDX3 was also shown to suppress HIV-1 replication, while being nontoxic to the cells (Yedavalli et al., 2008).

DDX3 was not only shown to be essential for HCV replication (Ariumi et al., 2007); but also to interact with HCV Core protein (Owsianka and Patel, 1999).The Core protein was suggested to disrupt the interaction between MAVS and DDX3 and therefore block the induction of antiviral IFNβ (Oshiumi et al. 2010) (Oshiumi et al., 2010). However, another study suggested that Core

protein can induce IFN via DDX3 (Kang et al., 2012), suggesting that the role of the DDX3 and HCV Core interaction is unclear. Most importantly, DDX3 knockdown decreased HCV RNA accumulation by 80-90 percent (Ariumi et al., 2007)

Hepatocellular carcinoma is a most prevalent form of cancer and is linked with hepatitis virus infection (Chang et al., 2006). In Hepatocellular carcinoma (Chang et al.) DDX3 expression is deregulated (Kang et al., 2012) (Chao et al., 2006) and DDX3 has been suggested to have tumour suppressor function in this context.

1.5 DDX3 in Antiviral Immune Signalling

Interferon is a soluble factor that was first described by Isaac and Lindenmann in 1957 and was shown to interfere with replication of Influenza A virus (Stunnenberg et al., 2018). Type-1 Interferons, IFNα (produced by dendritic cells (DC)) and IFNβ (produced by lots of different cell types including tissue cells, following viral infection and activation of RIG-I signalling) play major roles in antiviral immunity (Chen and Royer, 2010). DDX3 was shown to be involved in anti-viral immunity by enhancing IFN production downstream of anti-viral PRRs.

DDX3 was identified as a host target of the vaccinia virus protein K7 (Schröder et al., 2008). K7 was shown to inhibit IFNβ induction. The kinases IKKε and TBK1 phosphorylate and activate the transcription factors IRF3 and IRF7 that are essential for type-I interferon induction and the antiviral immune response (Gu et al., 2013). After Sendai virus infection, which triggers the RIG-I PRR pathway, DDX3 interacts with IKKε and enhances induction of the IFNβ promoter.

DDX3 was also shown to interact with and phosphorylate TBK1/ IKKε (Schröder et al., 2008, Soulat et al., 2008). DDX3 was in turn shown to be phosphorylated by TBK1/ IKKε (Schroeder , 2008; Soulat et al 2008).

The MU Host-Pathogen lab have demonstrated a collaborative role between DDX3 and IKKε in the anti-viral immune response, where DDX3 acts a scaffold binding IKKε, promoting its autophosphorylation. It was shown that DDX3 transiently associates with IKKε after SeV virus stimulation. IKKε then phosphorylates DDX3, allowing it to recruit IRF3 which is subsequently phosphorylated by IKKε. IRF3 is then recruited to the IFNβ promoter and stimulates IFNβ production, promoting viral clearance (Schroeder M., 2008). The N-terminus of DDX3 was shown to be essential for this, and the Vaccinia virus (VACV) protein K7 binds to the N-terminus of DDX3 to inhibit IFNβ promoter induction (Schroeder M., 2008). A DDX3 mutant containing only the amino acid 1-139 N-terminal region was shown to have a dominant negative effect on IFNβ

induction (Schröder et al., 2008). Importantly, ATPase activity of DDX3 was not required for its effect on IFN induction.

In contrast to this proposed role as a signalling adaptor, other modes of action of DDX3 in the RIG-I pathway were also proposed. DDX3 was suggested to be recruited directly to the IFNβ promoter (Soulat et al., 2008). In another publication, it was suggested to act jointly with RIG-I and mda5 in sensing viral RNA and inducing IFNB at early stages of viral infection (Oshiumi et al., 2010).

Thus, there are lot of studies highlighting DDX3's role in type-1 interferon induction, but there are some contradictory reports about its exact mechanism of action. However, previous work from the MU Host-Pathogen Lab suggests that the interaction between DDX3 and IKKε plays an important role in this pathway.

1.6 Cancer hallmarks and pathways

Cancer is a group of diseases involving abnormal cell growth with the potential to invade or spread to other parts of the body. Cancer hallmarks comprise biological capabilities acquired during the multistep development of human tumours; they are abnormal metabolic pathways, inflammation, self-sufficiency in growth signal, insensitivity to anti-growth signals, evading apoptosis, limitless replicative potential, sustained angiogenesis, evasion of the immune system, genome instability, tissue invasion and metastasis (Wilkins and LaFramboise, 2011).

1.7 Several pathways are commonly dysregulated in cancer

Receptor tyrosine kinase pathway:

Normal cells' ability to survive and proliferate depends on growth factor receptors that have tyrosine kinase activity (Receptor Tyrosine Kinase; RTKs). Mutations causing deregulated activation of RTKs or their downstream signalling components (Ras, AKT, PI3KCA, EGFR2, JAK2, ERK, MEK, KRAS, BRAF) are prevalent in human cancers.

Cell adhesion receptors and EMT:

Normal cells are attached to a support matrix via integrins and are only responsive to mitogens if they are not restrained by inhibitory action of cadherin-mediated contact inhibition. Deregulation of this pathway leads to EMT. The epithelial to mesenchymal transition (EMT) is a well-studied process in embryogenesis, fibrosis, tumour progression and metastasis. EMT is a process of change of epithelial cell to a mesenchymal phenotype that has invasive capacity. In EMT there is a loss of epithelial surface markers, such as E-cadherin and acquisition of mesenchymal markers such as, vimentin and N-cadherin. Downregulation of E-cadherin during EMT is mediated by transcriptional repression through the binding of EMT transcription factors

(EMT-TFs), such as SNAIL, SLUG, TWIST to the E-boxes present in the E-cadherin promoter. EMT-TFs can cooperate with different enzymes to repress the expression of E-cadherin and can regulate EMT at epigenetic and post-translational levels.

mTOR pathway:

It is a mediator of RTK signalling and a downstream target-effector of Akt. mTORC1 promotes translation of proteins that regulate cell growth, survival, and cell cycle progression (Ma and Blenis, 2009). In addition, mTORC1 suppresses autophagy and can indirectly activate transcription factors, such as SREBP, PPARγ and PCG1α, which promote lipid biosynthesis and mitochondrial function. DNA damage-induced activation of p53 inhibits mTORC1 through activation of AMPK, hypoxia exerts this effect through the HIF1 target gene REDD1 (Wullschleger et al., 2006) (Hsu et al., 2011).

Metabolic reprogramming:

Anaerobic glycolysis is usually activated in cancer cells (Warberg, 1956).Further, autophagy is a catabolic process that leads to the degradation of proteins and organelles and provides essential housekeeping functions (Cecconi and Levine, 2008) (Yen and Klionsky, 2008). Deregulation of autophagy under metabolic stress predisposes normal cells to acquire oncogenic mutations (Mathew and White, 2011).

Cell division and cell cycle progression:

These pathways are governed by cyclins and their catalytic subunits Cdks. Oncogenic mutations of several components of this signalling pathway are reported, which lead to overexpression of these components, e.g. Cyclin D1 is often upregulated in breast cancer (Alao, 2007).

1.8 DDX3's role in cell cycle control, proliferation and tumorigenesis

DDX3 has been implicated in cell cycle and cell growth control. Different studies have indicated a role for DDX3 in different aspects of cell cycle regulation, apoptosis and tumorigenesis. DDX3 has been shown to have contradictory effects on tumourigenesis, acting as a tumour suppressor or oncogene in different tissues and/or context. DDX3 was shown to affect cell cycle regulation and different cell cycle checkpoints. Therefore, it could affect different aspects of tumourigenesis, such as growth factor signalling, apoptosis, cell migration, and responses to cell stress (Ariumi, 2014).

1.9 DDX3 as a tumour suppressor

1.9.1 DDX3's role in the p53/p21 pathway

p53 is a tumour suppressor transcription factor that is mutated in many cancers. p53 is activated by many cellular stresses, most importantly DNA damage and oxidative stress. In cells expressing functional wild-type p53, DDX3 appears to positively regulate DNA damage-induced caspase activation, but in cells expressing non-functional p53, DDX3 seems to inhibit DNA damage-induced caspase activation and apoptosis. DDX3 was also shown to regulate apoptotic signalling and accumulation of p53 after DNA damage. DDX3 promoted retention and accumulation p53 in the nucleus by direct interaction in MCF7 breast cancer cells. One other DEAD-box helicase, DDX5 has been reported to regulate transcription of p53-dependent genes (Fuller-Pace, 2006).

P21waf1/cip1 is a tumour suppressor whose expression can be p53-dependent or p53 independent DDX3 was shown to transactivate the p21 promoter by interacting with Sp1 (which was previously shown to activate the p21 promoter (Botlagunta, 2008). In HCC, DDX3 was shown to be a tumour suppressor via its effect on p21 promoter activity (Chao et al., 2006).

DDX3 knockdown led to early entry of cells into S-phase and an increased cell growth rate. Knockdown of DDX3 led to altered expression of cell cycle regulators; namely Cyclin D1 and a dependent decrease in p21 (Chang et al.) (Chang et al., 2006). P21 (waf/cip1) is critical for CDK inhibitors, it modulates their kinase activity by interacting with Cyclin/ CDK. P21 also interacts with proliferating cell nuclear antigen (PCNA) and inhibits DNA synthesis.

1.10 DDX3 as an oncogene

DDX3 was shown to have a role as an oncogene in breast cancer. The active metabolite in tobacco smoke, Benzo[a]pyrene diol-epoxide was shown to upregulate DDX3 expression in mammary epithelial cells (Botlagunta et al., 2011). Over-expressing DDX3 in MCF10A mammary epithelial cell line was shown to promote epithelial-mesenchymal transition (EMT) and induce aggressive properties such as proliferation, motility and invasion (Botlagunta et al., 2008).

1.11 DDX3's effects on E-cadherin expression

E-cadherin is a cellular adhesion molecule. Loss of E-cadherin has been shown to result in EMT, increased cell proliferation, and migration leading to metastasis (Onder et al., 2008). DDX3 was shown to reduce E-cadherin promoter activity. Snail is an important transcription factor that regulates development and progression of cancer; it was shown to repress of E-cadherin expression leading to EMT. DDX3 knockdown was shown to result in decreased Snail expression, consequently increasing E-cadherin expression. DDX3 regulated Snail protein levels by promoting its retention in the nucleus (Sun et al., 2011). It was also shown that DDX3 binds either directly or as part of a heterogeneous complex to the endogenous E-cadherin promoter (Botlagunta et al., 2008).

1.12 DDX3 and hypoxia

In breast cancer, DDX3 expression was shown to be upregulated by hypoxia protein HIF-1α, which is correlated with more aggressive and invasive breast cancer phenotype (Bol et al., 2013). DDX3 expression was also shown to be correlated with expression of other proteins upstream of HIF-1α, like EGFR, HER2, Akt1, p53, COMMD1, FER kinase, PIN1, FOXO4.

1.13 DDX3 and the Wnt pathway

Wnt pathway deregulation is involved in different cancers, including colon cancer, medulloblastoma and melanoma (Clevers and Nusse, 2012) DDX5, a closely related helicase, was shown to be involved in Wnt signalling. DDX5 was shown to interact with nuclear β-catenin and stimulate EMT (Wang et al., 2015).DDX3 was later studied in this context and was found to be upregulated in Wnt-driven medulloblastoma tumours. DDX3 was later also shown to act as an allosteric activator of CK1ε activity, in phosphorylation of dishevelled and thereby activating β-catenin, in an ATP hydrolysis and helicase-independent fashion (Cruciat et al., 2013b).

1.14 Breast cancer

Breast cancer is the most common cancer, and the most common cause of mortality in females (Ghoncheh et al., 2016). The current molecular classification of breast cancer is divided into five subtypes after a subpopulation of the luminal A subtype with a Ki-67 proliferation index of >14% was designated as the luminal B subtype (Cheang et al., 2009).

The breast cancer molecular subtypes were redefined as follows, based on the receptors highly expressed (Goldhirsch et al., 2011) (Zhang et al., 2014):

Molecular subtype	Growth Hormone Receptor Status and Ki index
Luminal A:	ER+ and/or PR+, HER2− and Ki-67 ≤14%
Luminal B	ER+ and/or PR+, HER2− and Ki-67 >14%
Luminal B HER2/neu+	ER+ and/or PR+, HER2+ and any Ki-67
HER2/neu subtype	ER− and PR−, HER2/neu+ and any Ki-67
triple-negative subtype	ER−, PR−, HER2− and any Ki-67

Table 1.1: Molecular subtypes of breast cancer

Five different categories of breast cancer based on molecular subtypes, (ER – estrogen receptor, PR- progesterone receptor, HER- Human-epidermal growth factor receptor)

Among the different molecular subtypes ER+ breast cancer comprises ~75% of all breast cancers. Luminal A and B subtype in which ER+ and/or PR+ status is seen, are subjected to endocrine therapy with tamoxifen to inhibit ER function and aromatase inhibitors or inactivators that block estrogen production or to inactivate or downregulate the ER. Therefore, ER status has become important factor in discrimination of subtypes and the treatment options that target estrogen

synthesis (such as aromatase inhibitors) or the ones that disrupt the ER functions (Sieuwerts et al., 2014).

1.14.1 Treatments

The treatment options for Receptor positive (ER/PR and androgen-receptor, recently) fall into following categories:

Anti-estrogens

Antiestrogens consist of SERMs, SERDs and aromatase-inhibitors. SERMs (Arao et al.) and SERDs (selective estrogen receptor disruptors): Anti-estrogens act by blocking or competing with endogenous estrogen for activation of ERα. Tamoxifen is one such anti-estrogen and acts as an agonist in breast (Clevers and Nusse, 2012). Tamoxifen binds to the receptor and is known to exhibit agonist and antagonist effects in tissue and species-specific context (Robinson and Jordan, 1987), as it is selective in its response it is called selective estrogen receptor modulator (Arao et al.). Other drugs in this class are: raloxifene and toremifene.

SERDs on the other hand affect stability of the receptor. Fulvestrant is one such example and is shown to inhibit Estrogen receptor dimerization and targets the receptor for its degradation (Long and Nephew, 2006). Estrogens are synthesized from androgens by the aromatase enzyme (CYP19).

Aromatase inhibitors reversibly inhibit the aromatase enzyme, the examples of this drug class are letrozole and anastrazole and an irreversible inhibitor exemestane. The treatment with Aromatase exhibit longer disease-free survival but are only reserved for post-menopausal women due to their toxicity and in premenopausal women estrogen is alternatively also made

by ovaries. Therefore tamoxifen and fulvestrant are primarily used for treatment of premenopausal women (Aihara et al., 2014)

The treatment outcomes with anti-estrogens and response depends on hormonal responsiveness (Santen et al., 2005). Resistance to anti-estrogen therapy has become a major clinical problem, with ~30% ER+ cancers are reported to be non-responsive to anti-estrogen treatment (D'Souza et al., 2018, Giuliano et al., 2011). Anti-estrogens are known and are in use since the 1970s, and yet their mechanisms of action and resistance is still not fully understood (Clarke et al., 2001). Two forms of anti-estrogen resistance are reported; namely de novo resistance and acquired resistance. The most common de novo resistance mechanism is the absence of estrogen receptor expression, whereas a complete loss of ER expression (Arao et al., 2013) is not common. A class switch resistance or Anti-estrogen unresponsiveness is other major acquired resistance phenotype in which a switch to an anti-estrogen-stimulated growth is a minor phenotype. (Clarke et al., 2001, Clarke et al., 2003)

As the ER+ breast cancer is the most common type and is associated with recurrence and resistance, it is therefore the focus of the current study.

1.15 Estrogen receptor family

Estrogen receptors belong to the Nuclear Hormone Receptor family (NHR). NHRs are a large family of receptors that act as transcription factors. They play diverse roles in cellular processes in target tissues. Vertebrates have six evolutionary related nuclear receptors for steroid hormones. Two for estrogen (ERα and ERβ, also known as NR3A1 and NR3A2 respectively), and one for each androgen (AR), progesterone (PR), glucocorticoids (GR) and mineralocorticoid (Tamrazi et al.). NHR activity is modulated by their steroid hormone ligands that are cholesterol derivatives and can diffuse through plasma membranes and regulate tissue-specific intracellular events (Warner et al., 1999) (Yaşar et al., 2017)

There are two subtypes of estrogen receptor, ERα and ERβ, encoded by two different genes and expressed at varying levels in different and sometimes in the same tissues. ERα is predominantly expressed in mammary glands, uterus, pituitary gland, adipose tissue, skeletal muscle, and bone, whereas ERβ mediates estrogen (referred as E2 here onward) signalling in ovary, lung, prostate, cardiovascular, and central nervous systems. Within a single tissue, expression patterns of estrogen receptor subtypes are cell type specific. For example, in ovary, ERβ is expressed by granulosa cells but ERα is expressed more in theca cells (Yaşar et al., 2017) (Lee et al., 2012).

1.16 Estrogen receptor structure

Estrogen receptors are modular proteins, which means that they have distinct structural domains that have unique functional features (Kumar et al., 1987) (Green et al., 1986)

ERα is encoded by the ESR1 gene which is a ~300kb genomic segment located at q24-q27 of Chromosome 6 (Sand et al., 2002). The ESR1 gene has eight exons encoding 595 amino acids that make up a 66kDa full-length protein (Sand et al., 2002) Erβ is encoded by the ESR2 gene, ~254kb in size, located on q22-24 of chromosome 14 with eight exons (Enmark et al., 1997). It encodes a 530 amino-acid protein, with a 60kDa molecular mass.

ERα and ERβ share structural characteristics responsible for similar functional features, but the distinct amino acid composition gives subtype-specific properties to the receptors.

Estrogen receptors like other NHRs have six functionally distinct domains i.e. A, B, C, D, E and F (Kumar et al., 1987) (Figure 1.1). In both the ERα and ERβ genes, exon 1 encodes the A/B region. Exon 2 and 3 encode a part of the A/B region and the C region, i.e. the DNA binding domain. Part of the C-region is encoded by exon 4, which also encodes all of the D-domain and a part of the E-domain. Exons 4-8 encode the hormone-binding E/F domain (Hua et al., 2018).

There are two transcriptional activation domains on ER the one on the amino terminus is called AF-1 for Activation Function-1, and the second one at the carboxyl terminus is called AF-2 for Activation Function-2 (Figure 1.2).

A)

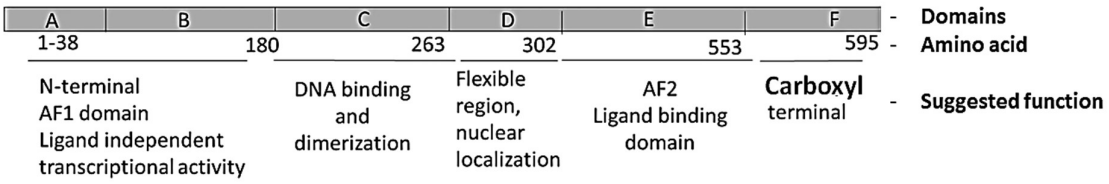

B)

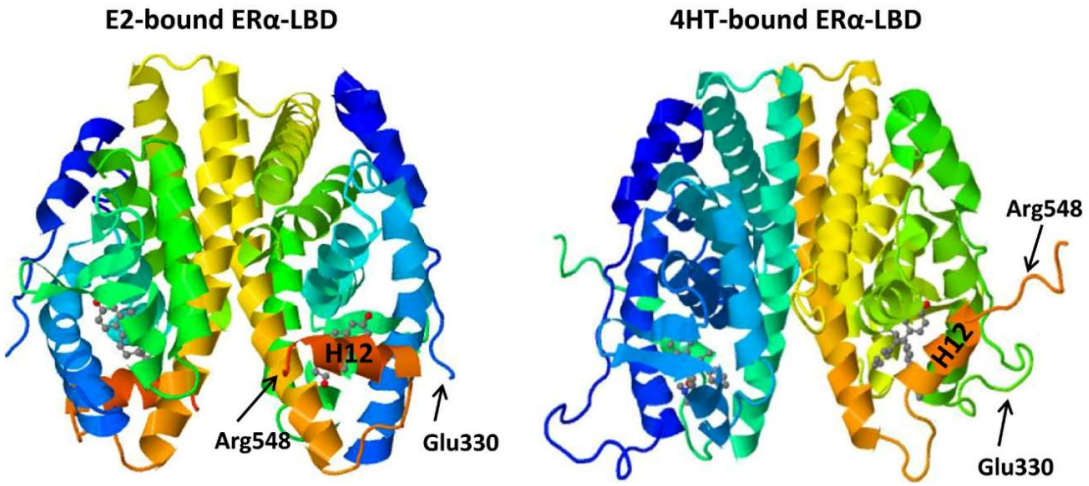

Figure 1.2: Schematic representation of different domains of Estrogen receptor alpha

A) Schematic representation of different domains of ERα. N-terminal domain has ligand-independent transcriptional activity, whereas ligand-dependent transcriptional activity is mediated by AF-2 domain, closer to C/ carboxyl terminal.

B) Tertiary structure of the estrogen receptor (ER)α-ligand-binding domain (LBD) dimer, bound to 17β-estradiol (E2) (left panel) or 4-hydroxytamoxifen (4HT) (right panel). Left panel: The binding of E2 induces a conformational change in the LBD, positioning the mobile H12 over the ligand-binding cavity. This positioning generates a surface for the interactions with co-activators to establish a competent activation function 2. (Protein Data Bank [PDB] identification [ID]: 1ERE; Brzozowski, et al.26). Right panel: The binding of 4-hydroxy-tamoxifen / 4-HT (grey), a selective estrogen receptor modulator, prevents H12 from docking in agonist conformation, therefore effectively preventing co-activator binding and transcription activation (PDB ID: 3ERT; Shiau, et al.38)

- **Molecular mechanism of estrogen–estrogen receptor signaling**

PelinYaşar,Gamze Ayaz,SırmaDamla User,GizemGüpür,Mesut Muyan (Yaşar et al., 2017)

AF-1 domain confers ligand-independent transactivation of the receptor, whereas AF-2 domain is strictly ligand-dependent for its transcriptional activation function. The ligand-binding domain (Tamrazi et al.) is a globular region and contains a ligand-binding site, a ligand-dependent co-regulator interaction domain, and AF-2, and also has a dimerization interface (homo-dimerization and hetero-dimerization) (Tamrazi et al., 2002).

Binding of estrogens to ER is a pivotal step in ER activation (Huang et al., 2005). Estrogens are steroid hormones and include estrone, estradiol (E2), and estriol.17β-Estradiol is the main circulating estrogen hormone that regulates various tissue and organ functions and is involved in a variety of important physiological functions that include development and maintenance of reproductive organs, cardiovascular, musculoskeletal, immune system and central nervous system homeostasis (Gruber et al., 2002) Estrogen binding induces a major structural re-organization of the ligand binding domain (Tamrazi et al.), converting inactive ER to functionally active ER that stabilizes the ER dimer and interactions with co-regulatory proteins (Bai and Giguére, 2003). The deregulation of E2-ER signalling contributes to the initiation and development of target tissue malignancies.

1.16.1 Structure of the ER Ligand-binding domain

The ligand binding domain (LBD) is a multifunctional domain and facilitates conformational changes in the receptor that direct gene activation or repression.

The LBD is located in the C-terminal region that includes domains E and F (Figure 1.2). The LBD has 12 helices and a three-layered antiparallel α-helical fold (Pike et al., 2000). This fold is unique to the nuclear receptor superfamily. The antiparallel α-helical fold comprises a central core layer made of three helices (H5/6, H9, H10), sandwiched between two additional layers of helices (H1-4 and H7, H8, H11). These helices create a scaffold that maintain the structure of the ligand

binding cavity. The other secondary structural elements, a small two-stranded antiparallel β-sheet and the highly mobile H12 helix, flank the three-layered motif described above. The ligand-binding pocket is hydrophobic and located in the bottom half of the LBD. (Huang et al., 2010).

The F domain or carboxyl terminus is largely unstructured. The F-domain of ERα contains an α-helical region and an extended β sheet. The F domain of ERα appears to modulate the transcriptional activity, dimerization, co-activator interactions, and stability of the receptor (Arao et al., 2013). This region plays an important part in ligand binding and dimerization of the receptor and is also a target site for SERMs and SERDs.

1.16.2 E2 binding and receptor dimerization

Dimerization of ERα is important for ERα function. Mutations that interfere with the dimerization domain render ERα transcriptionally inactive. The DNA-binding domain (DBD) also contributes to the dimerization of the receptor, where the H11 helices of each ERα-LBD monomer form the dimerization interface. A stretch of conserved hydrophobic residues at the amino-terminal end also play an important part in LBD interaction at the time of ERα dimer formation, the residues in H8 and the loop between H9 and H10 provide additional dimer interactions (Tamrazi et al., 2002).

The hydrophobic residues that line the cavity of the ERα ligand-binding pocket recognise the ligand (E2/ estradiol) though hydrogen bonds. When E2 binds to ERα, dynamically mobile H12 is packed against H3, H5/6 and H11 over a gap perpendicular to the dimerization interface. This forms a cover on the binding cavity. This H12 positioning is essential for transcriptional activation as it confers ligand-dependent activation function (through AF-2) and renders ERα capable of interactions with co-activators. While in this confirmation, the LBD can accept the

LXXLL motif from various co-activator proteins (L= Leucine and X= any residue), for example, members of the p160 steroid receptor co-activator (Yi et al.) family (SRC 1-3) (Yaşar et al., 2017).

1.16.3 The DNA binding domain of Estrogen receptor

The highly conserved C region harbours the DNA-binding domain (DBD). The ERα DBD and the ERα-complex with DNA was studied using nuclear magnetic resonance (NMR) and X-ray crystallography. The ERα DBD also contains sequences that contribute to receptor dimerization. The ERα DBD consists of a zinc finger-like motif that contains eight cysteines, which make up the tetrahedral coordination of two zinc ions and play a vital role in receptor dimerization and binding of ER to specific DNA sequences. Two DBD monomers bind to adjacent grooves on one side of the DNA double helix.

Residues in the first zinc finger module (also called P-box), in particular Glu203, Gly204, and Ala207, determine the DNA-binding specificity that is important for sequence discrimination and binding to Estrogen Response Elements (Nott et al.). Residues in the second zinc finger module, also called the D-box, play an important part in discrimination of half-site spacing via protein-protein interactions between two ER monomers.

1.16.4 The amino terminal domain of ERα

The amino terminus of the ER contains the Activation Function-1 (Yi et al.) domain and has ligand-independent transcriptional activity. It can function independently of the AF-2 domain which is ligand-dependent. However, in mammalian cells AF-1 is transcriptionally ineffective when it is separated from the carboxyl-terminus. Therefore AF-1 domain activity depends on the integrity of the hormone-binding domain. Both AF-1 and AF-2 domains are essential for full ER activity (Yi et al., 2002). Because of the intrinsically disordered amino terminus of the NHRs, its structure and exact mechanism of action are not known. The disorder in the amino terminus allows it to rapidly and reversibly adapt to various configurations. These changes are regulated cooperatively by domain and protein interactions, and post-translational modifications, in particular by phosphorylation. S118 phosphorylation in the amino-terminus of E2-bound-ERα or tamoxifen-bound ERα results in recruitment of peptidyl prolyl cis/trans isomerase, Pin1, which isomerizes the serine118-proline119 bond from a cis isomer to trans isomer. This leads to a conformational change within this region promoting ligand-dependent and agonist/SERM-induced ERα activity. These conformational changes that are mediated through phosphorylation are important for stable interaction with co-regulatory proteins to establish effective transcriptional activity (Rajbhandari et al., 2012).

1.17 Estrogen receptor mechanism of action

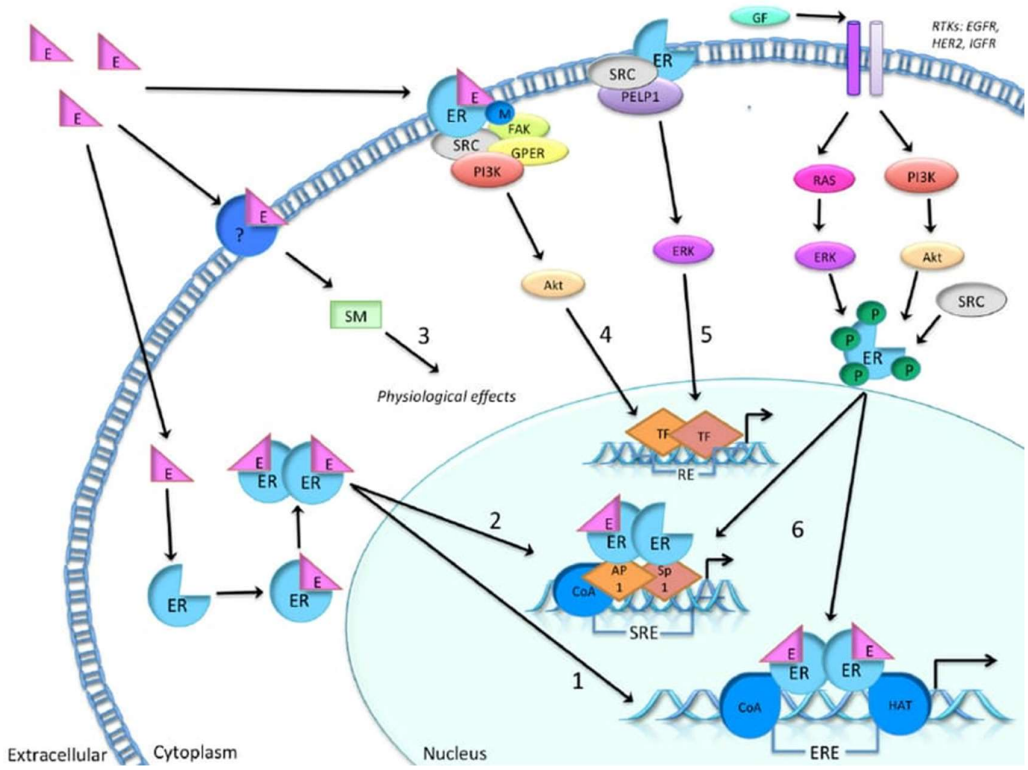

Figure 1.3: Simplified molecular signalling pathways associated with estrogen and estrogen receptors

(1) Classical and direct pathway: ligand activation is followed by binding to the estrogen response element (ERE), including coactivators (Goldhirsch et al.) and histone acetyl transferases (HATs) before gene regulation is modified; (2) tethered pathway: ligand dependent pathway which includes protein-protein interaction with other transcription factors, e.g., activator protein 1 (Ap1) and specificity protein 1 (Sp1), after ligand activation, thereby regulating genes by indirect DNA binding following serum response element (SRE) activation of transcription.

(3) non-genomic ligand dependent reaction: the receptor (e.g., classical ER, ER isoform or other receptors) is activated by a ligand, which may be associated with the membrane. This is then followed by signaling cascades initiated by second messengers (SM), initiating a rapid physiological response, which does not involve gene regulation.

(4) ligand-dependent reaction: ER is methylated by ligand induction and ER–phosphoinositide 3-kinase (PI3K)–steroid receptor coactivator (SRC)-focal adhesion kinase (FAK) forms a complex that further activates the serine/threonine–protein kinase Akt, which then activates transcription without ER binding to DNA; (5) ligand independent reaction: ER–SRC–proline-, glutamic acid and leucine-rich protein 1 (PELP1) forms a complex which then activates transcription, also without ER binding to DNA; (6) another ligand independent reaction activates through other signalling pathways, like growth factor signalling by downstream events of receptor tyrosine kinase (RTKs), such as epidermal growth factor receptor (EGFR), human epidermal growth factor receptor 2 (HER2) and the insulin-like growth factor receptor (IGFR).

- The Role of MicroRNAs as Predictors of Response to Tamoxifen Treatment in Breast Cancer Patients

- Nina G. Egeland and Håvard Søiland, 2015 (Egeland et al., 2015)

1.17.1 Classical pathway / Nuclear signalling

The nuclear ERs are the dominant receptors in manifesting cellular responses to E2. The D-region of the ER houses the nuclear localisation signal (NLS) that is required for translocation of ER to the nucleus. ERα was suggested to contain a leucine-rich nuclear export sequence (NES) in the LBD of the receptor. This NES was suggested to mediate the nuclear export of ERα through binding to an exportin.

In the absence of ligand, ERα exists as a monomer bound to chaperone heat shock protein 90 (Hsp90) and is sequestered in a multiprotein inhibitory complex. In the 'classical genomic' action of ERα, ERα dissociates from heat shock proteins upon ligand binding and binds either directly to estrogen response element (ERE) sequences in genes, or is tethered to promoters via interaction with other transcription factors [e.g. activation protein 1- AP1; specificity protein 1-SP1 (Safe), and recruits coregulators and the transcription machinery to induce transcription of ERα regulated genes.

Thus, nuclear ER interacts with target sites in gene promoters through two different modes, an estrogen response element (ERE)-dependent and an ERE-independent mode (Giraldi et al., 2010).

1.17.2 ERE-dependent transactivation

In the ERE-dependent pathway, target gene expression is regulated by binding of liganded ER to EREs present in promoter regions. This is the classical mechanism of E2-ER action. The events that are associated with ERE-dependent signaling can be similar between ERα and ERβ, but the mode and the extent of transcription differ significantly (Li et al., 2008). In ERE dependent promoters, ER interacts with the consensus ERE- sequence, which is a 5'-GGTCAnnnTGACC-3' DNA palindrome sequence (where n is a non-specific three nucleotide spacer). Estrogen-responsive genes contain one or more copies of EREs that differ from the consensus by one or more nucleotides. Ligand binding induces conformational changes within ERs which promote homo-dimerization and consequent binding to EREs, while binding to ERE induces a conformational change in the DBD of ERα (Hall et al., 2002). DNA bound receptor makes contact with the general transcriptional machinery either directly or indirectly via cofactors (such as, SRC-1, GRIP-1, AIB1, CBP/p300, TRAP220, PGC-1, P68 RNA helicase and SRA). ER coactivator interactions stabilize the formation of transcription pre-initiation complexes and facilitate remodelling of chromatin. Based on the cell type and the specific promoter, DNA-bound ER exerts either positive or negative effect on target gene expression.

The AF-2 domain of ERα interacts with an amphipathic a-helix containing LXXLL motifs in nuclear receptor interacting domains (NRIDs) of cofactors, anchors members of the P160 family of coactivators to the promoter and connects these proteins with upstream signaling. This then serves as a platform for P300 recruitment. This recruitment of P300 leads to an increase in histone acetylation, recruitment of initiation-competent unphosphorylated RNA pol-II and subsequent transcription initiation. ERα AF-1 cooperates with the carboxyl-terminus in a promoter context-dependent way. The ability of the A/B domain in recruitment and exchange of co-regulatory proteins is critical for AF-1 function as well as for the integration of both AF-1 and AF-2 to mediate full capacity transcription in response to estradiol/E2 (Yi et al., 2015).

Unliganded ERα can interact with heterogeneous co-regulator complexes through its carboxyl-terminus (Yi et al., 2015) to modulate the transcription of the target genes. Post-translational modifications (PTM), transcriptionally activate unliganded ERα and regulate several intracellular pathways by interfering with other signaling molecules in the nucleus (e.g. transcription factors like NF-Kβ or AP-1) or in the cytoplasm (e.g. IP3K, G proteins and others) (Maggi, 2011).

1.17.3 ERE-independent promoter transactivation

E2 plays an important role in growth, development, reproduction and maintenance of numerous physiological systems. Longer exposure to E2 stimulates breast cancer growth (Yager and Davidson, 2006) through rapid non-genomic / cytoplasmic signalling cascade (Levin, 2009).

E2-ER complexes can also alter transcription of genes lacking EREs but containing alternative response elements, this occurs through association of ER with other DNA-bound transcription factors such as AP-1 (by interacting with proteins- Fos/Jun), which tether the activated ER to DNA, resulting in an up-regulation of gene expression.

Liganded ER mediates functional interactions with transcription factors (TFs) such as (Cheung et al.) AP-1 and Stimulatory Protein-1 (SP-1). These transcription factors are bound to their cognate regulatory elements on DNA, through ERα's DBD making direct or indirect contact with these transcription factors. This pathway is dependent on receptor subtype, the ligand type, and the type of the cell (Lin et al., 2007).

AP-1 transcription factor is a member of the leucine zipper motif transcription factor family. Leucine zipper regions allow dimerization of transcription factors for regulating gene expression (e.g. Jun-Jun, Jun-Fos dimers). The dimerized Jun and Fos proteins interact with the consensus TGAGTCA sequence, also known as 12-O-tetradecanoylphorbol-13-acetate (TPA) response

elements (Clarke et al., Li et al., 2008). ERs do not directly bind to TREs, but are instead recruited by protein-protein interactions, e.g. to c-Jun through a region encompassing the ER-DBD (Cheung et al., 2005).

E2-ERα mediated activation of AP-1 responsive elements and transcription is dependent on both AF-1 and AF-2 that bind and enhance the activity of the p160 components (ex. SRC1, GRIP1) of the coactivator complex recruited to the site by c-Fos/Jun. Interestingly, the receptor ERβ that lacks AF-1 is unable to activate transcription of AP-1-regulated genes from TRE sites even when bound to E2, suggesting a distinct physiological action of ERβ compared to ERα in regulating this subset of genes (Webb et al., 1999).

SERMs and SERDs can activate rather than repress the transcriptional responses that are mediated by ERα at the TRE site, suggesting that altered pharmacology of these ER ligands can be explained by the amount and/or type of the co-regulatory proteins that show variations in cells from different tissues of origin (Webb et al., 1999).

In response to E2, ERα also cross-talks with SP-1 transcription factor to modulate the transcription of a variety of estrogen-responsive genes. SP-1 belongs to the Sp/KLF zinc-finger transcription factor family. SP-1 binds to consensus (G/T)GGGCGG(G/A)(G/A)(C/T) sequences, referred to as the – "GC box element". In this interaction ERα is tethered to the GC-box response element bound SP-1 protein. The Amino-terminus of ERα is important for responses from the promoters containing GC-box element (Safe, 2001).

1.18 Regulation of ERα function by phosphorylation

Though ERα function is mainly activated by ligand binding, ERα function is also regulated by posttranslational modifications (PTMs), most importantly phosphorylation. ERα phosphorylation occurs at multiple sites mostly in the N-terminal domain and can be mediated by various different kinases. Phosphorylation is regulated by ligand-dependent and ligand-independent mechanisms such as growth factor signalling (Merrell et al., 2011). Phosphorylation of ERα at different sites contributes to regulation of multiple functional activities, such as hormone sensitivity, nuclear localization, DNA binding, protein/ chromatin interactions, protein stability and gene transcription (Huderson et al., 2012).

ERα regulates transcription through its two activation domains, AF-1 and AF-2. As previously stated, AF-2 is located within the LBD and is activated upon ligand binding. However, AF-1 is activated by phosphorylation at several sites in a ligand-independent manner.

The N-terminal domain (NTD) has fourteen serine residues (Huang et al., 2010 84, 91, 102, 104, 106, 118, 137, 154, 167, 173, and 178), of which serines 102, 104, 106, 118, and 167 have been identified as phosphorylation sites by numerous laboratories (Le Romancer et al., 2011). Some of these phosphorylation sites have been functionally characterised, serines 102 (S102), 104 (S104), 106 (S106), 118, and 167 (Huderson et al.) in the AF-1 domain, serine 236 (S236) in the DNA binding domain, and serine 305 (S305), threonine 311 (T311), and tyrosine 537 (Y537) in the ligand binding domain (LBD) (Fig 1.2).

Mutations of these phosphorylation sites to non-phosphorylatable alanine (A) decrease ERα transcriptional activity (eg. S104, S106, S118, S167). Apart from E2 induced phosphorylation of ERα, numerous signalling pathways regulate ERα phosphorylation, such as mitogen activated protein kinase (MAPK) (Thomas et al., 2008), casein kinase 2 (CK2) (Huderson et al., 2012, Williams et al., 2009), protein kinase A (PKA), phosphatidylinositol-3-kinase/AKT (PI3K/AKT)

(Shah and Rowan, 2005), cyclin dependent kinase 2/cyclin A (CDK2/cyclin A) (Rogatsky et al., 1999), glycogen synthase kinase 3 (GSK3) (Medunjanin et al., 2005), cyclin dependent kinase 7 (CDK7) (Guo et al., 2010a), inhibitor of kappa B kinase α (IKKα). S118 is a well-studied phosphorylation site, which is phosphorylated by a number of kinases that include MAPK, GSK-3, IKKα, CDK7 and mTOR (Likhite et al., 2006) (de Leeuw et al., 2011).

For example, Epidermal growth factor (EGF) can enhance E2-induced ERα activity through CDK7- and MAPK-dependent pathways, stimulating ERα activity in the absence of E2 (Guo et al., 2010a).

1.18.1 S118 phosphorylation

S118 phosphorylation functionally mediates the interaction of ERα with coregulator proteins, such as CBP/p300 and the p160 family of coactivators (Dutertre and Smith, 2003) Phosphorylation of ERα at S118 by MAPK increases steroid receptor coactivator 3 (SRC3) binding (Likhite et al., 2006) and induces ERα hypersensitivity to E2 (La Rosa et al., 2012).

ERα S118 phosphorylation through continuous activation of the MAPK pathway thus bypasses ligand-dependency and renders tumour growth hormone-independent. However, S118 phosphorylation in breast cancer is associated with a more differentiated tumour phenotype, better prognosis, and a better response to adjuvant therapy (de Leeuw et al., 2011). Interestingly, in these studies S118 phosphorylation was not associated with disease progression or recurrence-free survival among patients that were not in tamoxifen therapy, indicating that S118 phosphorylation is a predictive marker for tamoxifen response.

S118 phosphorylation has selective effects on gene transcription. For example, after E2 treatment, phosphorylated ERα is recruited to the cyclin D1 promoter after 120 minutes, and

unphosphorylated ERα is recruited to cyclin D1 promoter at 150 minutes. Mutation of S118 to alanine results in reduction of ERE-driven genes but complete loss of genes regulated by tethered ERα interaction (c-myc and cyclin D1 are regulated by tethered interactions through ATF-2/c-Jun and FOS/c-Jun heterodimers, respectively).

1.18.2 S167 phosphorylation

S167 can be phosphorylated by ERK1/2 MAPK, AKT, p90 ribosomal kinase (p90RSK), CK2 and mTOR/p70S6K (de Leeuw et al., 2011, Likhite et al., 2006).

Phosphorylation of S167 increases binding of ERα to DNA, in vitro. It also enhances binding of the coactivator SRC3 to ERα in the presence of E2, and consequently enhances transcription.

CK2-mediated phosphorylation of S167 regulates ERα's interaction with ERE sequences in vitro (Shah and Rowan, 2005). AKT overexpression was shown to increase phosphorylation of ERα and reduce tamoxifen sensitivity. Vice versa, AKT inhibition using RNAi decreased phosphorylation of ERα at S167 and restored tamoxifen sensitivity. AKT-mediated S167 phosphorylation of ERα increased DNA binding and interaction with co-activators in the presence of E2 (Likhite et al., 2006). Increased levels of activated AKT correlated significantly with decreased survival and increased S167 phosphorylation in tamoxifen treated patients. Therefore, for better prediction of patient survival and endocrine therapy response, it might be important to measure both levels of ERα phosphorylation and levels of activated kinases. SRC kinase activates PI3K/AKT, and AKT in turn phosphorylates S167 of ERα. This stabilizes ERα and coregulators interaction with endogenous promoters (Shah and Rowan, 2005).

A few other novel ERα phosphorylation sites have been identified, S154, S212, S294, S554 and S559. Out of these, S294 and S559 were confirmed as bona fide ERα phosphorylation sites which had functional significance (Williams et al., 2009).

Loss of ERα phosphorylation at S118 and S167 in breast cancer cells impacts cancer growth, cell morphology and ERα signalling. These are often used as surrogate markers for a functional ERα signalling pathway, to predict outcomes for Tamoxifen adjuvant therapy in breast cancer. In the MCF7 breast cancer cell line, phosphor-deficient mutations S118A or S167A showed profound changes in cell morphology (Huderson et al.), growth, migration/invasion and gene expression patterns (Huderson et al., 2012). Cells expressing phospho-deficient ERα increased growth and colony formation compared to parental MCF7 cells and were more resistant to apoptosis. They were more invasive but still maintained epithelial markers and sensitivity to E2 and anti-estrogens was as good as in parental MCF7 cells. However, these stably transduced cells had markedly altered E2-regulated ERα target gene expression in an 84 gene qPCR array of genes relating to ERα signalling and breast cancer. Therefore, a single change in ERα phosphorylation can have a profound impact on the expression of ERα regulated genes as well as cell growth and morphology.

While there is evidence from cell line models that ERα S167 phosphorylation promotes anti-estrogen resistance, evidence for a role of S167 phosphorylation in anti-estrogen resistance in breast cancer patients is not substantiated. The majority of studies report a positive association between S167 phosphorylation and the response to endocrine therapy and patient survival. In a study published by Yamashita et al. phosphorylated S167 and expression of ERα and PR were associated with an improved response to endocrine therapy and survival. ERα S167 phosphorylation was also demonstrated to be a predictive marker for a positive response to

endocrine therapy in breast cancer patients and longer survival after relapse (de Leeuw et al., 2011).

The most important sites are serine 118 (Huderson et al.) and serine 167 (S167), whose phosphorylation is regulated by multiple signalling pathways and associated with drug-resistant breast cancer. Therefore, to understand ERα function in breast cancer better, it is important to understand its regulation through phosphorylation and understand its effects on chromatin interaction, gene expression, its impact on protein complexes at target promoters that result in breast cancer growth and endocrine therapy response.

1.19 Regulation of ERα gene expression

Breast cancer cells often show increased expression of ERα. The ERα gene (ESR1) has a complex genomic organisation pattern in humans. The upstream region of the ESR1 gene has several distinct promoter sequences which can also generate several mRNA transcripts that encode the same ERα protein. There are six human ERα mRNA isoforms that encode the same 66-kDa protein but differ in their 5’ untranslated region that regulates expression of the protein. The ESR1 promoter region also undergoes epigenetic modifications, such as DNA methylation (Hua et al., 2018).

1.19.1 Transcriptional regulation of ERα expression

Transcriptional regulation of ERα is controlled by multiple promoters. There are nine putative promoters upstream of the transcription start site of human ERα. This multiple promoter system plays a role in tissue-specific and temporal regulation of ERα gene expression. ERα promoters A and C are used in MCF7 cells which are human breast adenocarcinoma cells, whereas promoter A is used in ZR-75-1 human breast carcinoma cells. The transcription factor Estrogen Receptor Promoter B Associated Factor 1 (ERBF-1) is critical for the transcriptional activity of a distal promoter B. ERα mRNA is transcribed from promoter B in cells that express ERBF-1 (Liu and Shi, 2015).

While encoding the full-length ERα protein, the usage of multiple Esr1 promoters changes the choice of transcriptional activators and repressors and leads to variation of alternative splicing of mRNA transcripts. Another transcription factor that plays an important role in ERα transcription is AP2, which binds to the sequence CCCTGCGGGG in the ERα promoter. ERα expression is associated with AP-2 activity in breast and endometrial cancer. The two subtypes AP2α and AP2γ can trans-activate the human ERα promoter. The forkhead box protein FOXO3a is also positive regulator of ERα transcription; but can interact with ERα and ERβ proteins and inhibit ligand-dependent ER signalling and tumorigenesis. FOXO3a is inactivated by AKT. A different forkhead transcription factor FOXM1 activates and regulates transcriptional activity of the ERα promoter through two closely located forkhead response elements at the proximal region of the ER promoter. On the other hand, FOXM1 protein and mRNA expression is regulated by estrogen in breast cancer.(Arao et al.). FOXM1 expression is downregulated when ERα is depleted in MCF7 cells. FOXM1 and ERα can simultaneously bind to the same genomic sites and stimulate ERα transcriptional activity, making ERα and FOXM1 two key components within a positive cross-regulatory loop. (Guo and Sonenshein, 2004).

GATA proteins are a family of zinc finger DNA binding proteins that recognise the consensus motif T/A GATA A/G. GATA3 is expressed in mammary glands only by epithelial cells, it is an essential regulator of mammary gland morphogenesis and luminal cell differentiation. GATA3 expression is highly correlated with ERα expression in breast cancer. ERα transcription is stimulated by the binding of GATA3 to two cis-regulatory elements located within the ERα promoter (Eeckhoute et al., 2007).

The negative regulators of ERα transcription are less widely studied. These include the zinc finger repressor B-lymphocyte-induced maturation protein (BLIMP1) and Enhancer of Zeste Homolog2 (EZH2). BLIMP1 can bind to the ERα promoter and inhibit ERα transcription. EZH2 negatively regulates ERα transcription by inducing the di-, tri- methylation of histone-3 residue 27. NF-kB can both repress ERα transcription through inducing expression of BLIMP1 and EZH2 and enhance ERα transcription by enhancing the recruitment of ERα to target DNA. Lastly like other human genes, alternate promoters of ER exist. The promoter switch was

mediated by the DDX5/DDX17 (Dutertre et al., 2010a).

1.19.2 Alternative splicing of ER

Alternatively spliced ERα mRNA has been detected in both normal and cancerous tissues. Variances in ERα transcripts may lead to loss of ligand-dependent transactivation activity, gain of ligand-independent transactivation activity, and differential response to tamoxifen (Dutertre et al., 2010b). The best characterized isoform of ERα is the 66-kDa protein encoded by a 6.6-kb mRNA with eight exons (Enmark et al., 1997). There are six human ERα mRNA isoforms that encode the same 66-kDa protein but differ in their 5' untranslated region. Moreover, other variant isoforms of ERα mRNA that encode different protein isoforms occur in the presence or absence of the full length ERα transcript. The variance in ERα mRNA may be attributed to frame-

shift mutations or alternative splicing. A genomic rearrangement in which ERα exons 6 and 7, which encode part of the ligand-binding domain of ERα, are duplicated in an in–frame fashion results in an ERα mRNA that can be translated into an 80 kDa ERα. In addition, a 46-kDa amino-terminal truncated form of ERα, ERα-46, has been identified in endothelial cells and breast cancer cells. ERα-46 is encoded by an ERα transcript that lacks the first exon of the ERα gene (Dago et al., 2015). The high mobility group A protein 1a (HMGA1a) induces alternative splicing of ERα and thereby increases ERα-46 expression, which reduces tamoxifen sensitivity in breast cancer cells. Moreover, some normal or cancer tissues may express an ERα variant that lacks exon 7. While the splicing factor HTRA2-β1 is responsible for ERα exon 7 inclusion, heterogeneous nuclear ribonucleoprotein (hnRNP) G induces exon 7 skipping and then promotes the generation of the exon 7-skipping isoform of ERα. In addition, a 36-kDa spliced variant of ERα, ERα-36, has also been isolated. ERα-36 is defective of exons 1, 7 and 8, which encode transcriptional activation domains AF1 and AF2. This suggests that it is a negative regulator of ERα. Both ERα-46 and ERα-36 are located in the plasma membrane, cytosol, and nucleus ERα-36 also negatively regulates the transactivation activity of ERα-66 and ERβ. Finally, overexpression of the nuclear protein E3-3 (NPE3-3) promotes the generation of another alternatively spliced variant of ERα, ERαV, which contains only exons 1, 2, 7 and 8, and encodes a 37-kDa ERα.

1.20 Wnt signalling pathway

Wnt signalling plays a central role in development and disease (Tamai et al., 2004). The Wnt signalling pathway is a conserved pathway in metazoan animals. The name Wnt is resultant from a fusion of the name of the Drosophila segment polarity gene 'wingless' and the name of the vertebrate homolog, 'integrated' or 'int-1'. Wnt signalling plays important role in embryonic, postnatal development and adult homeostasis by regulating development and stemness and has been highly associated with cancer. Wnt signalling pathway in carcinogenesis is mostly described for colorectal cancer, but abnormal Wnt signalling was observed in many other cancers as well (Ng et al., 2019) (Clevers and Nusse, 2012). A connection of the Wnt signalling pathway to cancer was implicated by the discovery that activation of int1 (Wnt1), resulted in mammary hyperplasia and tumours in mice (Tsukamoto et al., 1988). The first mammalian Wnt signalling gene, mouse Int-1, was identified in 1982 as a proto-oncogene in the mouse genome. Its expression was activated by mouse mammary tumour virus (MMTV) proviral DNA integration leading to mouse mammary cancers (Nusse et al., 1984). This gene was subsequently found to be a homolog of the Drosophila Wingless gene that controls segment polarity in fly larva development (Rijsewijk et al., 1987) (De Ferrari and Moon, 2006).

Deregulated or defective WNT signalling is a causative factor for a number of pleiotropic human pathologies. Most notably, these pathologies include cancers of the breast, colon and skin, skeletal defects and human birth defect disorders including the most common human neural tube closure; spina bifida. The function of signalling in cancer biology is intriguingly complex and not completely understood.

The extra-cellular signal stimulates several intra-cellular signal transduction cascades, including the canonical or signalling /β-catenin dependent pathway and the non-canonical or β-catenin-independent pathway.

Wnt proteins are secreted glycoproteins and can be tethered to the plasma membrane or exit the cell via multiple routes, like solubilization and direct release from plasma membrane, exosomes or lipid protein particles. Secreted signalling proteins bind to cell surface receptors and coreceptors and activate downstream signal transduction cascade. There are several types of signalling receptors, such as N-terminal extra-cellular cysteine-rich domain of the Frizzled (FZD) receptor family. The FZD protein is a seven-transmembrane-span protein with topological homology to G-protein coupled receptors. In addition to the interaction between the signalling molecule Wnt and FZD, the co-receptors that also mediate WNT signalling are lipoprotein-receptor replated protein-LRP5/6 (canonical pathway) and a few others: GPR124, Reck, TMEM59, Ror and Ryk (non-canonical pathway).

A key signal transduction pathway is the canonical β-catenin signalling, which by regulating cytosolic β-catenin protein level controls the activation of signalling -responsive genes. β-catenin plays central role in signalling pathway or β-catenin is the important ligand in activation of signalling pathway. In this study the canonical or signalling / β-catenin dependent pathway will be discussed.

β-catenin is encoded by the CTNNB1 gene and plays a central role in this pathway. β-catenin has dual function it is involved in both cell-cell adhesion and regulation of gene transcription. β-catenin forms a protein complex at the cell membrane forming adherenes junctions, fundamental for maintenance of the epithelial cell layer. Nuclear β-catenin acts as transcriptional regulator. β-catenin is regulated by a destruction complex that contains the scaffold protein AXIN, APC (encoded by tumour suppressor gene adenomatous polyposis coli (APC), Casein kinase 1 alpha (CK1α) and Glycogen synthase kinase 3 alpha and beta (GSK3A/B).

1.20.1 Wnt signalling mechanism

When signalling ligands bind to their various receptors this activates different downstream signalling pathways.

<u>In the absence of signalling stimulation:</u>

β-catenin is the transcriptional co-activator of Wnt signalling. In the absence of wnt, β-catenin is rendered inactive due to its phosphorylation by GSK3. Phosphorylated β-catenin forms a "destruction complex" comprising of GSK3, Adenomatosis Polyposis Coli (APC), Axin, and Casein Kinase-1α (CK1α) (Polakis, 2002). CKI and GSK-3 sequentially phosphorylate β-catenin (Li et al., 2002) (Amit et al., 2002), thereby marking β-catenin for ubiquitination/degradation by an E3 ubiquitin ligase called β-TrCP and targets it for proteasomal degradation (Polakis, 2002).

As a result, β-catenin is not translocated to the nucleus and the repressor complex containing T-cell specific factor (TCF)/lymphoid enhancer-binding factor (Lefebvre and Sol) and transducing-like enhancer protein-/Grouche binds and represses the activity of the target gene (Hutti et al.).

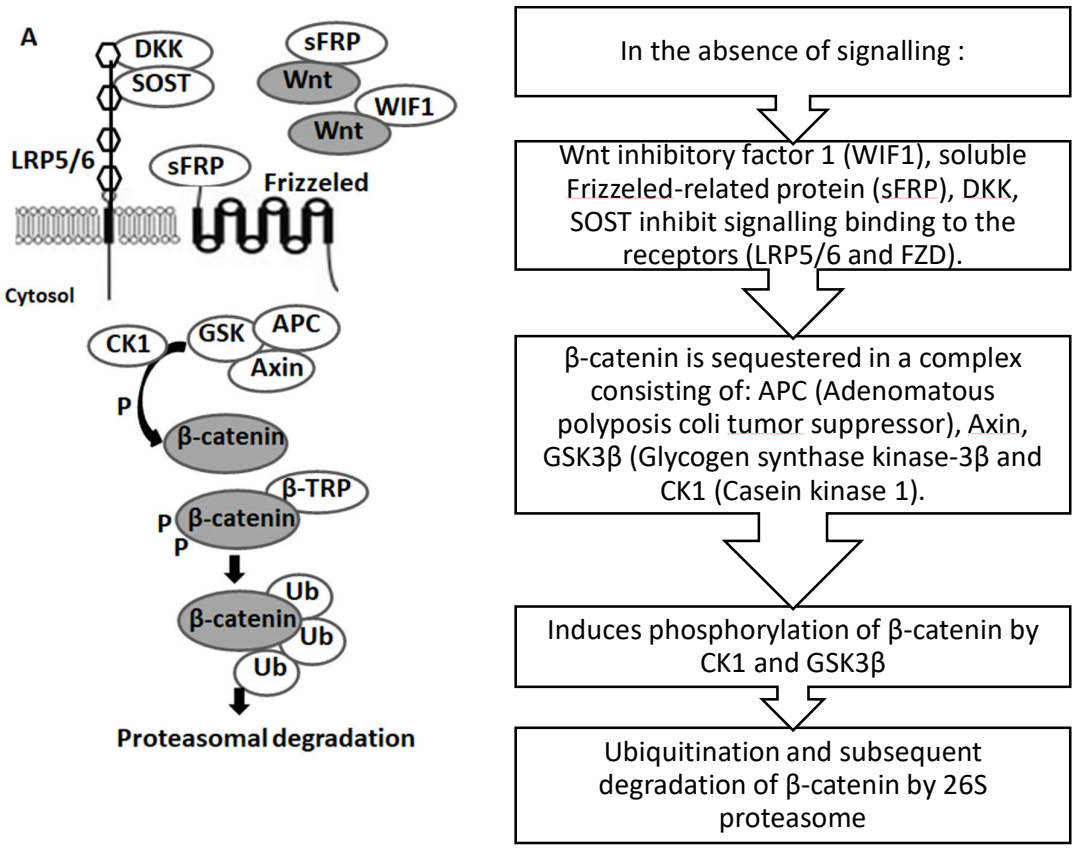

Figure 1.4: Canonical signalling in absence of signalling stimulation

In the absence of a signalling ligand, the phosphorylation of β-catenin by destruction complex (composed of axin, APC, CK1, and GSK3β) leads to its ubiquitination by β-TrCP targeting it for proteasomal degradation. The absence of β-catenin in the nucleus results in the binding of the repressor complex containing TCF/LEF and TLE/Grouche to the target gene and thereby repressing its activity.

In the presence of signalling stimulation:

Following the binding of signalling ligand wnt to Frizzled-Axin-LRP-5/6 complex co-repressor complex stimulates the canonical signalling pathway. After activation, FZD interacts with a cytosolic protein called Dishevelled (Dvl or Dsh), that acts upstream of β-catenin this prevents the β-catenin destruction complex comprising of CK1, GSK3β and axin, from binding and phosphorylating β-catenin (Stamos and Weis, 2013). Cytosolic GSK-3β (Glycogen synthase kinase-3 beta) is sequestered, and the phosphorylation of β-catenin is blocked. The accumulation of hypo-phosphorylated β-catenin in the cytosol allows its migration to the nucleus, where it regulates target gene expression by interacting with the TCF/LEF family of transcription factors. This signalling is implicated in the regulation of cell differentiation and proliferation (Clevers and Nusse, 2012).

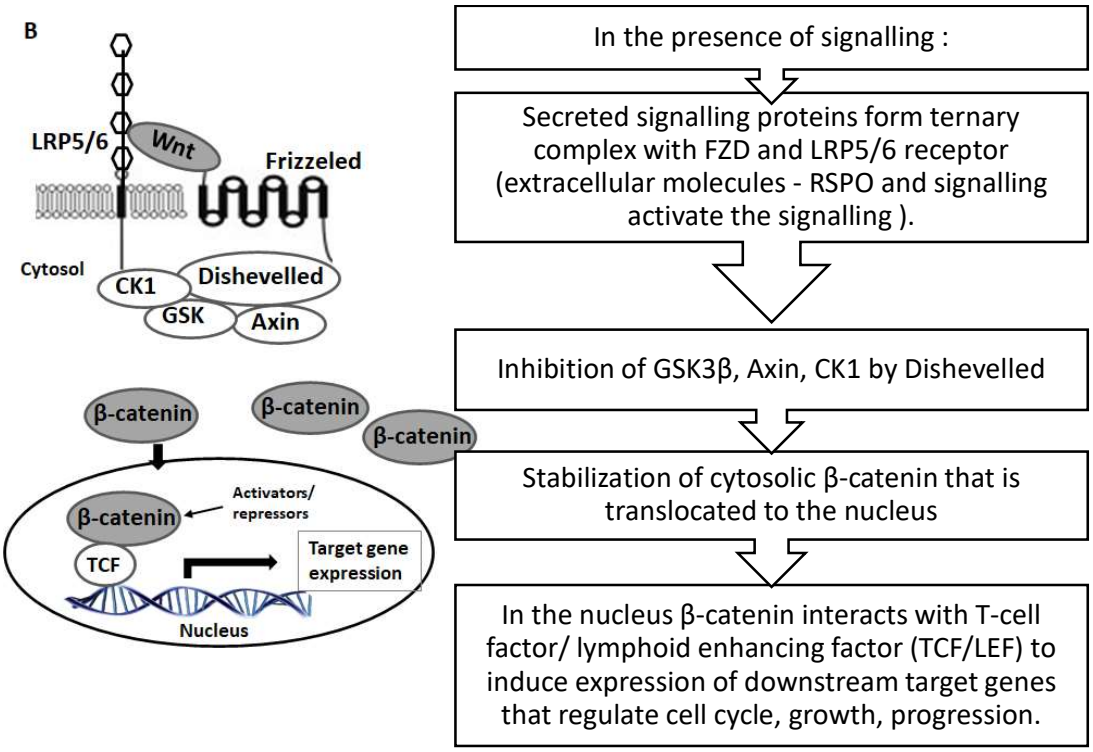

Figure 1.5: Canonical signalling in presence of signalling stimulation

Once the signalling ligand binds to the Frizzled receptor and LRP co-receptor, LRP receptors are phosphorylated by CK1 and GSK3β, resulting in the recruitment of Dvl proteins to the plasma membrane where they activate and scaffold the β-catenin destruction complex. This results in the accumulation of β-catenin in the cytoplasm and its translocation to the nucleus where it forms a complex with TCF/LEF and transcribes target genes.

1.20.2 Wnt signalling in breast cancer

Wnt signalling is activated in over 50% breast cancer patients and is associated with reduced overall survival. canonical signalling was shown to play important role in triple negative breast cancer development and progression and has been studied extensively. High nuclear expression of β-catenin was also seen in other breast cancer subtypes. A small fraction of tumours had somatic mutations of key pathway regulators, like β-catenin, but canonical signalling -ligands and receptors were found to be overexpressed in breast cancer where secretory antagonists were silenced (Ng et al., 2019).

1.20.3 CK1ε in Wnt signalling pathway

<u>CK1 dependent β-catenin mediated TCF-promoter activity:</u>

The Casein kinase 1 (CK1ε) family of protein kinases are serine/threonine-selective enzymes. They function as regulators of signal transduction pathways in most eukaryotic cell types. Different CK1ε isoforms are involved in Wnt signalling , circadian rhythms, nucleo-cytoplasmic shuttling of transcription factors, DNA repair, and DNA transcription (De Ferrari and Moon, 2006)

The kinase CK1ε, forms a part of β-catenin destruction complex, in the absence of signalling. CK1ε was suggested to play role in phosphorylation and activation of the scaffold protein Dishevelled (Dvl) (Gao and Chen, 2010), which binds components at the interface of signalling receptors and the β-catenin destruction complex, in the signalling pathway. Dvl phosphorylation by CK1ε promotes binding of co-effecter Frat, dissociation from β-catenin degradation complex, and stabilization of β-catenin (Amit et al., 2002) (Gao et al. 2002).

1.20.4 DDX3 in the Wnt signalling pathway

DDX3 was previously studied in the genetic analysis of wingless (wg) signalling in Drosophila, in mammalian cells, signalling through the Frizzled family of receptors, to Dishevelled. DDX3 is required for β-catenin signalling in mammalian cells and during Xenopus and Caenorhabditis elegans (a nematode) development (Jenny and Basler, 2016).

DDX3 was shown to be a regulator of the signalling –β-catenin network, where it acts as a regulatory subunit of CK1ε (Cruciat et al., 2013b). DDX3 binds to CK1ε, in a signalling -dependent manner, and directly stimulates its kinase activity, promoting phosphorylation of the scaffold protein dishevelled and promotes β-catenin activation. (The kinase-stimulatory function extends to other DDX and CK1 members, opening fresh perspectives for one of the longest-studied protein kinase families).

This facilitates β-catenin translocating into the nucleus. In the nucleus β-catenin can interact with two major transcription factors, the T-cell factor (TCF) and lymphocyte enhancer factor (Lefebvre and Sol) (Cadigan and Waterman, 2012) , accompanied with several transcription co-activators, BCL9, CBP, p300, Pygo, to regulate multiple genes transcription. These downstream target genes mainly include Snail1, MMP7, PAI1, RAS, and Fibronectin. Moreover, up-regulation of DDX3 expression contributes to the induction of TCF reporter activity and the elevation of mRNA expression levels of TCF-regulated downstream genes, such as c-MYC, AXIN2, CCND1 and BIRC5A (Herbst et al., 2014).

In 1991, it was discovered that the mutations of the adenomatous polyposis coli (APC) gene were the underlying cause of the hereditary colon cancer syndrome termed familial adenomatous polyposis. The APC gene was found to interact with β-catenin. The loss of function of APC resulted in overactive T-cell factor (TCF)4/β-catenin signalling. This suggested a direct link between Wnt signalling and human colorectal cancer (Nakamura et al., 1991).

In breast cancer, a direct link between β-catenin mediated increase in ERα protein expression level was suggested. In this study, the effects of DDX3 and CK1ε on Wnt signalling will be investigated and the possible role of DDX3 in Wnt signalling mediated ERα activation will be explored.

1.21 Hypothesis/ Background of the project

In innate immune signalling, DDX3 associated with IKKε after virus stimulation. The MU Host-Pathogen lab have previously demonstrated a collaborative role between DDX3 and IKKε in the anti-viral immune response, where DDX3 acts a scaffold binding IKKε, promoting its autophosphorylation. IKKε then phosphorylates DDX3 allowing it to recruit IRF3, which is subsequently phosphorylated by IKKε. IRF3 is then recruited to the IFNβ promoter and stimulates IFNβ production (Schröder et al., 2008).

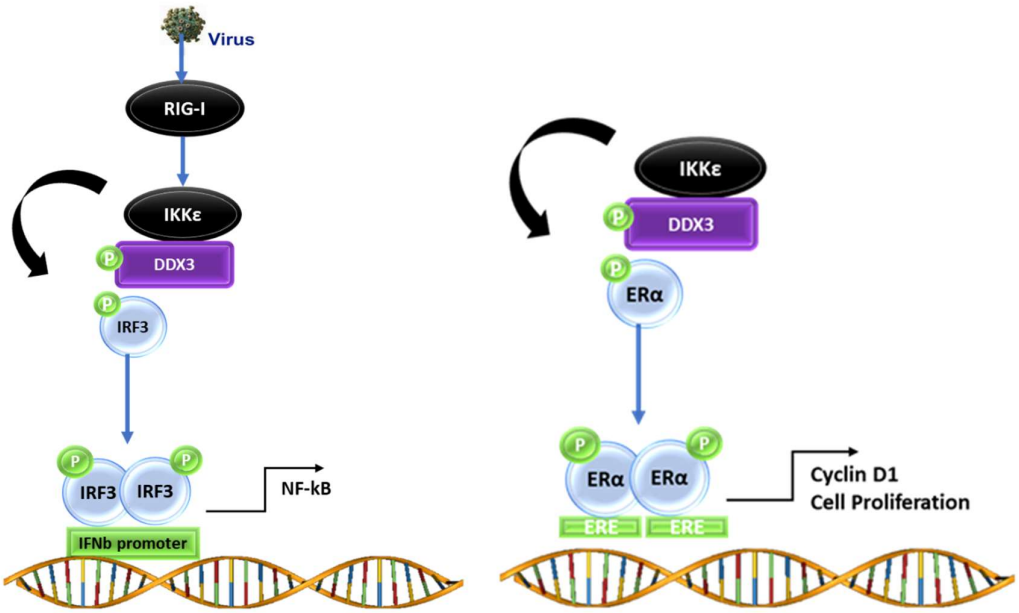

A) DDX3 in Innate immune signaling **B) hypothetical role of DDX3 in ERα activation**

Figure 1.6: Schematic representation of the hypothesis

A) In innate immune signalling pathway, DDX3 promotes autophosphorylation of IKKε, and then links the activated kinase to its substrate, the transcription factor IRF3. Phosphorylated IRF3 drives transcription of IFN-β and other antiviral genes.

B) IKKε has been shown to phosphorylate ERα at Ser167. We propose that DDX3 might mediate IKKε-dependent phosphorylation of ERα, similar to its role in innate immune signalling, and thereby drive expression of ERα target genes.

DDX3 and IKKε were both independently shown to be breast cancer oncogenes, but their collaborative role was not studied. DDX3's expression was shown to be upregulated in breast cancer cells via HIF1-α, and IKKε was shown to activate ERα independent of estrogen, rendering cells insensitive to tamoxifen (anti-estrogen) treatment (now retracted paper by Guo et al 2010). Based on DDX3 and IKKε's role in driving anti-viral immune response, the hypothesis for the project was developed that DDX3 and IKKε might play a similar role in the activation of ERα in breast cancer cells akin to their collaborative role in activation of IFNβ production and elicit innate immune response (Figure 1.5).

The project aims to gain mechanistic insights into ERα activation by DDX3 and IKKε and to analyse the functional impact on downstream targets of ERα.

1.22 Aims of this project

- Investigate DDX3 and IKKε's potential collaborative role in activation of ERα by determining whether DDX3 physically interacts with ERα to enhance ERα activation.
- Understand the functional consequences of DDX3's role in ERα activation (estrogen responsiveness, cell proliferation, tamoxifen sensitivity) and downstream effects of DDX3 knockdown on ERα target gene expression.
- Determine whether DDX3's regulation of the Wnt signalling pathway contributes to its effects on ERα activation and/or target gene expression.

2 Materials and methods

2.1 Standard laboratory procedures

2.1.1 Cell culture

The MCF7 cell line is derived from pleural effusion of metastatic human breast cancer. It is an adherent, epithelial luminal cell line with estrogen, progesterone and glucocorticoid receptors. Although they are referred to as hormone-dependent, the minimal amount of steroid hormones present in serum is sufficient to ensure their growth. For normal maintenance of MCF7 cell line, the cells were cultured in Dulbecco's Modified Essential Medium (DMEM) (Sigma) supplemented with 10% (v/v) fetal bovine serum (FBS) (Sigma) and antibiotics (10µg/ml Gentamicin) (Sigma). Cells were maintained at 37^0C at 5% CO_2 in a humidified incubator. For normal maintenance of cells, they were passaged at 1:10 ratio in T75 cm2 tissue culture flasks (Corning), every three days. Cells were dissociated using 5% (w/v) trypsin-EDTA solution (Sigma-Aldrich) and then resuspended in DMEM.

The T47D cell line is also a hormone-dependent human breast cancer cell line derived from pleural effusion with infiltrating ductal carcinoma of the breast. T47D cells also express receptors for estrogen, progesterone, androgen, glucocorticoid. T47D cells were cultured in RPMI-1640 medium (Invitrogen) supplemented with 10% (v/v) fetal bovine serum (FBS) (Sigma) and antibiotics (10µg/ml Gentamicin) (Sigma); and maintained as described above.

Estrogen depletion

For some experiments involving estrogen responsiveness, cells were starved of estrogen for three days by culturing them in estrogen-depleted medium, to clear out any residual estrogen from the system so that the basal ERα activity was at minimum level. As phenol red from the normal cell culture media was shown to bind to the estrogen receptor and stimulate the proliferation of ERα-positive cell line (Węsierska-Gądek, et al. 2007). MCF7 cells were cultured in commercially available estrogen depleted Phenol red- free Dulbecco's Modified Essential Medium (DMEM) (Sigma) supplemented with 10% (v/v) charcoal stripped-fetal bovine serum (CSFBS) (Sigma), L-glutamine (5µg/ml) and antibiotic (10µg/ml Gentamicin (Sigma) and maintained as described above.

For experiments involving estrogen responsiveness, T47D cells were cultured in commercially available estrogen depleted RPMI-1640 medium (Gibco Lab Technologies) supplemented with 10% (v/v) charcoal stripped-fetal bovine serum (CSFBS) (Sigma), L-glutamine (5µg/ml) and antibiotic (10µg/ml Gentamicin (Sigma) and maintained as described above, for three days. After estrogen depletion, cells were trypsinised as usual and then washed with Dulbecco's phosphate buffered saline (PBS) and then seeded for experiments.

2.2 Long term storage of cells

For long term storage of cells, cells were frozen from a 70-80% confluent culture, at a density of 1-2x10^6 cells/ml in a freezing medium (FBS containing 10% v/v DMSO (Sigma-Aldrich). Cells were trypsinized and resuspended in DMEM or RPMI. Cells were pelleted by centrifugation at 1400g and then resuspended in freezing medium (10% DMSO made in FBS). The cell suspension was transferred into cryotubes (Nunc) and then kept in Mr Frosty (Nalgene), a special freezing container that allowed gradual freezing by lowering the temperature by -1°C/minute, the optimal rate for cell preservation. The vials were transferred to Mr Frosty and stored at -70^{0}C for 24 hours before being transferred to liquid nitrogen for long term storage.

When required, cells were recovered by thawing quickly at 37^{0}C and then added to cold complete culture medium; they were then centrifuged to remove the freezing medium. Cell pellet was then re-suspended in warm medium and transferred to a sterile tissue culture flask and incubated.

2.3 Lentiviral transduction to generate DDX3 knockdown cells

Preparing DDX3 knockdown cells using lentivirus consisted of two parts, transfection of HEK293T cells for virus preparation using the calcium phosphate precipitation method and transduction of the cells in which knockdown of DDX3 gene expression will be enabled. Lentiviral transduction uses TRIPZ inducible lentiviral short hairpin RNA (shRNA) system.

2.3.1 pTRIPZ ShRNA

pTRIPZ DDX3X shRNA (V2THS_228965, Thermo Scientific) or a matching non-silencing control (NSC) plasmid were previously validated. Lentiviral particles were generated by transfecting HEK293T cells with a pTRIPZ shDDX3 vector (V2THS_228965, Thermo Scientific) that inducibly expressed shRNA targeted against either DDX3 or a corresponding Non-Silencing control (NSC) shRNA and the packaging vectors pSDAX2 and pMD2 in the presence of chloroquine sulfate. HEK293T cells were transfected using lentivirus. Stably transduced cells were selected using 2µg/ml puromycin. Knockdown was induced by addition of 2µg/ml doxycycline when cells were being plated. Knockdown was assessed by western blotting.

2.3.2 DDX3 siRNA sequence

siRNA	Sequence	Identifier
DDX3-2	5'-UUCAACAAGAAGAUCCAACAAAUCC-3'	(HSS102713)

Table 6: siRNA sequence and Identifier (Invitrogen)

2.3.3 Transfection of HEK293T cells for preparing virus

HEK293T cells were seeded in 10cm tissue culture dishes (3 – 3.5x10^6 cells in 10 ml culture medium), 24hrs before transfection. Medium on the cells was replaced with the fresh medium 2hrs before transfection with 9 ml fresh culture medium (around afternoon).

For transfection in the afternoon (4pm):

The following plasmids were mixed in sterile Eppendorf tubes:

13.2µg Sh vector (knockdown)/ NSC vector (non-silencing control)
10µg pSPAX2
4µg pMD2
add 450 µl TE/H_eO
+ 500 µl 2xHBS (dropwise/Vortex mixer)
+ 50 µl 2,5M $CaCl_2$ (dropwise/Vortex mixer)

The DNA mixture in the eppendorf tubes was incubated at room temperature for 10 – 20 minutes. Chloroquine (100µM) was added to the cells to enhance transfection efficiency. The precipitates formed in DNA and $CaCl_2$ buffer mixture were then added onto the HEK293T cells to be transfected. The medium was removed and replaced with fresh medium 14-16 h after transfection (first thing in the morning). Precipitates were removed by gently rocking the dishes before replacing medium, followed by addition of 5 ml of fresh medium. For the next two days supernatant containing virus was collected (5ml each) first thing each morning. The supernatant containing the virus of day one was kept in the fridge till the next day and combined with virus of day 2 and frozen to facilitate complete lysis of cells and release of virus particles. Freezing and thawing step for the combined supernatant was followed, as it is possible that some cells that contain virus may detach while handling, so freezing and thawing the cells, ruptures the cell membrane and releases virus particles. Before transducing cell lines, this frozen virus

supernatant was thawed at room temperature, centrifuged and the filtered through 0.45um filter to remove cell debris. Alternatively, the virus was concentrated by ultracentrifugation or Peg-precipitation for long term storage.

2.3.4 Transduction of cells

Prior to transducing the cell lines with lentivirus, selection antibiotic- Puromycin kill curve was determined by treating the cells with serial dilutions of puromycin and cultured for 5 days. The Puromycin concentration that killed non-transduced wildtype cells by day 5 was later used as selecting concentration for knockdown cells, after transduction.

For viral transduction, cells were seeded in a 6 well-plate at 3x10^6/2ml and incubated overnight (one control well each, and two duplicates for NSC and SH). The medium on the cells was taken off in the morning and 700ul-1ml of virus supernatant was added. Cells were transduced three times (morning, afternoon and evening) with 700µl virus supernatant. If concentrated virus was being used it was added to the 2 ml of medium. In addition, 4 µg/ml protamine sulfate was added to enhance the transduction efficiency.

The next day, the medium on the transduced cells was changed and Puromycin (at previously determined) at the selected concentration was added and left for selection until un-transduced control cells are dead (usually by day 5).

Transduced NSC and ShDDX3 cells were maintained in the original transduction plates until they were confluent enough to be split (always with puromycin to maintain the knockdown). They were then split and one batch was frozen at an early stage, and the rest of the cells were allowed to grow at larger scale to be saved by freezing in liquid nitrogen and / or to be seeded to establish whether suppression of the targeted protein i.e. DDX3 knockdown has occurred during transduction by using western blot analysis.

2.4 Plasmid transfections into mammalian cell lines

Cells were transfected with different plasmids using either or calcium phosphate transfections, as follows:

2.4.1 Transfections using Lipofectamine-2000

Cells were transfected using Lipofectamine for ERE reporter gene assays. Cell were seeded at a density of 1 x 10^5/ml and allowed to adhere for 24hr before transfection. Transfection was carried out as follows: Lipofectamine was diluted at 1:24 dilution in Serum free medium and added to previously mixed DNA (230ng total DNA) (in 96well v-bottomed plate). The DNA and lipofectamine mix was incubated for 15 min at room temperature before adding to the cells in a 96 well-plate. A total of 230ng DNA was added in to each well. Cells were incubated at 37^0C for 24-48 hours before harvesting for analysis.

2.4.2 Calcium Phosphate Transfection

For immunoprecipitations (Ips) and western blot analysis, cells were transfected using the calcium phosphate transfection method. Cells were seeded at 2-2.5 x 10^5/ml and allowed to adhere for 24hr before transfection. Culture medium on the cells was changed 1hr prior to transfection. For a 10cm dish, 20µg of plasmid DNA was taken in sterile 1.5 ml microfuge tubes. 2xHBS was added to bring the combined volume to 500µl. 30µl 2.5M $CaCl_2$ was then added and mixed gently. After 20min incubation, the DNA precipitates were added dropwise to the cells. Cells were then incubated at 37^0C for 24-48 hours before harvesting. For a 6-well plate, 12- well plate or 24-well plate, volumes were scaled down appropriately.

2.5 Luciferase Reporter Gene Assays

Cells were plated in flat-bottomed 96wwell-plate at a density of 1 x 10^5/ml and transfected with 60 ng of ERE reporter construct containing a firefly luciferase gene under the control of 3x Estrogen Response Element (ERE) promoter. In addition, 20µg pGLRenilla construct was added, which contains Renilla luciferase under control of a constitutively active promoter. pGLRenilla was transfected to allow normalization of the data for transfection efficiency. Other constructs relevant to the experimental condition were also transfected (e.g. expression constructs for DDX3, IKKε, ERα, etc.). The total DNA concentration transfected into each well was brought to 230 ng with the appropriate matched empty vector, usually PCMV-myc or PCMV-Ha.

Where indicated, cells were stimulated 48 hours post-transfection with 25nM estradiol for an additional 8 hours and then harvested. For harvesting, the medium was first removed from the wells. 50 µl of 1X Reporter Lysis Buffer (made from 5X Reporter Lysis Buffer, Promega) was added to each well. The plate was placed on a rocker at room temperature for 15 min and frozen. The cell lysates were thawed at room temperature on a rocker. 20 µl of each lysate was pipetted into two separate white 96-wells plates. Firefly luciferase activity was assessed by adding 40 µl of Firefly luciferase substrate mix (see section) to one white 96wp, whilst Renilla luciferase activity was assayed by adding its substrate Coelenterazine (Promega) (diluted at 14000 in PBS before use). Luminescence was then measured in a BMG-Labtech Clariostar plate reader. All experiments were carried out in triplicate and repeated 3-6 times.

2.6 SDS-PAGE and Western Blotting

2.6.1 SDS-PAGE

Samples to be subjected to SDS-page were prepared from cell lysates/protein samples by mixing with 2x Laemmli sample buffer with subsequent boiling for 10mins. SDS-polyacrylamide gel electrophoresis (SDS-PAGE) was conducted in a Biorad Mini-Protean® Tetra System. The gels were assembled together using rigs, the tetracell was filled with SDS-PAGE running buffer. The prepared samples were loaded into the wells of a pre-prepared gel (typically a 5% poly-acrylamide stacking gel and a 10% resolving gel) along with a protein molecular weight marker (Fermentas). Samples were then subjected to SDS- PAGE at 100-150 V constant voltage for 50-90 minutes, or until sufficiently resolved.

2.6.2 Western Blotting

Once the proteins had been separated by SDS-PAGE, they were transferred to a polyvinylidene fluoride (PVDF) membrane (Millipore) in a semi-dry electrophoretic transfer unit (Biometra) at 90mA/gel. Prior to use, the membrane was activated by soaking in methanol (Sigma-Aldrich) and in transfer buffer for 5 min. After transfer, the membrane was allowed to dry at room temperature overnight. The membrane was reactivated in methanol followed by a quick wash in PBS Tween. The membrane was then incubated in blocking buffer (5% semi-skimmed milk powder in PBS-Tween) at room temperature for 1h to prevent non-specific antibody binding. After the incubation with blocking buffer the membrane was washed 3 x 5min with PBS-Tween. Subsequently, the membrane was incubated with primary antibody, in blocking buffer, at 4°C overnight. After 3 x 5min washes with PBS-Tween, the membrane was then incubated with the appropriate horseradish peroxidase (HRP) conjugated secondary antibody in blocking buffer for

1h at room temperature, and then washed again 3 x 5 min with PBS-Tween, followed by enhanced chemi-luminescence detection (La Rosa et al.).

2.6.3 Chemiluminscence detection

Enhanced Chemi-Luminescence (La Rosa et al.) solution was prepared by mixing ECL A (1ml), hydrogen peroxide (0.610ul) and ECL B (1ml) and then added to the membrane for 30 secs. Membranes were placed between two layers of clear plastic sheets and placed in a film cassette. In the dark room, Autorad film (UltraCruz ^{TM} Autoradiography Film, Santa Cruz Biotechnology) was placed on top of the membranes in the cassette for 1-30 min. The exposure time was increased to up to 4hr for weaker signals. Autorad film was then developed and fixed. Autrad films were then scanned and processed to generate figure.

2.6.4 Reprobing of the membranes

Some of the PVDF membranes were reprobed for detection of two different proteins with similar molecular weights. Prior to reprobing the PVDF membrane, commercially available western blots stripping buffer from Sigma Aldrich, Re-blot plus was used to strip the membrane. Specifically, re-blot stripping solution was diluted using distilled water by mixing 1ml of the stripping buffer with 9 ml of distilled water (1:10 dilution). Diluted buffer was then poured oven the activated PVDF membrane to be reprobed in a tray and subjected to gentle shaking for 5-10 minutes. The membrane was then washed 3 times x 5 minutes with PBS, followed by blocking the membrane with blocking solution for one hour, as described above and then re-probed for the antibody of interest.

2.6.5 Coomassie staining of the SDS gels

Coomassie staining was used to detect proteins after on the SDS gel after the SDS-PAGE for recombinant proteins. Purified recombinant protein was subjected to on SDS-PAGE, the gel was gently removed and placed in a clean tray and stained with Coomassie Blue Staining Solution for 5 minutes on a rocker, followed by de-staining in de-stain solution or by gently warming up the gel in a microwave oven with distilled water until the background was clear.

2.7 RNA Isolation and RT-PCR

2.7.1 RNA isolation and cDNA synthesis

Total RNA was isolated from T47D NSC and T47D ShDDX3 cells using a Nucleospin RNA isolation kit (Macherey-Nagel), as per manufacturer's instructions. cDNA was synthesized using RT iScript cDNA synthesis kit (Biorad) from 11µls of RNA as follows:

11 µl RNA

4 µl H2O

4µl Buffer

1µl iScript reverse transcriptase

Cycling conditions:

5 minutes at 25°C

30 minutes at 42°C

5 minutes at 85°C

cDNA was then quantified (using Thermo scientific NanoDrop® ND-1000 Spectrophotometer machine), and appropriate dilutions were made to get 200ng/well concentration of cDNA to set-up the RT-PCR in triplicate for each gene and housekeeping gene in a 96 well RTPCR-plate.

List of Primers for used for RT-PCR:

Gene	Ta	Primer sequence
HPRT	60^0C	For 5'- GGT GAA AAG GAC CCC ACG AA-3' Rev 5'- GGC GAT GTC AAT AGG ACT CCA-3'
DDX3	60^0C	For 5'-AGT CGT GGA CGT TCT AAG AGC AGA-3' Rev 5'- AAG CCT CCA TAG CCA CCT CCA CC-3'
NRIP1	60^0C	For 5'-AGC AAA GAC CCA CCA GGA GAG A-3' Rev 5'- GTC TCT GCT CTT CCA CTG ACA TG-3'
PS2	60^0C	For 5'- CCA GTG TGC AAA TAA GGG CTG C-3' Rev 5'- AGG CAG ATC CCT GCA GAA GTG T-3'
EGR3	60^0C	For 5'- GAC TCG GTA GTC CAT TAC AAT CAG-3' Rev 5'-AGT AGG TCA CGG TCT TGT TGC C-3'
GREB1	60^0C	For 5'-GGT CTG CCT TGC ATC CTG ATC T-3' Rev 5'- TCC TGC TCC AAG GCT GTT CTC A-3'
ABCA3	60^0C	For 5'- CTT GAC AGT CGC AGA GCA CCT T-3' Rev 5'- CTC CGT GAG TTC CAC TTG TCC T-3'
Cathepsin-D	60^0C	For 5'- GTA CAT GAT CCC CTG TGA GAA GGT-3' Rev 5'- GGG ACA GCT TGT AGC CTT TGC-3'
Cyclin D1	60^0C	For 5'-CTA CAC GGA CAA CTC CAT CC-3' Rev 5'- TGT TCT CCT CCG CCT CTG-3'
MYC	60^0C	For 5'- TCC GGG TAG TGG AAA ACC AG-3' Rev 5'- CAG CAG CTC GAA TTT CTT CC-3'
TRIM24	60^0C	For 5'-GTG GAT CAG CAA GCA GAA G-3' Rev 5'-TTT GTC AAG AAA GGG TGT AAC G-3'
EPSIN-1	60^0C	For 5'- GGC AAG AAG TGG CGT CAG GTT T-3' Rev 5'-ACT GGA AGT CCT TCA GCG TCT G-3'
EIF4EBP1	60^0C	For 5'-CAC CAG CCC TTC CAG TGA TGA C-3' Rev 5'- CCT TGG TAG TGC TCC ACA CGA T-3'

Table 2.1: List of primers used for RTPCR

2.7.2 Quantitative real-time PCR

Evagreen (Metabion) was used to perform the RT-PCR, as per manufacturer's instructions. A primer master mix was made for each gene. 200ng cDNA was used per well for each PCR reaction. For each gene, RT-PCR was run in triplicates, along with housekeeping gene (HPRT) for every cDNA for data normalization purpose.

<u>The cycling conditions:</u>

2 minutes at 95^{o}C
15 seconds at 95^{o}C
20 seconds at 60^{o}C
30 seconds at 72^{o}C

After the RT-PCR cycling, melt curves for each triplicate were checked for overlay. CT Mean for each triplicate was calculated and checked if the Ct values for triplicates were close (Ct values must not vary more than 1). Relative mRNA expression was calculated using ΔΔCT method, as follows:

ΔCt (ref) value= Ct NSC gene – Ct housekeeping gene
ΔCt (sample) value= Ct Sh gene – Ct housekeeping gene
ΔΔCT value= ΔCt ref - ΔCt sample
Relative expression = 2^ -ΔΔCT.

Primers to be used in RTPCR were first tested using a conventional end-point PCR with Taq polymerase (KOD- Hot start polymerase kit).

2.8 Preparation of competent *E. coli* cells

Competent cells were prepared from *E. coli* strain BL21/DH5α (NEB) with $CaCl_2$ solution, which facilitates transformation of the cells with DNA. More specifically, 50 µl of *E. coli* cells were added to 2 ml of LB broth and cultured overnight at 37°C. LB broth (400ml) was inoculated with 2ml of the *E. coli* overnight pre-culture and incubated at 37°C with shaking (200rpm) to mid-log phase until the OD600 of the culture reached 0.4-0.5 (after approximately 2-3 hours). Then, the bacteria were pelleted by centrifugation at 4°C for 20 minutes at 3,000g. The pellet was immediately resuspended in 30ml of ice-cold transformation buffer (100mM $MgCl_2$) and incubated on ice for 10 minutes. The cells were pelleted as before and resuspended in 2 x 50 ml ice-cold PIPES buffer. Cells were then pelleted again by centrifugation, resuspended in 2 x 20 ml of PIPES buffers. Aliquots of 200-300 µl were snap frozen in liquid nitrogen and stored immediately at – 80°C.

2.8.1 Transformation of chemically competent cells

Competent cells were thawed on ice. 50 µl of cells were transferred into a cold 1.5ml tube containing 50 ng of plasmid DNA and kept on ice for 10 mins before being heat- shocked for 30 seconds at 42°C, and then placed on ice for a further 2 minutes. 100 µl of SOC medium or Ampicillin free LB broth was added to the transformed cells. The cells were either immediately plated onto LB agar plates (LB broth with 1.5 % (w/v) agar) containing 100µg/ml ampicillin and incubated at 37°C overnight or after heat-shock 100µl of SOC medium or LB broth was added to cells, and the tube was left shaking at 37°C in a bacterial incubator for 1h. Outgrowth at 37°C for 1 hour is best for cell recovery and maintenance of antibiotic resistance. Transformed cells were then spread onto LB agar plates containing 100µg/ml ampicillin and incubated at 37°C overnight.

2.8.2 Large scale DNA preparation

Plasmid purification from transformed bacterial cells was performed using the Nucelobond Xtra Midi Kit (Macherey-Nagel) according to the manufacturer's protocol. Specifically, a single transformed *E.coli* colony was inoculated in LB broth (100ml) containing appropriate antibiotic (e.g. ampicillin) and incubated over night at 37^0C with constant shaking at 180-200 rpm. The bacterial cells were centrifuged at 3000g for 20mins at 4^0C and subjected to lysis and purification as per the manufacturer's instructions. All plasmids were eluted in molecular grade water. DNA concentrations and purity were determined using a Thermo scientific NanoDrop® ND-1000 Spectrophotometer according to the manufacturer's protocol.

2.9 Methods for investigating Protein interactions

2.9.1 Production of recombinant His-tagged proteins in BL21 *E. coli*

1µl plasmid DNA (pHis-Parallel-2 expression plasmid) was transformed into chemically competent *E. coli* strain BL21 (New England Biolabs). An overnight pre-culture was performed at 37°C by inoculating with one transformed colony in 12 ml of LB (AMP) overnight. Alternatively, 5µl of a glycerol stock was used to inoculate the 12ml pre-culture of LB (AMP).

On the next day, 10 ml of the overnight pre-culture was inoculated into a 100 ml LB (AMP) culture and incubated at 37°C up to the logarithmic phase of growth. When OD600 = 0.6 was reached, protein expression was induced by the addition of isopropyl β-D-1 thiogalactopyranoside (IPTG) to a final concentration of 100 µM followed by incubation at room temperature for 5 hrs.

2.9.2 Purification of His-tagged recombinant protein from BL21 *E. coli*

The *E. coli* cells were pelleted by centrifugation of 4000g for 15min at 4°C, and then resuspended in 1 ml lysis buffer for His-tagged proteins. Cells were then freeze-thawed to facilitate lysing. Additional sonication (30% power for 30sec x 3) was performed on the lysates to completely lyse the bacteria with intermittent 30 sec incubation on ice. The lysates were cleared by centrifugation at 13000g for 30 min. 50µl of supernatant was removed and added in a separate eppedorf tube to check for protein expression later by using Coomassie staining. The rest of the supernatant from lysate was added to a washed Ni-NTA beads slurry and subjected to gentle agitation on a roller at 4°C. (see section 2.9.3 for preparation of beads for pulldown assay)

Pellet extraction was performed to extract the maximum amount of protein by resuspending pellet in His-lysis buffer added with inhibitors followed by storing on ice for 30 minutes with intermittent mixing using a vortex mixer. After centrifugation the supernatant from this step

was mixed with the previous supernatant and rolled with the beads from previous step to purify his-tagged recombinant protein. In addition, 50µl of this supernatant was saved as a pellet sample and checked by SDS-PAGE and Coomassie to establish if protein was present in the pellet. Similarly, protein purification, SDS-PAGE and Coomassie staining was performed for full-length DDX3 and truncated proteins. To have roughly similar amount of proteins (for full-length DDX3 and truncated protein) the purified protein samples were subjected to SDS-PAGE and Coomassie staining. By comparing band intensity between full-length DDX3 and truncated protein the amount of beads required for the pulldown assays was decided.

2.9.3 Preparation of beads for pulldown assay

100 µl Ni-NTA bead (50%) slurry (Qiagene) for his- tagged proteins was washed three times with His-lysis buffer. At the end of washes, beads were resuspended in his-lysis buffer added with Imidazole (at an appropriate concentration) to make a 50% slurry.

The beads were then washed thrice with 1.5 ml of the appropriate washing buffer (His-lysis buffer) and then subjected to SDS-PAGE and Coomassie staining to check and compare amount of protein on the beads. The purified recombinant proteins were eluted by boiling with 2x Laemmli sample buffer (50µl). Aliquots of protein were run on SDS-PAGE and stained with Coomassie Blue (see section Coomassie staining) to assess purity and amount of purified recombinant proteins.

2.9.4 Preparation of mammalian cell lysate for pulldown assays

MCF7 and T47D cells were cultured in appropriate culture medium. 5-10x10^6 Cells were harvested by trypsinising and resuspending in PBS followed by centrifugation. Cell pellets were lysed using 1650µl of mammalian lysis buffer for pulldowns as below:

Tris/Cl pH 7.5 50 mM

NaCl 150mM

EDTA 1mM

Glycerol 10%

NP-40 0.5-1%

Imidazole 50mm

NaV 1:100 (1mM final concentration)

PMSF 1:100 (1 mM final concentration)

Aprotinin 2:100 (2µg/ml)

After resuspending in lysis buffer, cells were kept on ice for 45 minutes with intermittent vortexing. Then centrifuged at 13000rpm for 15 minutes. The supernatant was transferred to a fresh Eppendorf tube. 50µl of the supernatant was saved as a control for the pulldown assay in SDS-PAGE analysis.

200µl of lysate (supernatant after lysis) was added with 25 µl diluted recombinant-protein-beads. Same amount of cell lysate was also incubated with empty beads as a control to check if there was any non-specific binding to the beads.

Beads were added to the cleared mammalian cell lysates from above step to set up pulldown.

2.10 In vitro pulldown assay

For pull-downs, equal amounts of the different His-tagged recombinant proteins were used, as estimated by SDS–PAGE and Coomassie Blue staining prior to use. 250µl Cell lysates from MCF7 and T47D cells or HEK293T cells with over-expressed proteins were incubated with the purified His-tagged proteins pre-coupled to Nickel-Agarose (25µl), with constant rotation for 4h or overnight at 4°C. Beads were washed three times in 1.5ml lysis buffer, and then all the wash buffer was removed using gel-loading tip. Beads were then resuspended in 2x Laemmli sample buffer and boiled for 5min at 95^0C. Samples were analysed for interactions by SDS-PAGE and Western blotting.

2.11 Co-Immunoprecipitations

2.11.1 Precoupling of beads

Protein A/G beads (Santa Cruz) were washed with IP lysis buffer three times by centrifugation at 4000rpm for 2 minutes and then resuspended in the lysis buffer added with inhibitors, to make a 50 % slurry.

Coupling of Beads and antibodies:

For DDX3 antibody coupled beads, 30µl beads were mixed with 5 µl DDX3 antibody (Santa Cruz mouse polyclonal). For ERα antibody coupled beads, 30µl beads were mixed with 3µl ERα antibody (Santa Cruz Rabbit polyclonal). For ERα isotype control, IgG antibody coupled beads were prepared by mixing 30µl beads with 3µl of IgG antibody (Santa Cruz) and for DDX3 isotype control 30µl beads were mixed with 3µl of IgG2 (Santa Cruz). 30µl of antibody pre-coupled beads were used to set up one IP. For more IP conditions (cells cultured in replete/complete (complete), estrogen deplete (deplete) and estrogen deplete+E2 treated (deplete+E2)) the amounts of beads and antibodies were increased proportionately.

Washed A/G beads were precoupled with anti-ERα antibody (rabbit polyclonal Ab from Santa-Cruz Biotech) for 1hr. Antibody pre-coupled beads were washed 4 times with lysis buffer after 1 hr incubation with the antibody, the mixture was subjected to centrifugation at 4000rpm for 2 minutes. The beads were then resuspended in IP lysis buffer to make 50% slurry (to make up to same volume as at the start) and then used to set up Immunoprecipitations.

2.11.2 Generating cell lysates for Immunoprecipitation (IP)s

4x10^6 cells were washed with ice cold PBS, detached from the culture vessel using a scraper and pelleted by centrifugation at 6000rpm for 15 minutes. The cell lysates were prepared by adding 800µl of IP lysis buffer with protease inhibitors to the cell pellets followed by 45 minutes incubation on ice with intermittent vortexing (see Buffers section below).

The samples in lysis buffer were then centrifuged at 13000g for 15-20 min. 30µl of each type of cell lysate was saved to be run on SDS-PAGE later as input, and the remaining amount of lysates were transferred to a fresh 1.5ml Eppendorf tube to be used in Immunoprecipitation, separately.

2.11.3 Co-Immunoprecipitation

Pre-coupled beads (30µl per IP) were transferred to a fresh 1.5ml microfuge tube for setting up immunoprecipitations. 250µl cell lysate was then added to 30µl of antibody pre-coupled protein A/G beads. The beads with the lysates were incubated for 3hr or overnight at 4^0C with constant rotation. After the incubation with lysates, the beads were washed 4 times with lysis buffer followed by centrifugation at 4000rpm for 2 min. At the last step all the lysis buffer was removed by using narrow tipped- gel loading tips and 50µl Laemmli sample buffer was added to the beads. The beads were boiled at 95^{o}C for 5 min and subjected for SDS-PAGE and western blot analysis to identify co-immunoprecipitated proteins.

2.12 Proliferation assay

Cell proliferation assays were set up in 24 well-plates for DDX3 knockdown (SH) cells (MCF7 and T47D) using non-silencing control (NSC) cells as controls, in estrogen depleted and supplemented conditions (25nM Estradiol).

DDX3 knockdown was induced by culturing cells in the presence of puromycin (2µg/ml) and doxycycline (2µg/ml) in both complete and estrogen depleted culture conditions. T47D cells were seeded at 5000 cells/well in a 500µl volume. MCF7 cells were seeded at 1x10^5 cells/well in 500µl in a 24 well-plate. Cells were allowed to adhere for 24 hours and then estrogen was added to the cells where indicated. Cell proliferation rates in estrogen-depleted and estrogen-treated conditions were measured by trypan blue-exclusion method of cells counting for 5 consecutive days as indicated in the figure. For counting the cells on each day, the medium in the wells to be counted was taken off, cells were washed with PBS and then 250 µl trypsin/EDTA was added to detach and separate cells. Trypsin was neutralized after 5 minutes using PBS to make up to the initial volume of 500 µl. The cell suspension was transferred to Eppendorf tubes, 10 µl of which was mixed with 10µl of trypan blue (cell suspension: trypan blue ratio of 1:1) and then 10 µl of this was loaded onto the hemacytometer and then cells were counted for 5 consecutive days. Medium on the cells was replaced with fresh medium with all additives, including puromycin and doxycycline, on day 3 of the assay.

2.13 MTT assay

In T47D cells knockdown was induced as described above. The MTT proliferation assay was set up using T47D DDX3 knockdown (SH) and non-silencing control (NSC) cells in a 96 well-plate format. T47D cells were seeded at 6500 cells/well in 250µl volume in presence and absence of estrogen and allowed to adhere for 24 hours. Cells were then treated with 10nM estrogen and 0.1µM-20µM Tamoxifen. Medium was replaced with fresh medium on day3 of the assay. At the end of day 5 medium on the cells was taken off by aspiration and 30 µl of MTT solution (5mg/ml) was added on the cells, from Sigma. Cells were incubated with MTT for 5 hours during which MTT reagent was reduced to a blue-purple coloured compound due to metabolic activity of the cells leading to formation of formazan crystals. At the end of 5 hr incubation with MTT, MTT was aspirated from the well and 200 µl of DMSO was added in each well to dissolve the formazan crystals. The plate was gently rocked on the shaker for 5 minutes. OD at 550 nm was measured and the results were normalized to media blank and plotted against untreated control for comparison.

2.14 Colony formation assay

DDX3 knockdown was induced as indicated before in T47D and MCF7 cells and colony formation assay were set up to compare colony forming ability in DDX3 knockdown T47D and MCF7 (SH) cells in comparison to their non-silencing control (NSC) cells. T47D cells were seeded at 500 cells/well in a 6 well-plate and MCF7 cells were seeded at 1500cells/well in the presence or absence of estrogen (25nM). Cells were incubated for about 15-20 days to allow colony formation, with medium being replaced with fresh medium every 3rd day. At the end of incubation time, the medium was removed from the wells and cells were fixed by dehydration using methanol. Methanol was removed and 2% Crystal violet solution was added to each well to stain the colonies, which was then removed onto tissue paper and disposed appropriately. Wells were then washed gently under running tap water, dried and then colonies were counted.

2.15 Filter aided sample preparation (FASP) method for protein purification

For the proteomics analysis, samples were prepared as follows:

The FASP method generates tryptic peptides from crude lysates for LC-MS analysis. Since the essential steps of this method occurs within a filtration device, the method has been termed Filter Aided sample Prep (FASP). This method allows analysis of detergent lysed cells and tissues and is therefore suitable for studying entire proteomes and fractions containing biological membranes. The key features of the method making that make it superior over other sample preparation methods are:

- The method provides protein digest that are from nucleic acid and other cell components
- This method can be applied to samples containing high concentrations of detergents
- There are no precipitation and the concentration steps, and the concentration of sample is kept high
- 0.2-200µg of protein can be processed in a single filter device
- The yield and the purity of peptides can be monitored by UV-spectrometry allowing QC of the digest.

Materials for FASP:

Microcon YM-30 (Millipore),

3M Empore HP Extraction disk cartridge (C18-SD); 7mm/ 3 ml (Varian Cat. No. 12144002)

Solutions:

UA 8 M urea (Sigma, U5128) in 0.1 M Tris/HCl pH 8.5 (1 ml per sample) and IAA 0.05 M iodoacetamide in UA (0.1 ml per sample) solutions were prepared and used on the same day.

Trypsin, was prepared as a stock 0.4 µg/µl 0.5 M NaCl in water (0.05 ml per sample)

Ammonium bicarbonate (ABC): 0.05M NH4HCO3 in water (0.25 ml per sample)

2.15.1 Cell treatment and Sample preparation

Lysis and thiol-reduction:

Heating of samples in the presence of a high concentration of SDS and reduction of disulphide bridges was used for maximal cell lysis, as follows:

DDX3 knockdown was induced in T47D shDDX3 cell line and its matching non-silencing control cell line by the addition of doxycycline (2µg/ml) to the culture medium, in tandem with estrogen deplete (phenol-red free RPMI-1640 medium supplemented with charcoal stripped FBS) and complete medium (normal RPMI-1640 medium supplemented with FBS) for 3 days.

4x10^6 cells were harvested, and samples were prepared for proteomics analysis using the Filter Aided Sample Preparation (FASP) method. Protein concentration was determined using the BCA Assay (Sigma) following the manufacturer's protocol. Aliquots of 50 µg of proteins in

10µL lysis buffer were transferred into individual 1.7 mL microtubes. Cells were lysed by mixing with 150µl of lysis solution that contained 4%SDS, 100mM Tris/HCl pH 7.6, 0.1M DTT and incubated at 95°C for 3 min. DNA was sheared by sonication to reduce the viscosity of the sample. Before sample processing, the lysate was clarified by centrifugation at 16,000 x g for 5 min at room temperature or 20^0C.

Sample processing:

30µl of protein extract was mixed with 200µl of UA in the filter unit and centrifuged at 14,000 x g for 15 min. 200µl of UA was added to the filter unit again and centrifuged at 14,000 x g for 15 min. Flow through was discarded from the collection tube.

100 µl of IAA solution was added and the sample was mixed at 600rpm in a thermo-mixer for 1 min and incubated without mixing at 20 min. Filter units were centrifuged at 14,000 x g for 15 min. 100µl of UA was added to the filter unit and it was centrifuged at 14,000 x g for 15 min (repeated twice).

40 µl of ABC and Trypsin mix (enzyme to protein ratio 1:100) was then added and followed by mixing at 600 rpm in a thermo-mixer for 1 min. The filter units were then incubated in a wet chamber at 37^0C for 4-18hr.

Next day, the filter units were transferred to new collection tubes, and centrifuged at

14,000 x g for 10 min. Next, 40µl ABC was added on the top of the filters and the filters were centrifuged again at 14,000 x g for 10 min. The filtrate was acidified and desalted using Trifluoroacetic acid (CF_3COOH).

2.15.2 Peptide yield determination using Bradford

Bradford assay was performed for quantification of yield as follows:

Serial dilutions of BSA were prepared and used as standards. The Bradford's assay was performed to get an estimate for protein concentration of the samples using the Bradford ultra (Expedeon) kit as per manufacturer's instructions. Absorbance values for standards i.e BSA dilutions were plotted to generate a standard curve. The corrected absorbance (Abs. Sample-Abs. blank) of the samples was then plotted on the standard curve to get the approximate protein concentrations. Samples were diluted in PBS to get 0.2µg/µl protein concentration. Aliquots of 50 µg of proteins in 10 µL lysis buffer were transferred into individual 1.7 mL microtubes. Diluted samples were then added to the sample vials and subjected to mass spectrometry.

2.15.3 LC-MS/MS run

An Ultimate 3000 NanoLC system (Dionex Corporation, Sunnyvale, CA, USA) coupled to a Q-Exactive mass spectrometer (Thermo Fisher Scientific) was used for mass spectrometry-based analysis. Four experimental replicates were analysed using label-free LC-MS/MS. Re-suspended peptide mixtures (a maximum load of the equivalent 1 µg pre-digested protein) were loaded by an autosampler onto a C18 trap column (C18 PepMap, 300 µm id × 5 mm, 5 µm particle size, 100 Å pore size; Thermo Fisher Scientific). The trap column was switched on-line with an analytical Biobasic C18 Picofrit column (C18 PepMap, 75 µm id × 500 mm, 2 µm particle size, 100 Å pore size; Dionex). The peptides generated were eluted over either 65 min or 180 min using the following binary gradients: solvent A [2% (v/v) ACN and 0.1% (v/v) formic acid in LC-MS grade water] and 0-90% solvent B [80% (v/v) ACN and 0.1% (v/v) formic acid in LCMS grade water]. The column flow rate was set to between 0.25 and 0.3 µL/ min. The Q-Exactive was

operated in positive, data dependent mode and was externally calibrated. Survey MS scans were conducted in the 300–1700 m/z range with a resolution of 140,000 (m/z 200) and lock mass set to 445.12003. CID (collision-induced dissociation) fragmentation was carried out with the fifteen most intense ions per scan and at a resolution of 17,500. A dynamic exclusion window was applied within 30s. An isolation window of 2 m/z and one micro-scan were used to collect suitable tandem mass spectra.

2.15.4 Data analysis for proteomics

Data analysis of all statistically significant proteins with altered abundance Protein identification and label-free quantification (LFQ) normalization of LC-MS/MS data was performed using MaxQuant v1.5.2.8 (http:// www.maxquant.org). The Andromeda search algorithm incorporated in the MaxQuant software was used to correlate LC-MS/MS data against the Homo sapiens Uniprot reference proteome database and a contaminant sequence set provided by MaxQuant. Perseus v.1.5.6.0 (www. maxquant.org/) was used for data analysis, processing and visualization. Normalised LFQ intensity values were used as the quantitative measurement of protein abundance for subsequent analysis. The data matrix was first filtered for the removal of contaminants and peptides identified by site. LFQ intensity values were log2 transformed and each sample was assigned to its corresponding group. ANOVA-based multi-sample t-test were performed using a cut-off of $p < 0.05$ on the post imputated dataset to identify statistically significant differentially abundant proteins. Differentially expressed proteins were identified by filtering rows based on proteins expressed in one group and then listed using Numeric venn diagram analysis function. Data was copied to excel for further analysis to calculated protein expression fold change.

2.16 Buffers

Solutions used for making SDS-PAGE gel

10% w/v ammonium persulphate (10% APS)

0.1g APS was dissolved in 1 ml dH_2O and stored at -20°C.

1.5M Tris-HCL (pH 8.8) (Resolving gel)

90.75g Tris was dissolved in 400 ml dH_2O

pH was adjusted to 8.8 with HCL and the volume was made up to 500 ml by adding H_2O

and stored at room temperature

1.0 M Tris-HCL (pH 6.8) (stacking gel)

155g Tris was dissolved in 150 ml dH_2O

pH was adjusted to 6.8 with HCL and the volume was made up to 250 ml

by adding dH_2O and stored at room temperature.

10% w/v SDS

10g SDS was dissolved in 100 ml of dH_2O

10X SDS-PAGE running buffer

30.3 g TRIZMA BASE

144 g Glycine

10g SDS

dH_2O to 1 litre

Diluted to 1X before use with dH_2O

10x Transfer Buffer

30.3 g Tris

144g Glycine

Made up to 1L with dH_2O

1x Transfer buffer was made using 15% Methanol prior to use.

2X Laemmli sample buffer

2ml 0.5M Tris/HCL pH 6.8 3 tone

2% SDS (10% stock was used)

10ml Glycerol

200µl bromophenol blue (1% stock ethanol) - 6mg bromophenol

2ml 1M DTT

0.53 ml distilled water

Distilled water was added to make 20ml and stored at room temperature.

1M DTT

1.54 g DTT in 10 ml dH_2O

IP Lysis Buffer:

50 mM Hepes pH 7.5 (or Tris/HCL pH 7.5)

150 mM NaCl

1 mM EDTA

10% Glycerol

0.5% NP-40 (or 1% NP-40)

Protease and phosphatase inhibitors:

Added freshly just before use:

Aprotinin (20 μl/ml)

1mM sodium orthovanadate (10 μl/ml)

1 mM PMSF (10 μl/ml)

The lysis buffer was stored in the fridge, kept on ice after the inhibitors were added (PMSF unstable even on ice, only keeps for about 1h).

Other general buffers:

10x PBS

85g NaCL

4.68g NaH_2PO_4

4.68g Na_2HPO_4

Made up to 1L with dH_2O (requires heat)

PBS/Tween

1 x PBS

0.1% Tween-20 (1ml in 1L)

Blocking Solution (for Westerns)

5% Dried Milk (Marvel) in PBS/Tween (5g in 100ml)

0r 5% BSA (Sigma-Aldrich) in PBS/Tween (5g in 100ml)

50 x TAE (1 l, pH 7.6):

242 g Tris Base

57.1 mls glacial acetic acid

100mls 0.5M EDTA (pH 8.0)

Make up with distilled water to 1L.

Ampicillin Stock:

100mg/ml in distilled water, filter-sterilised, aliquoted, and stored at -20^{0}C. Used at 1/1000 dilution.

LB media and LB Agar plates:

20 g of LB pre-mix / 1L of water (autoclave before use)

For plating LB agar medium: 1.5 g Agar was added and autoclaved.

Selection antibiotic was added once the LB agar medium was cooled to ~ 50-55^{0}C.

His-Lysis buffer for recombinant protein:

10mM Tris/Cl pH 7.5,

300mM NaCl,

20mM Imidazole,

PMSF and protease inhibitor tablet (range of different NaCl concentrations was tried, at lower salt concentration the binding is reduced, and higher concentration of salts increased protein binding).

IP lysis buffer:

50 mM Hepes/ Tris HCl pH 7.5

300mM NaCl

1mM EDTA

10% Glycerol

0.5% NP-40

20µl/ml Aprotinin

10µl/ml NaV

10µl/ml PMSF

Buffers for Calcium phosphate-mediated transfection:

2.5M $CaCl_2$:

36.75g $CaCl_2.2H_2O$ in 100ml dH_2O

2x HBS buffer:

42mM HEPES

10mM KCL

12mM Dextrose

1.5 mM $Na_2HPO_4.7H_2O$

280mM NaCl

pH adjusted to 7.5 with NaOH.

Luciferase substrate recipe:

Stock solutions:

500mM $MgSO_4x7H_20$:

6.162g/50ml, stored at RT

10 mM ATP:

165.345mg/30 ml prepared freshly each time

50mM Magnesium Carbonate Hydroxide:

1.214g/50mls, stored at RT (this doesn't dissolve, but it was resuspended before adding into the luciferase mix).

Amounts adjusted for 100mg Acetyl-CoA:

1.73g Tricine

2.56 ml of $MgSo_4$ stock solution

96.5 µl of EDTA stock (500mM)

2.48g DTT (dissolved first in 10 ml H20)

25.4 ml of fresh ATP stock solution

4mls of H_20 to Acetyl-CoA, was added and dissolved

63.5 mg of Luciferin and from this step onward solution was kept in the dark

dH_20 was added to make up to 471.11 ml

1.206 ml of 2M NaOH was added

2.561 ml of Magnesium Carbonate Hydroxide was added

made up to final volume of 482.54 ml

aliquoted in 50 ml tubes, wrapped in tin foil, and stored in -20 freezer

Defrosted before use and diluted to ½ in dH_2O.

Chemiluminescence detection solutions: ECL A and ECL B:

Solution A:

1ml of 250mM luminol (0.44g in 10ml DMSO),

0.44ml of 90mM p-Coumaric acid (0.15g in 10 ml DMSO)

10ml 1M Tris-HCl pH 8.5

-made up to 100ml with dH_2O.

Solution B:

10ml Tris HCl pH 8.5

61µl 30% H_2O_2

-made up to 100ml with dH_2O.

Solution A and B were mixed 1:1 immediately before use.

Buffers for Transduction:

Protamine sulphate:

4 µg/µl in H_2O, sterile filtered (0.22 µM filter)

- stored at 4°C

100 mM Chloroquine:

515,87 mg in 10 ml 1xPBS, sterile filtered (0.22 µM filter)

- stored at 4°C

1 x TE-Buffer (diluted 1/10 in H_2O before use):

10 mM Tris

1 mM EDTA

pH 8

121.14 mg Tris

29.23 mg EDTA (or 0.2 ml of 0.5M solution)

Dissolved in 100 ml dH_2O and sterile filtered (0.2 µm filter).

-Stored at 4°C

2.17 Statistical analysis

Experiments were performed in triplicates where indicated and represented as average ±SD of at least three independent repeat experiments, as indicated in figure legends. Statistical analysis was performed where indicated using two tailed paired t-test with * $p \leq 0.05$, ** $p \leq 0.01$, and *** $p \leq 0.001$.

2.18 Antibodies used for Immunodetection:

Antibody	Supplier (Ab clone, catalogue no.)	Species	Dilutions	Blocking buffer
Tubulin	Abcam (ab7291)	Mouse	1:3000	5% skimmed milk in PBS+tween
Beta-actin	SCBT	Mouse	1:3000	5% skimmed milk in PBS+tween
DDX3	SCBT (sc-81247)	Mouse	1:1000	5% skimmed milk in PBS+tween
DDX3	Bethyl lab (A300-474A)	Rabbit	1:3000	5% BSA in PBS+Tween
ERalpha	SCBT (HC-20)	Rabbit polyclonal	1:3000	5% BSA in PBS+Tween
ERalpha	SCBT (sc-8002)	Mouse monoclonal	1:3000 or 1:2000	5% BSA in PBS+Tween
Phospho-ERalpha S167	Cell signalling (D5W3Z) #64508	Rabbit polyclonal	1:3000	5% BSA in PBS+Tween
Myc-tag	Thermofisher (# PA5-85185)	Mouse polyclonal	1:3000	5% skimmed milk in PBS+tween
Flag-tag	SCBT (sc-7945)	Mouse polyclonal	1:3000	5% skimmed milk in PBS+tween

Antibody	Supplier (Ab clone, catalogue no.)	Species	Dilutions	Blocking buffer
Ha-tag	SCBT (sc-7392)	Mouse polyclonal	1:3000	5% skimmed milk in PBS+tween
IKKepsilon	Cell signalling (D20G4 #2905)	Rabbit	1:3000	5% BSA in PBS+Tween
CathepsinD	Cell signalling (E179 #69854)	Rabbit	1:3000	5% BSA in PBS+Tween
PS2	Cell signalling (D2Y1J #15571)	Rabbit	1:3000	5% BSA in PBS+Tween
HIF1α	Cell signalling (#3716)	Rabbit	1:3000	5% BSA in PBS+Tween
Non-phospho-active beta-catenin	Cell signalling (D13A1 #8814)	Rabbit	1:3000	5% BSA in PBS+Tween

Table 2.2 List of antibodies used for Immunodetection

Chapter 3. Results

3. DDX3X functionally and physically interacts with Estrogen Receptor-alpha

DDX3 and IKKε were both independently shown to be breast cancer oncogenes. The expression of DDX3 is upregulated in many types of cancers, and in breast cancer its expression is mainly upregulated in hypoxic conditions through a mechanism involving hypoxia inducible factor (Giuliano et al.) (Botlagunta et al., 2011).

The oncogenic effects of IKKε might be partially mediated through ligand independent activation of the Estrogen receptor alpha. IKKε was suggested to phosphorylate and activate estrogen receptor alpha at Ser167 independently of estrogen, leading to ligand independent activation of the receptor and resistance to anti-estrogen tamoxifen treatment (retracted paper) (Guo et al., 2010b).

The MU Host-Pathogen Lab previously identified a mechanism where DDX3 and IKKε collaborate in antiviral innate immune signalling to activate the transcription factor IRF3, resulting in anti-viral gene expression such as IFNβ.

The current study aimed to test the hypothesis that DDX3 and IKKε might also jointly activate ERα.

3.1. Optimisation of ERE reporter gene assays in MCF7 cells

To test the hypothesis that DDX3 and IKKε might have joint role in activating ERα, a Firefly luciferase reporter gene assay system was used. The estrogen-responsive reporter luciferase plasmid (ERE-luc) contains six consensus ERE motifs wherein, firefly luciferase expression is controlled by a promoter that contains 6xERE. When there is activation of the ERE motifs or phosphorylation of ERα, there is an increase in luciferase production. The ERE-luc plasmid was transfected into the MCF7 and T47D cells along with a control Renilla luciferase plasmid as a control for transfection efficiency. After 24 h incubation, cells were harvested with 50 µl cell lysis buffer (Promega) and the Firefly and Renilla luciferase activities were determined by measuring luminescence. Firefly luciferase reporter activity was normalized to the Renilla luciferase activity to control for transfection efficiency.

In the initial experiments the ERE activation levels were very low. Therefore, assay conditions were optimised first, by comparing the activation of the ERE reporter in complete/estrogen-replete medium to estrogen-depleted medium, as trace amounts of estrogen in fetal bovine serum (FBS) and phenol-red that mimics estrogen action inside the cells could interfere with the ERα activation in my assay system.

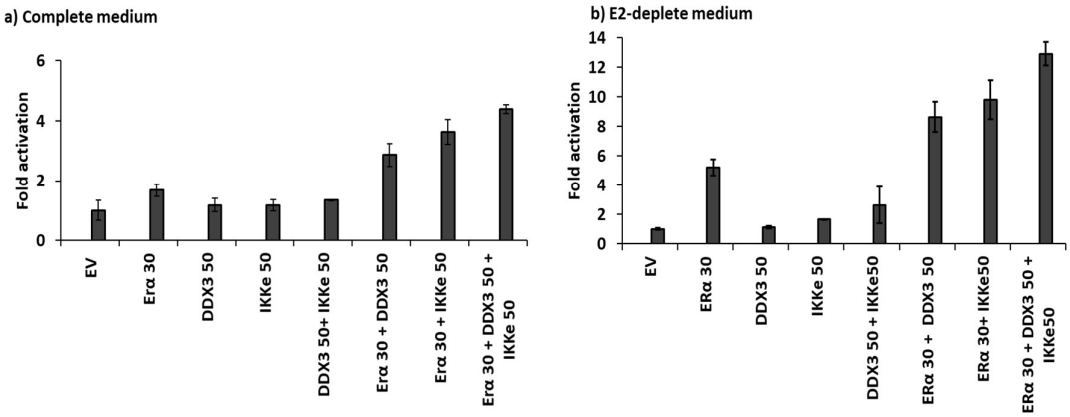

Figure 3.1: Deplete medium was optimal for measuring activation of ERE reporter construct

MCF7 cells were cultured in normal complete DMEM medium (a) and estrogen-depleted DMEM medium (b) and transfected with an ERE Firefly luciferase reporter gene construct (60ng), a Renilla control luciferase construct (20ng), and expression constructs for Empty vector- EV, DDX3, IKKε, and ERα as indicated. Firefly and Renilla luciferase activity were measured 24h post transfection. Data is normalized to Renilla luciferase levels and expressed as fold induction relative to control levels. Each experiment was performed in triplicate. Shown here is one representative experiment with error bars indicating SD.

It was found that that estrogen depleted medium was better suited for activation of ERE activity, as the basal ERE activity was lower due to the absence of estrogens and estrogen-like substances from the medium (FBS/ phenol red), therefore the effect of over-expression of different constructs was recognizable. For this reason, estrogen depleted medium was used in experiments measuring ERE activity ERE reporter assays (Figure 3.1).

3.2. DDX3 and IKKε jointly enhance ERα activity

The ERE reporter gene assay was used to understand DDX3 and IKKε's effect on ERα activity, using MCF7 cells grown in estrogen-deplete medium. In this data, transfection of ERα alone enhanced ERE activity as expected. DDX3 or IKKε co-expression individually with ERα caused an approximately 1.5-fold increase in ERα activity (Figure 3.2). However, when both proteins were co-expressed along with ERα there was an approximately 3-fold increase in ERα activity when compared to ERα alone (Figure3.2). This increase in ERα activity upon co-expression of DDX3 and IKKε with ERα suggested that they might indeed synergistically enhance ERα activity, similar to their role in IRF3 activation in innate immune signalling.

ERE reporter assays were also performed using the T47D ER+ breast cancer cell line. The ERE activation levels were low in T47D cells, which suggested they might be difficult to transfect, and it was not clear whether DDX3 and IKKε were reliably co-expressed. However, a similar trend in T47D cells was observed, showing a collaborative effect of DDX3 and IKKε in enhancing ERα activity in one experiment (data not shown).

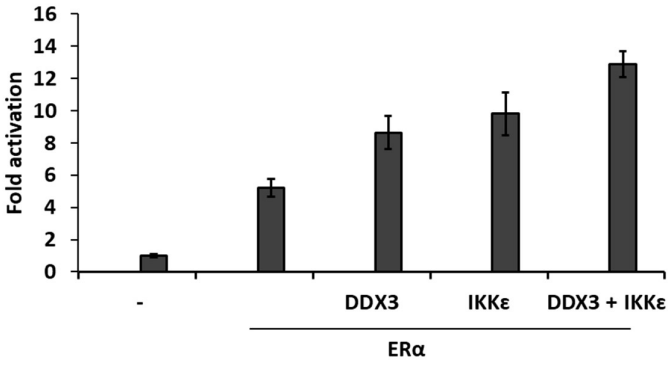

Figure 3.2: DDX3 and IKKε enhance ERα activity.

MCF7 cells were cultured in estrogen-deplete medium and transfected with an ERE firefly luciferase reporter gene construct (60ng), a Renilla luciferase control construct (20ng), and expression constructs for DDX3 (50ng), IKKε (50ng), and ERα (30ng), as indicated. Firefly and Renilla luciferase activity was measured 24h post transfection. Firefly luciferase values were normalised to Renilla luciferase values and expressed as fold induction relative to control levels. Shown is the mean fold activation of three independent experiments ± SD, performed in experimental triplicates.

As DDX3 belongs to the DEAD-box helicase family, it can remodel RNA in ATP-dependent manner, it was essential to investigate whether DDX3's ATPase activity was required for its effect on ERα activity. To test this, wild-type DDX3 was compared to the enzymatically inactive mutant DDX3-K230E in ERE reporter gene assays (Figure 3.3). K230E is a single point mutant, that bears a substitution in motif I (Walker A), this mutated residue is known to be essential for ATP binding and hydrolysis. Yedavalli et al (2004) had shown that DDX3's ATP dependent RNA helicase activity was required to function in the CRM1 RNA export pathway, essential for the export of HIV1 RNA. However, it was not required for its role as an enhancer of IFNβ promoter's activity in previous work from the lab (Schroder et al., 2008).

3.3. The enzymatic activity of DDX3 is not required for ERα activation

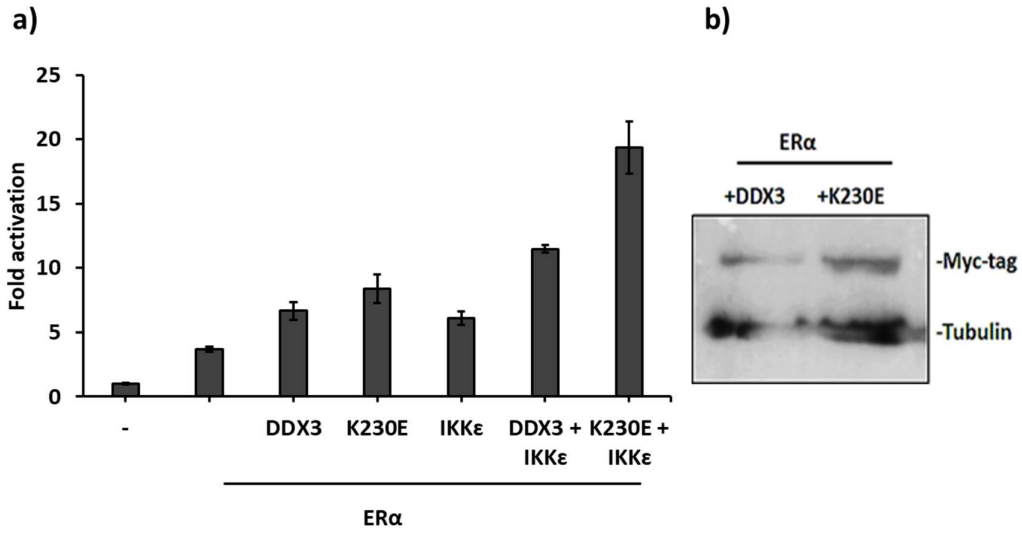

Figure 3.3: The enzymatic activity of DDX3 is not required for ERα activation

(a) MCF7 cells were cultured in estrogen-deplete medium and transfected with an ERE Firefly luciferase reporter gene construct (60ng), a Renilla control luciferase construct (20ng), and expression constructs for DDX3 (50ng), IKKε (50ng), and ERα (30ng), and DDX3 (K230E) as indicated. Firefly and Renilla luciferase activity was measured 24h post transfection. Firefly luciferase values were normalized to Renilla luciferase values and expressed as fold induction relative to control levels. Shown here is the mean of three independent experiments ± SD. (b) The expression levels of DDX3 and K230E constructs were analysed by subjecting reporter assay samples to SDS-PAGE and Western Blot analysis, followed by immunodetection using myc antibody for myc-epitope tagged DDX3 and myc-epitope tagged K230E and a loading control tubulin. Shown here is one representative experiment of two independent experiments. with an antibody for the myc epitope tag was performed on cell lysates, with tubulin levels detected as a loading control.

As seen in the previous experiment, wild-type DDX3 again enhanced ERα activity. The enzymatically inactive mutant of DDX3 K230E also enhanced ERα activity, which was further increased with co-expression of K230E, ERα and IKKε together (Figure 3.3a).

The expression levels of DDX3 wildtype and K230E were compared by performing western blot analysis on reporter assay lysates and probing for the myc-tag present on both WT and K230E DDX3. It was found that K230E expressed better than the wild type DDX3 expression construct,

which might explain the higher level of activation observed with K230E compared to WT DDX3 in the ERE reporter assay. In any case, this result demonstrates that enzymatic activity of DDX3 is not essential for inducing ERα activity.

3.4. Endogenous DDX3 mediates full ERα activity in breast cancer cell lines

Next whether endogenous DDX3 also plays a role in ERα activation was investigated. To this end, DDX3 knockdown (shDDX3) T47D and MCF7 cells and matching non-silencing control (NSC) cells to study the effects of DDX3 knockdown on estrogen-mediated ERα activation in these breast cancer cell lines were used. T47D DDX3 knockdown (shDDX3) and NSC cells were generated by stably transducing cells with either a pTRIPZ shRNA expression construct that knocks down DDX3 expression or a non-silencing control (NSC) using a lentiviral system. The pTRIPZ vector provides an inducible knockdown system, where addition of doxycycline (2µg/ml) to culture medium results in expression of shRNA that knock-down DDX3 expression or of a non-silencing-control RNA. The DDX3 knockdown was induced for three days by culturing the cells in appropriate estrogen-depleted culture medium supplemented with 2µg/ml doxycycline (DMEM for MCF7 and RPMI for T47D cells). Cells were then re-seeded in estrogen depleted medium, allowed to settle for a day, then transfected with reporter and expression plasmids for 18-24 hrs, and then stimulated with 25nM estradiol for 8 hrs as indicated in the Figure 3.4.

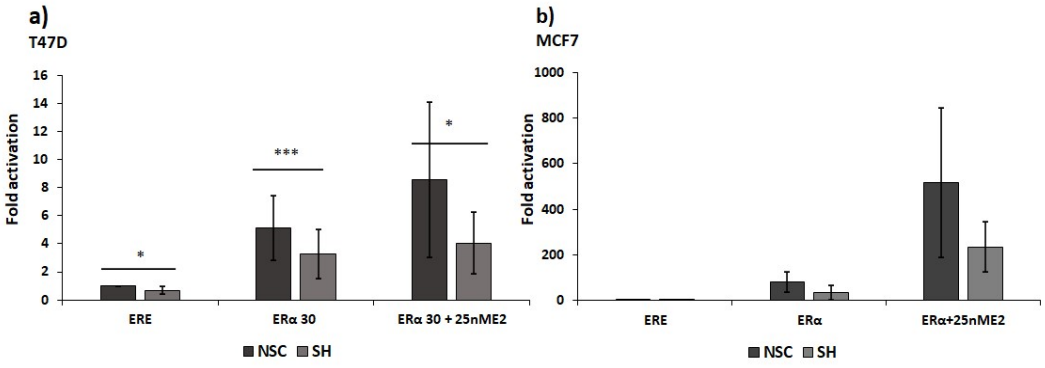

Figure 3.4: Endogenous DDX3 is required for full ERα activity in T47D and MCF7 cells

T47D (a) and MCF7 (b) cells were stably transduced with a doxycycline-inducible shRNA construct to knock-down endogenous DDX3 expression, or a matching non-silencing control (NSC) plasmid. Knockdown was induced in T47D NSC and shDDX3cells cultured in estrogen deplete medium for 3 days prior to seeding for reporter gene assays.

Next, the cells were transfected with an ERE Firefly luciferase reporter gene construct (60ng), a Renilla control luciferase construct (20ng), and expression constructs for ERα (30ng) as indicated. 24h post transfection cells were stimulated with 25nM Estradiol (25nM E2) for 8h. Luciferase activity was then measured, and data normalized to control as described above. Shown here is the mean data from five independent experiments with error bars indicating ±SD for T47D cells and two independent experiments for MCF7 cells, each performed in triplicate with error bars indicating ±SD. Statistical analysis was performed using a paired t-test (p=0.0289,0.0004, 0.0277).

In both cell lines, basal ERE activity was already reduced in DDX3 knockdown cells (shDDX3) compared to non-silencing control (NSC) cells. ERα overexpression increased ERE activity in NSC by ~1.5 fold, while there was only a marginal increase in DDX3sh cells, which indicated that endogenous DDX3 mediates ERα activity in breast cancer cell lines. Upon estrogen stimulation ERE activity was increased by ~4-5 folds in NSC cells, whereas estrogen responsiveness was mostly unchanged in DDX3 knockdown (ShDDX3) cells compared to their NSC counterparts. Overall ERE activation was much higher in MCF7 cells which transfected better, compared to lower level of ERE activation in T47D that are much more difficult to transfect.

This data suggests that DDX3 might also contribute to ligand-dependent ERα activation in breast cancer cell lines.

3.5. Hypoxia enhances DDX3 expression and ERα activity

DDX3 was previously shown to be upregulated in hypoxic conditions, through hypoxia inducible factor HIF1α (Botlagunta et al., 2011). Since from the results presented above provided the evidence that DDX3 could mediate ERα activity and estrogen responsiveness, it was next sought to answer whether increased DDX3 expression under hypoxic conditions also enhances ERα activity. Hypoxia was induced using DMOG (Dimethyloxallyl Glycine) in T47D NSC and shDDX3 cells and compared ERα activity in ERE reporter gene assay. DMOG is a synthetic analogue of α-ketoglutarate, commonly used to induce HIF signalling, as it inhibits O2 consumption in cancer cells. DMOG can mimic the effects of hypoxia by activating HIF even under normal oxygen tension.

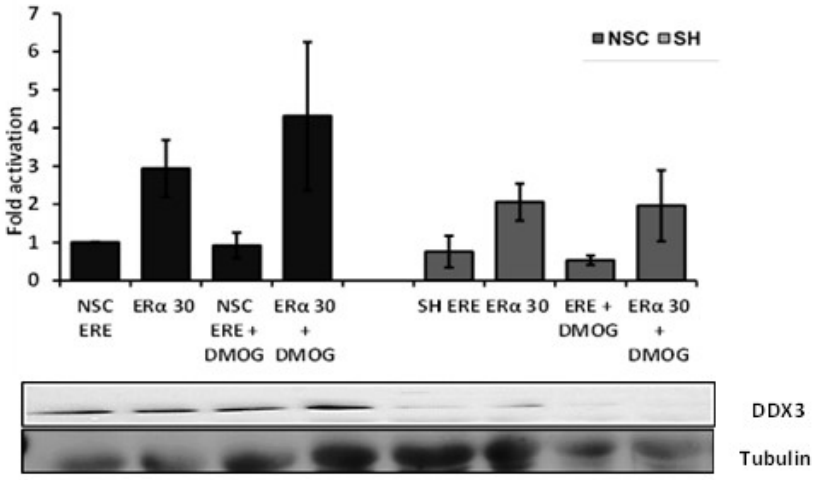

Figure 3.5: Hypoxia enhances DDX3 expression and ERα activity

DDX3 knockdown was induced in T47D NSC and shDDX3cells cultured in estrogen deplete medium for 3 days prior to seeding for reporter gene assays. Cells were transfected with an ERE Firefly luciferase reporter gene construct (60ng), a Renilla control luciferase construct (20ng), and expression constructs for ERα (30ng) as indicated. Hypoxia was induced using DMOG at (1mM) concentration. 24h post transfection cells were stimulated with 25nM Estradiol (25nM E2) for 8h. Luciferase activity was then measured, and data normalized to control as described above. Shown here is the mean data from two independent experiments (±SD) for T47D, each performed in triplicate. Western Blot analysis of reporter assay samples is shown underneath the bars in the graph.

As previously seen basal ERE activity was reduced in DDX3 knockdown shDDX3 cells compared to NSC controls for all conditions. DMOG treatment (hypoxia) indeed led to higher ERE activity when ERα was overexpressed in NSC cells, as well as slightly increased DDX3 expression (Figure 3.5). There was no increase in ERα activity with DMOG (hypoxia) in DDX3 knockdown cells (shDDX3). This might suggest that hypoxia leads to more ERα activity and that this is mediated by increased DDX3 expression.

3.6 DDX3 truncation mutants can activate ERE

For identifying regions of DDX3 required in activation of ERα, ERE activation levels mediated by full-length DDX3, and different truncation mutants expressed together with ERα was compared to ERE activation level mediated by additional over-expression of IKKε, in ERE reporter gene assays.

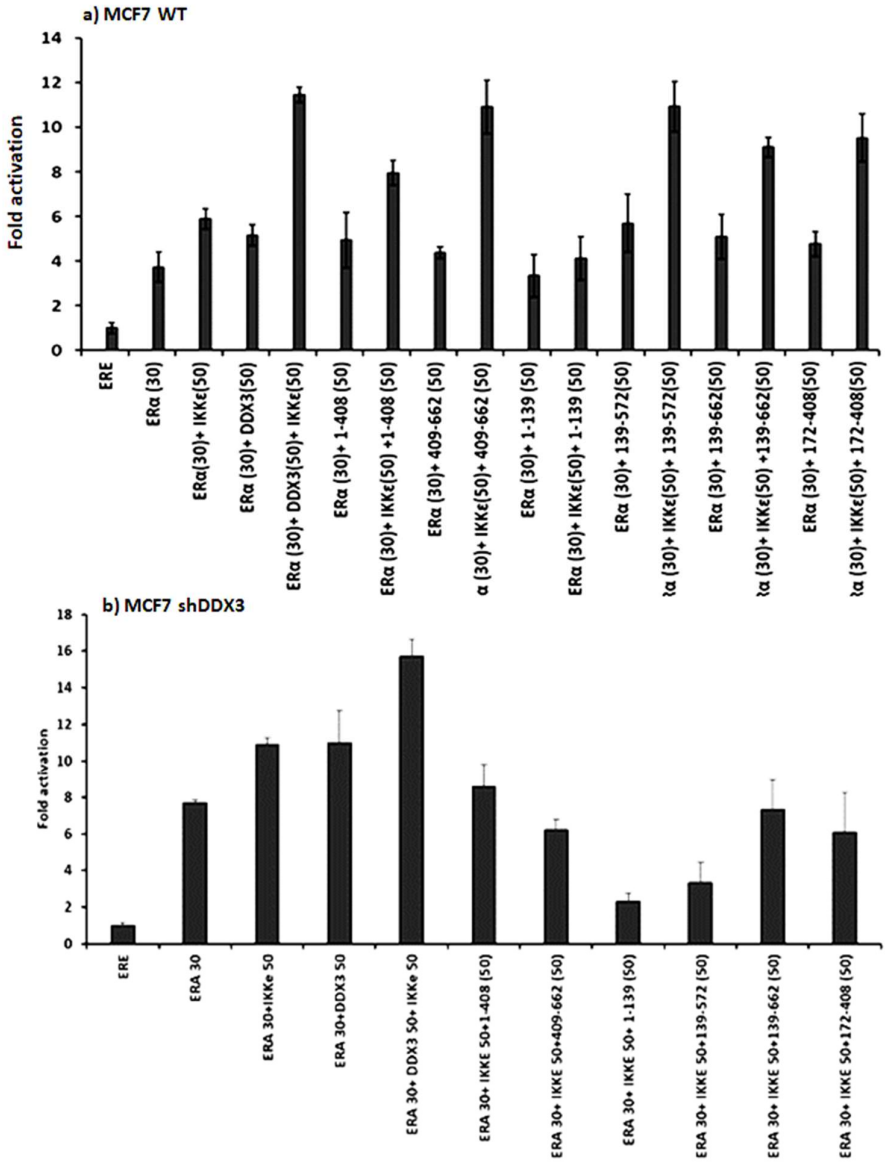

Figure 3.6: DDX3 truncation mutants can activate ERE by enhancing IKKε's effect

a) WT-MCF7 cells were cultured in estrogen-deplete medium and transfected with an ERE Firefly luciferase reporter gene construct (60ng), a Renilla control luciferase construct (20ng), and expression constructs for myc-DDX3 (50ng) and myc-tagged DDX3-truncation construct, IKKε (50ng), and ERα (30ng), as indicated. Firefly and Renilla luciferase activity was measured 24h post transfection. Data is normalized to Renilla luciferase levels and expressed as fold induction relative to control levels. Shown here is one representative experiment of two independent experiments. Each experiment was performed in triplicates.

b) MCF7 ShDDX3 cells were cultured in estrogen-deplete medium and transfected with an ERE Firefly luciferase reporter gene construct (60ng), a Renilla control luciferase construct (20), and expression constructs for myc-DDX3 (50ng) and myc-tagged DDX3-truncation construct, flag-tagged IKKε (50ng), and ERα (30ng), as indicated. Firefly and Renilla luciferase activity were measured 24h post transfection. Data is normalized to Renilla luciferase levels and expressed as fold induction relative to control levels. Shown here is one representative experiment of three independent experiments + SD. Each experiment was performed in triplicates.

In MCF7 cells, full length DDX3 activated ERE to a greater extent when co-expressed with IKKε, as previously seen DDX3 409-662 and 139-572 truncations activated ERE to a similar extent compared to full-length DDX3, followed by 172-408 and then 139-662. 1-408 mediated activation was less compared to other truncations. And 1-139 seemed to inhibit ERE-activation as it was less compared ERα + IKKε mediated ERE activation. The C-terminus of DDX3 was previously shown to dimerize with full-length DDX3 (Floor et al., 2016), so there is a possibility that the ERE activation in this assay setup might be partially mediated through dimerization with endogenous DDX3. To rule out a role for endogenous DDX3 in this setup, next ERE-reporter gene assays were performed with a similar setup in MCF7-ShDDX3 cells. DDX3 knockdown was induced in MCF7-ShDDX3 cells, and the cells were then seeded and transfected as indicated.

In MCF7 shDDX3 cells, full-length DDX3 activated ERα activity to the greatest extent. All other truncations activated to a lesser degree than ERα+ IKKε together. 1-139 inhibited the activation mediated by ERα+ IKKε the most, followed by 139-572, with 409-662, 139-662, 172- 408 being close to ERα+ IKKε mediated activation. Data from repeat experiments was not entirely clear and was variable between repeat experiments. It is also possibly that ERE activation need full-length DDX3, because different regions of DDX3 might contribute together.

3.7. DDX3 knockdown reduced expression of ERα target genes

To confirm that the effects observed in ERE reporter assays translate into altered expression of endogenous ERα target genes, mRNA expression levels of selected well-established ERα target genes in T47D and MCF7 control (NSC) and DDX3 knockdown (shDDX3) cells were compared using real-time PCR. NRIP1, PS2 and EGR3 were previously shown to be direct ERα target genes (Lin et al., 2004).

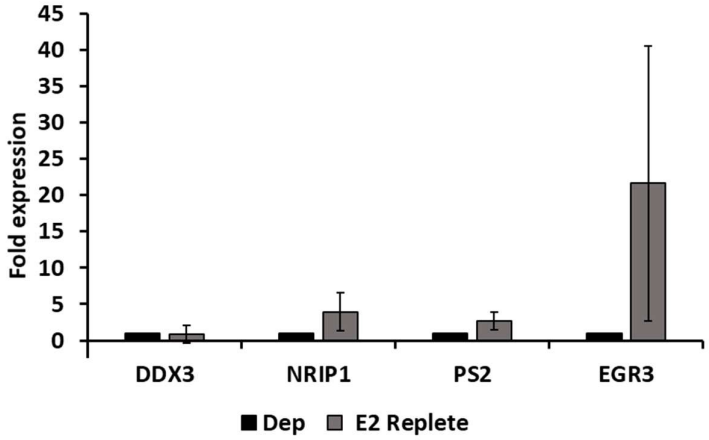

Figure 3.7: ERα target gene expression in estrogen replete medium compared to deplete medium

T47D cells were cultured in estrogen replete and estrogen deplete medium for 3 days, prior to processing for RNA isolation, followed by cDNA synthesis and RTPCR for indicated genes. Gene expression for DDX3, NRIP1, PS2 and EGR3 was quantified in T47D cells using the ΔΔCT method (target gene expression was normalized to the expression of housekeeping gene HPRT). To determine effect of estrogen depletion, the gene expression from estrogen replete medium normalized to gene expression in T47D cell from deplete medium to calculate fold change. Each experiment was performed in triplicates. Shown here is the average of four independent experiments. Maximum fold change was seen for EGR3, which was affected by estrogen depletion the most. (Statistical analysis was done using paired t-test. The results were not significant However EGR3 expression was reduced by estrogen depletion in each experiment).

To confirm that expression of these genes is indeed driven by estrogen, mRNA expression levels of NRIP1, PS2 and EGR3 in T47D cells cultured in complete medium was compared to the expression levels in estrogen-deplete medium. In Figure 3.7, mRNA expression levels of these

genes in complete medium were normalized to their expression in estrogen-deplete medium. PS2 expression was 3-fold, NRIP1expression was 4-fold and EGR3 expression was approximately 4-5-fold higher in complete (estrogen-containing) medium when compared to estrogen-deplete medium. This data confirms that all three genes are responsive to estrogen in this system albeit to varying degrees, with EGR3 expression showing the strongest dependency on estrogen. However, it was difficult to achieve similar levels of estrogen depletion for repeat experiments which was reflected in EGR mRNA expression level (hence the high standard deviation). Nonetheless EGR3 was most strongly reduced by estrogen depletion.

The mRNA expression levels of these ERα target genes were compared between T47D DDX3 knockdown (shDDX3) and control (NSC) cells (Figure 3.8).

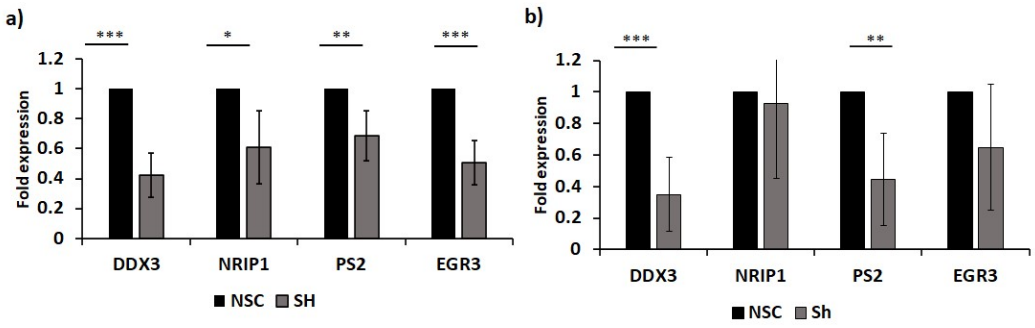

Figure 3.8: ERα target gene expression in Estrogen replete and estrogen deplete medium

DDX3 knockdown was induced in T47D ShDDX3 and NSC cells by the addition of puromycin (2µg/ml) in estrogen replete (Figure a) and estrogen deplete medium (figure b) for 3 days, prior to processing for RNA isolation, followed by cDNA synthesis and RTPCR for indicated genes. Gene expression for DDX3, NRIP1, PS2 and EGR3 was quantified in T47D cells for both the conditions using ΔΔCT method with expression of target genes normalised to expression of the housekeeping gene HPRT (ΔCT). Gene expression in ShDDX3 cells was normalized to gene expression in NSC cells, to calculate fold expression (ΔΔCT). Each experiment was performed in triplicates, shown here is the average of 6 independent experiments with $\pm$SD. Statistical analysis was performed using paired t-test with * p≤0.05, **p≤0.01, and *** p≤0.001. (Replete medium, p-values: 0.000, 0.010, 0.005,0.000) (Deplete medium, p-values: 0.001, 0.73, 0.012, 0.082)

NRIP1 and PS2 mRNA expression levels were reduced by approximately 20% in both complete and deplete medium, whereas EGR3 expression in complete medium was reduced by 60% (Figure 3.8a). In estrogen-deplete medium (figure 3.8b), EGR3 expression levels were already barely detectable in NSC cells, hence no further reduction could be observed for DDX3 knockdown cells.

Next, western blot analysis was carried out on T47D NSC and shDDX3 cell lysates to confirm that protein expression levels of ERα-dependent genes were also reduced (Figure 3.9).

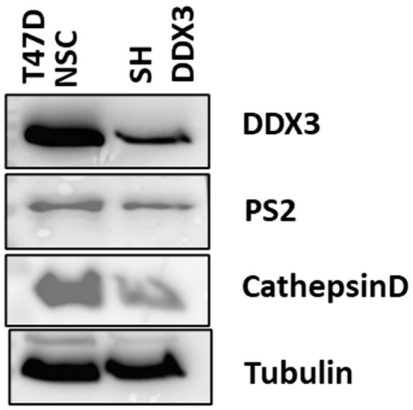

Figure 3.9: DDX3 knockdown reduced protein expression levels of ERα target genes in T47D shDDX3 cells

DDX3 knockdown was induced in T47D NSC and ShDDX3 cells by addition of doxycycline (2μg/ml) for three days. Cells were harvested and samples were prepared for SDS-PAGE and western blot analysis. (Shown here is one representative experiment of two independent experiments).

As expected, PS2 protein expression was reduced in DDX3 knockdown (shRNA) compared to control (NSC) cells. Cathepsin D is also transcriptionally regulated by ERα, and its protein expression was also reduced by DDX3 knockdown in T47D cells compared to control cells. This data further confirms that endogenous DDX3 plays a role in regulating ERα target gene expression.

The mRNA expression levels of ERα target genes were also compared between MCF7 NSC and ShDDX3 cells, as most of the other experiments in this study were performed in MCF7 cells.

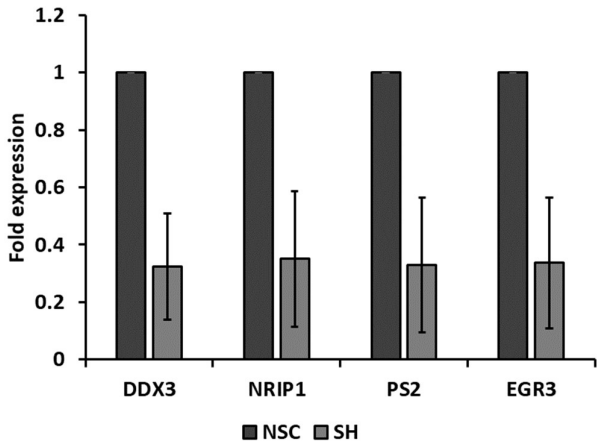

Figure 3.10: ERα target gene expression in MCF7 NSC and ShDDX3 cells

DDX3 knockdown was induced in MCF7 ShDDX3 and NSC cells by the addition of puromycin (2μg/ml) in estrogen replete medium (figure b) for 3 days, prior to processing for RNA isolation, followed by cDNA synthesis and RTPCR for indicated genes. Gene expression for DDX3, NRIP1, PS2 and EGR3 was quantified in MCF7 cells for both the conditions using ΔΔCT method with expression of target genes normalised to expression of the housekeeping gene HPRT (ΔCT). Gene expression in ShDDX3 cells was normalized to gene expression in NSC cells, to calculate fold expression (ΔΔCT). Each experiment was performed in triplicates, shown here is the average of 4 independent experiments. Statistical analysis was performed using paired t-test with * p≤0.05, **p≤0.01, and *** p≤0.001. (p-value: 0.024, 0.041, 0.038, 0.037).

ERα target gene expression was significantly reduced in MCF7 ShDDX3 cells compared to NSC cells, by approximately 2.5-fold. As MCF7 cells were less responsive to estrogen stimulation, ERα target gene expression was not measured in estrogen deplete medium.

T47D and MCF7, NSC and ShDDX3 samples were also analysed to understand the effect of DDX3 knockdown on expression levels of these other downstream target genes (GREB1, ABCA3, Cyclin D1, Myc) in T47D cells also.

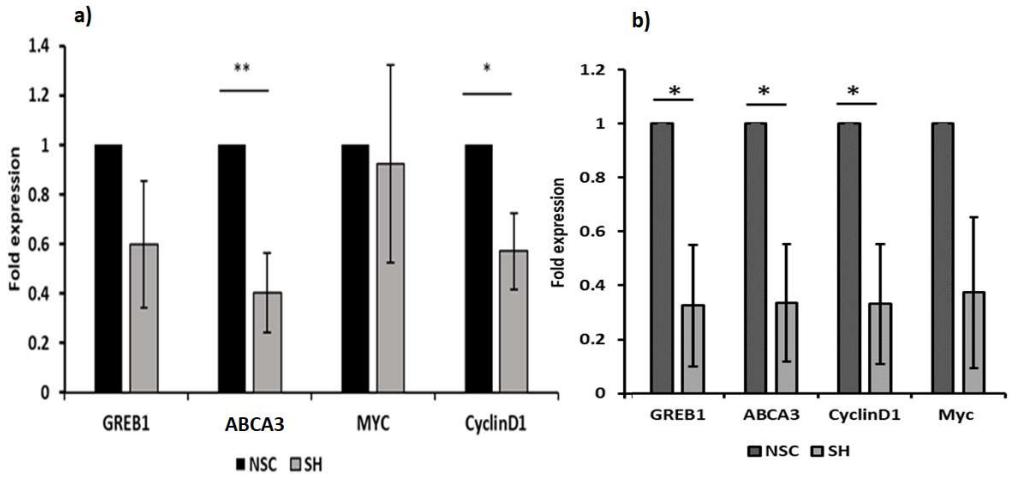

Figure 3.11: Additional downstream target genes of ERα were also reduced in T47D and MCF7 DDX3 knockdown cells

DDX3 knockdown was induced in T47D (Figure 3.11a) MCF7 (Figure 3.11b) ShDDX3 and NSC cells by the addition of puromycin (2µg/ml) in estrogen replete medium for 3 days, prior to processing for RNA isolation, followed by cDNA synthesis and RTPCR for indicated genes. Gene expression for additional ERα target genes, GREB1, ABCA3, Cyclin D1 and Myc was quantified in T47D and MCF7 cells using ΔΔCT method with expression of target genes normalised to expression of the housekeeping gene HPRT (ΔCT). Gene expression in ShDDX3 cells was normalized to gene expression in NSC cells, to calculate fold expression (ΔΔCT). Each experiment was performed in triplicates, shown here is the average of 4 independent experiments for T47D cells and 3 independent experiments for MCF7 cells. Statistical analysis was performed using paired t-test with * p≤0.05, **p≤0.01, and *** p≤0.001. (T47D, p-values: 0.072662, 0.002492, 0.557351, 0.024243) (MCF7 p-values: 0.035, 0.034, 0.034, 0.06).

GREB1, ABCA3 and CyclinD1 expression were also reduced by DDX3 knockdown in T47D cells. However, expression of Myc was not reduced by DDX3 knockdown, as opposed to in MCF7 cells where DDX3 knockdown reduced Myc expression by ~50%.

3.8. DDX3 regulates ERα phosphorylation

As DDX3 knockdown resulted in reduced expression of ERα target genes, it was essential to test whether DDX3 regulated ERα activity by supporting relevant phosphorylation events of ERα. To understand the role of DDX3 in activation of ERα, changes in S167 phosphorylation were analysed by performing western blot analysis using the samples expressing DDX3 with/ without ERα, which might suggest that DDX3 can indeed enhance S167 phosphorylation mediated by IKKε (or other kinases).

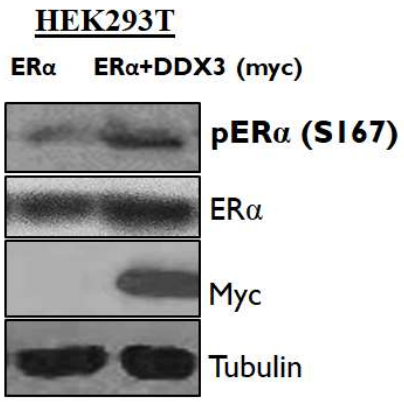

Figure 3.12: DDX3 over-expression increased phosphorylation of ERα at S167

HEK293T cells were cultured and seeded at an equal cell density and transfected with expression constructs for ERα and myc-tagged-DDX3 using the calcium-phosphate transfection method. Cells were incubated for 24 hours after transfection after which cells were harvested and cell lysates were subjected to SDS-PAGE and western blot analysis to analyse phospho- ERα (S167), total ERα, DDX3 and tubulin levels. Shown here is a representative experiment of 3 independent experiments.

Western blot analysis of these samples showed that DDX3 over-expression increased the phosphorylation of ERα at S167, whereas ERα levels were comparable for cell lysates without and with DDX3 overexpression. When DDX3 was co-expressed with ERα a clear increase in S167 phosphorylation was observed, suggesting that DDX3 can indeed enhance S167 phosphorylation of ERα (Figure 3.12).

IKKε was independently shown to enhance ERα phosphorylation at S167 as mentioned in the introduction, to facilitate activation of ERα in an estrogen-independent manner (Ref. retracted) (Guo et al., 2010b). As to this end, DDX3 also phosphorylated ERα at S167, it was hypothesized that DDX3 might support ERα activation by facilitating its phosphorylation by IKKε. First it was tested and confirmed that IKKε can indeed mediate strong phosphorylation of ERα at S167 when both proteins are co-expressed in HEK293T cells.

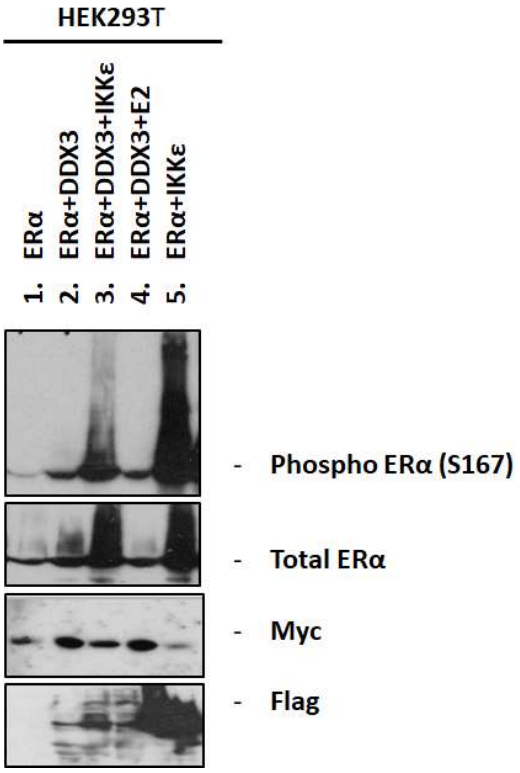

Figure 3.13: IKKε over-expression enhanced phosphorylation of ERα at S167

HEK293T cells were cultured and seeded at an equal cell density and transfected with expression constructs for ERα, myc-tagged-DDX3, and/or flag-tagged IKKε as indicated using the calcium-phosphate transfection method. Cells were incubated for 24 hours after transfection after which they were stimulated with 25nM estrogen for 8 hours where indicated. Cells were then harvested, and cell lysates were subjected to SDS_PAGE and western blot analysis to analyse phospho- ERα (S167), total ERα, DDX3, and IKKε levels. Shown here is a representative experiment of 3 independent experiments.

As previously observed, DDX3 overexpression enhanced phosphorylation of ERα at S167 (Figure 3.13, top panel, lane 2), estrogen stimulation did not have an additional effect on ERα phosphorylation in the presence of exogenously expressed DDX3 (Figure 3.13, top panel, lane 4). DDX3-mediated phosphorylation was further increased by co-expression of IKKε (Figure 3.13, top panel, lane-3). IKKε over-expression alone with ERα greatly enhanced ERα phosphorylation. Indeed, when ERα, IKKε and DDX3 were jointly expressed phosphorylation of ERα was enhanced compared to DDX3+ERα, but actually decreased compared IKKε + ERα. This was unexpected, as it was initially hypothesized that DDX3 would enhance IKKε -mediated phosphorylation of ERα.

To try and resolve this issue, IKKε was over-expressed at different DNA concentrations with ERα and ERα+DDX3 in HEK293T cells to better demonstrate a potential supporting effect of DDX3 on IKKε-mediated phosphorylation of ERα. To test this, western blot analysis was performed on HEK293T cell lysates expressing exogenous ERα, DDX3 and different amounts of IKKε (100ng and 400ng of the relevant expression vector).

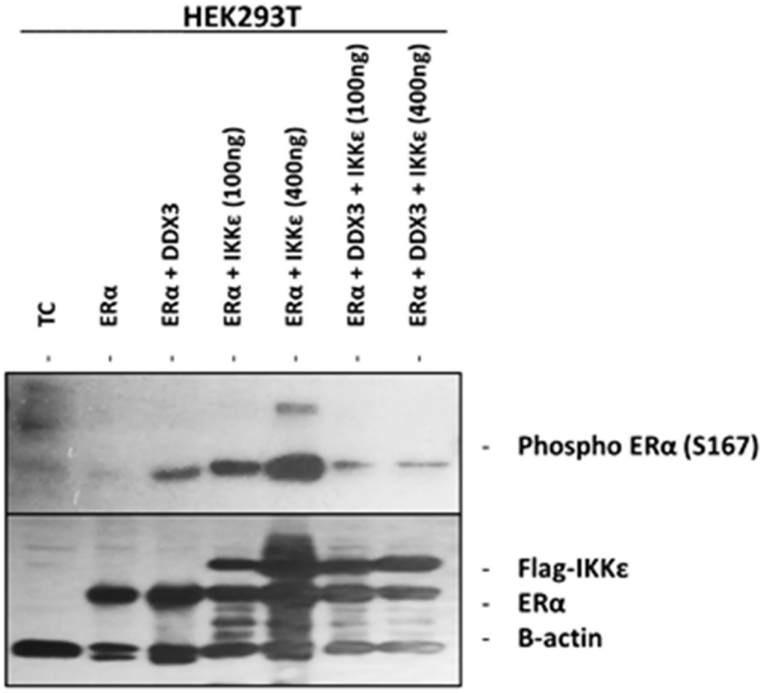

Figure 3.14: IKKε expression had a dose-dependent effect on phosphorylation of ERα

HEK293Tcells were cultured and seeded at an equal cell density and transfected with expression constructs for ERα, myc-tagged-DDX3 and/or flag-tagged IKKε as indicated using the calcium-phosphate transfection method. 24 hours later cells were harvested, and cell lysates were subjected to SDS-PAGE and western blot analysis to analyse phospho- ERα (S167), total ERα, DDX3, and IKKε levels. Shown here is a representative experiment of 3 independent experiments.

This analysis showed again that DDX3 overexpression enhanced phospho-ERα (S167) levels. IKKε strongly phospho-ERα levels (S167) and showed a dose dependent effect on phosphorylation of ERα, as seen when comparing the levels of phosphorylation achieved with a low (100ng) and high (400ng) amount of IKKε expression vector transfected. However, co-expression of DDX3 still resulted in reduced rather than enhanced ERα phosphorylation levels, even at the lower level of IKKε when compared to cells transfected with IKKε plasmid alone.

This was unexpected, because the hypothesis was that DDX3 would enhance IKKε -mediated phosphorylation of ERα and because we saw positive effects of DDX3 on basal ERα

phosphorylation levels in Figures 3.12 and 3.13. The reduction in phosphorylation of ERα when all three proteins were expressed together compared to ERα and IKKε alone, could be because of a possible inhibition of protein interaction complexes by over expression of DDX3.

This led to further investigating whether DDX3 knockdown would result in reduction of IKKε mediated phosphorylation of ERα. For this HEK293T DDX3 knockdown Sh cells were used and along with their non-silencing control NSC cells, in ERα and IKKε overexpression system as described above.

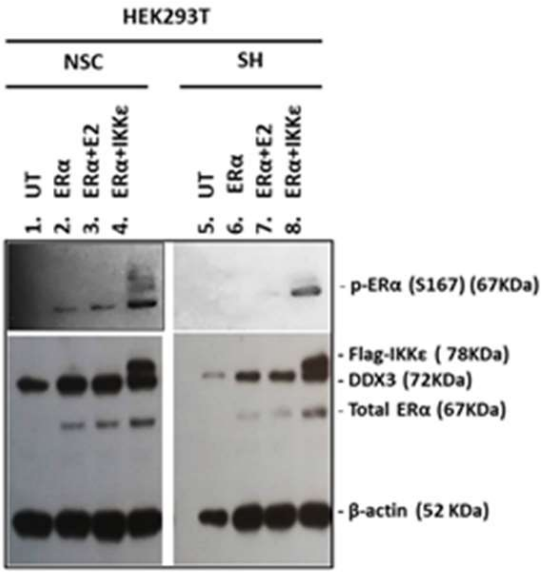

Figure 3.15: IKKε mediated phosphorylation of ERα was reduced by DDX3 knockdown

DDX3 knockdown was induced in HEK293T ShDDX3 and their non-silencing control NSC cells by using doxycycline (2μg/ml) for 3 days. Cells were then transfected with expression constructs for ERα, and/or flag-tagged-IKKε as indicated. Cells were stimulated with 25nM E2 8h before harvesting, as indicated. Cells were harvested and subjected to SDS-PAGE and Western Blot analysis with the indicated antibodies. Shown here is one representative experiment of 3 independent experiments.

DDX3 knockdown resulted in reduction of IKKε mediated phosphorylation of ERα in ShDDX3 cells compared to control NSC cells (figure 3.15). Smearing of phosphor-ERα band was seen for NSC cells overexpressing ERα and IKK which was not observed in DDX3 knockdown ShDDX3 cells (lane 4 and 8) total ERα levels were comparable between NSC and DDX3 knockdown ShDDX3 cells. NSC and ShDDX3 cells were also stimulated with E2 to test effect DDX3 knockdown on ligand-dependent phosphorylation of ERα. DDX3 knockdown resulted in reduced phosphorylation of ERα induced by E2 treatment. In summary, this data supports the evidence that endogenous DDX3 might play a role in IKKε mediated phosphorylation of ERα phosphorylation at S167.

3.9. DDX3 knockdown reduced intrinsic phosphorylation of ERα in T47D and MCF7 cells

Next, the effect of DDX3 knockdown on intrinsic phosphorylation of ERα at Ser167 were analysed by western blot analysis on MCF7 and T47D, NSC and Sh DDX3 cells. DDX3 knockdown clearly reduced the levels of phosphorylated ERα (pERα S167) in T47D and MCF7 cells, whereas total ERα levels remained unchanged (Figure 3.16). This suggests that DDX3 at least partially mediates ERα activity by supporting its phosphorylation at Ser167.

a) T47D NSC and ShDDX3 cells

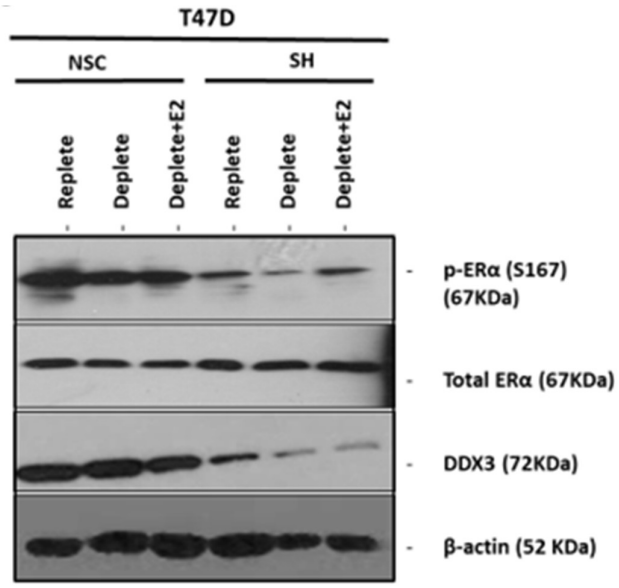

b) MCF7 NSC and ShDDX3 cells

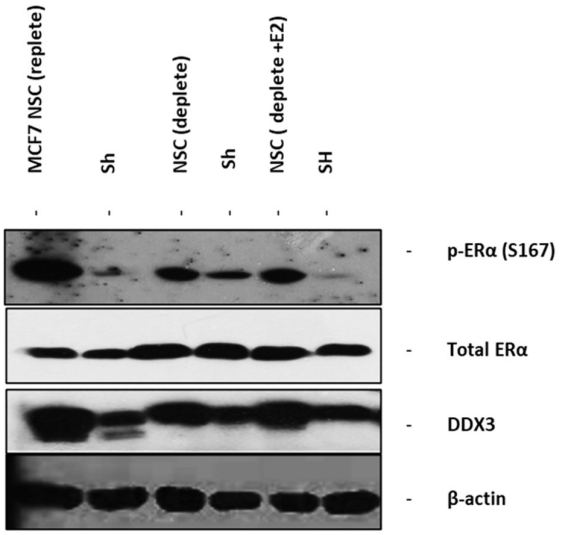

Figure 3.16:DDX3 knockdown reduced intrinsic phosphorylation of ERα

DDX3 knockdown was induced in T47D and MCF7 breast cancer cells using doxycycline (2µg/ml for 3 days). The cell lysate was subjected to SDS-PAGE and western blot analysis with indicated antibodies (shown here is a representative experiment of 3 independent experiments for replete medium conditions and one experiment from deplete and deplete+E2).

DDX3 knockdown clearly reduced the levels of phosphorylated ERα (pERα S167) in both T47D and MCF7 cells grown in different medium conditions (complete, estrogen-deplete, and estrogen-deplete with reconstituted E2), whereas total ERα levels remained unchanged (Figure 3.16). As shown in Figure 3.16, DDX3X knockdown reduced ERα phosphorylation in T47D and MCF7 cells in all three conditions. Based on this data, it is conceivable that DDX3X at least partially mediates ERα activity by supporting its phosphorylation at Ser167.

3.10. DDX3 physically interacts with ERα

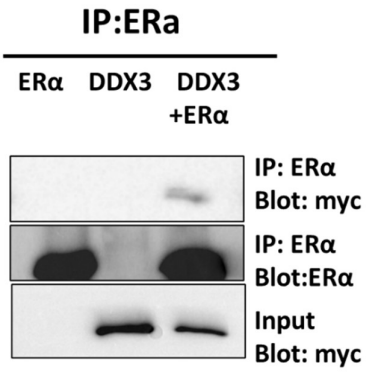

Figure 3.17: DDX3 co-immunoprecipitates with ERα

HEK293T cells were transfected with expression constructs for myc-DDX3 and ERα. Cell lysates were subjected to immunoprecipitation with an anti-ERα antibody coupled with Protein G Sepharose beads, followed by SDS-PAGE and WB analysis with indicated antibodies (shown here is a representative experiment of 3 independent experiments).

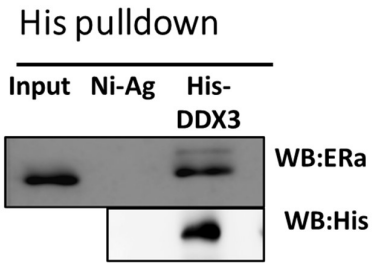

Figure 3.18: DDX3 directly interacts with ERα

Nickel-agarose (Ni-Ag) beads were coupled with purified recombinant full-length His-DDX3. The beads were then incubated with T47D whole cell lysate. Interacting proteins were subjected to SDS-PAGE and WB analysis with indicated antibodies (shown is a representative experiment of 3 independent experiments)

Further, to investigate whether DDX3 can interact physically with ERα to regulate its activity, ERα and myc-tagged DDX3 were overexpressed in HEK293T cells. ERα was immunoprecipitated, followed by detection of ERα and co-immunoprecipitated myc-DDX3 by Western Blot analysis.

Importantly, DDX3 was not pulled down in cells that were not transfected with ERα, confirming the specificity of the interaction band. This interaction was further validated/ confirmed using His-pulldown assays with recombinant His-tagged DDX3 expressed in and purified from *E.coli* (BL21). ERα from MCF7 cell lysates was pulled down with His-tagged DDX3 coupled to Nickel Agarose beads but did not bind to empty Nickel Agarose beads that were used as a control.

This pulldown also showed a higher molecular weight band for His-DDX3, which possibly can be a phosphorylated form of ERα suggesting that DDX3 can also interact with phospho- ERα. This might suggest and support DDX3's role as an adapter molecule to facilitate phosphorylation and activation of ERα (through IKKε). When the same blots were probed for Phospho-ERα 167 or IKKε, no bands were detected for these proteins. This could possibly be due to a transient interaction commonly mediating phosphorylation events.

3.11. DDX3 interacts physically with ERα at endogenous level

By performing co-immunoprecipitations on MCF7 and T47D cell lysates, endogenous DDX3 and endogenous ERα interaction was also tested at endogenous level in relevant breast cancer cell lines.

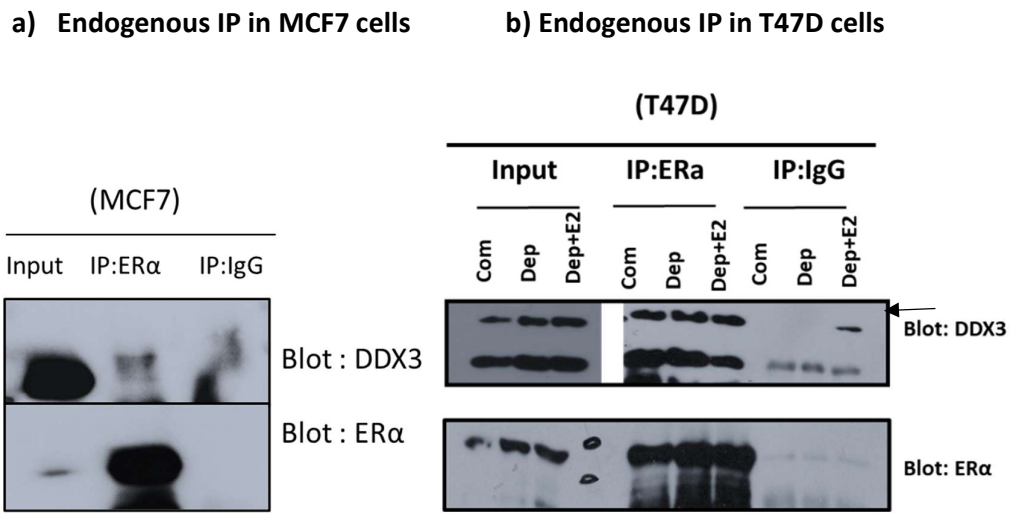

Figure 3.19: DDX3 interacts physically with ERα at endogenous level

MCF7 cells were cultured in replete medium and T47D cells were cultured in normal complete/ replete medium (com), estrogen deplete medium, and estrogen deplete + estrogen stimulated for 8 hours (dep+E2). Protein G Sepharose beads coupled with ERα antibody were used to immunoprecipitate DDX3 from the cell lysates, which was followed by SDS-PAGE and WB analysis with the indicated antibodies (shown here is one representative experiment of 3 independent experiments). The input blot for DDX3 is the lower exposure image of the same blot (top-left panel).

The DDX3 and ERα interaction was also detected at an endogenous level. Specifically, immunoprecipitations were carried out using ERα antibody and an isotype control antibody for MCF7 and T47D cells. In both MCF7 and T47D cells DDX3 and ERα interacted at endogenous levels. In MCF7 cells an interaction band was seen and the absence of band in IgG isotype control indicated the specificity of the interaction (Figure 3.19a).

As T47D cells were more responsive to estrogen, in these cells it was important to evaluate whether estrogen has any effect on the interaction. To answer this, immunoprecipitations were performed with T47D cells were cultured in estrogen depleted, estrogen stimulated or normal replete medium. Endogenous DDX3 interacted with endogenous ERα in all 3 conditions. The interaction might be stronger in complete medium, because even though the interaction bands (IP: ERα blot: DDX3 band) were similar intensity across all 3 conditions, the input band for DDX3 in complete medium was weaker, indicating less DDX3 in this lysate which gave a strong interaction band for ERα. This may suggest that the DDX3 and ERα interaction was potentially stronger in the complete/ replete medium. The absence of bands in IgG isotype control lanes shows specificity of the interaction (except for a weaker non-specific band in the Deplete+E2 stimulated sample in the last lane). Nonetheless, the results indicate that DDX3 interacts strongly with ERα at endogenous level.

3.12. Mapping the regions of DDX3 involved in ERα interaction:

Next, the regions of DDX3 involved in the interaction were explored. To do this, a series of DDX3 truncation mutants were used to map the interaction between different sites of DDX3 and ERα. DDX3 truncation mutants used in this mapping consisted of full length DDX3 (1-662 amino acids), DDX3 (1-408), and DDX3 (409-662). For the two truncated halves of DDX3, the protein was split at the flexible linker region that connects the two RecA-like domains.

Pulldown experiments were carried out with recombinant His-tagged DDX3 and two truncated versions of DDX3 (1-408, 409-662) with T47D cell lysate cultured in normal and estrogen deplete medium (to again evaluate effects of estrogen on the interaction).

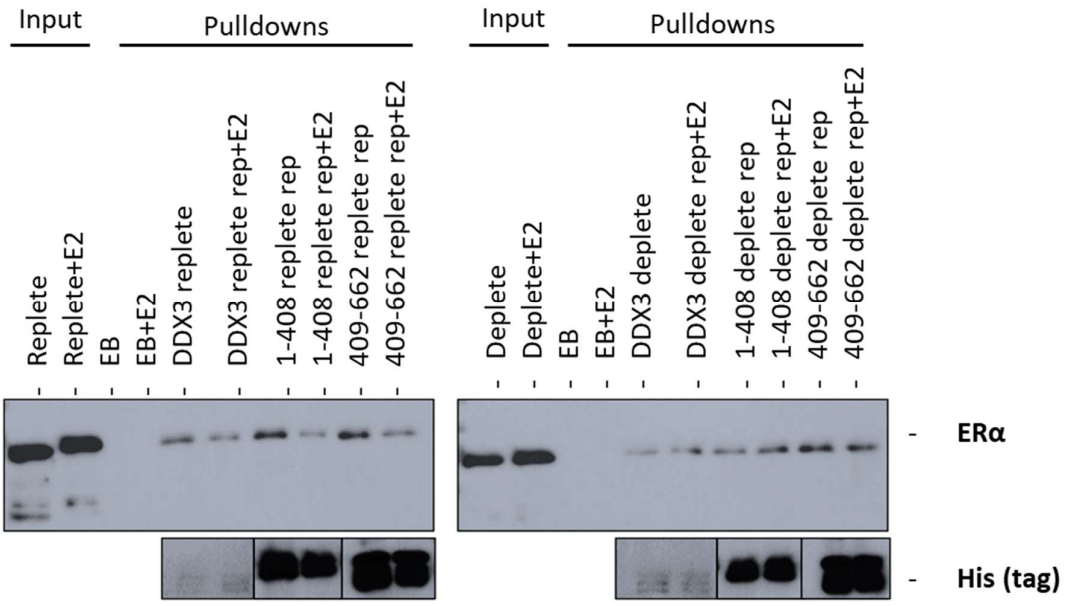

Figure 3.20: DDX3 and truncations interact physically with ERα in replete, deplete and estrogen treated conditions

T47D cells were cultured in normal complete/ replete medium (com), estrogen deplete medium and estrogen deplete + estrogen stimulated for 8 hours (dep+E2). His-tagged recombinant DDX3 and truncations were purified, and pulldown was setup with the cell lysate as indicated, this was followed by SDS-PAGE and WB analysis with the indicated antibodies (shown here is one representative experiment of 3 independent experiments).

The cell lysates from cells cultured in complete medium and cells cultured in complete medium with estrogen stimulation showed comparable levels of ERα (lane 1 and 2 top panel). Estrogen treated lysate gave rise to a higher band compared to untreated lysate, indicating potentially phosphorylated ERα. In deplete and deplete with estrogen treated cell lysates the ERα level was also comparable. However, E2 treated lysate did not show a similar shift in the band.

The results showed that, the full-length DDX3 and both halves of the protein (1-408 and 409-662) interacted with ERα in complete and complete+E2 treated, as well as deplete and deplete+E2 treated conditions (Figure 3.20 left panel and right panel). There was no effect of estrogen stimulation on the DDX3 and ERα interaction. They all could bind to ERα in estrogen treated, untreated (normal culture) and estrogen deprived conditions. Furthermore, truncations were expressed at a much higher level than the full-length DDX3, as seen in the His-blot (Figure 3.20 lower panel) that shows very low DDX3 expression compared to truncations. Despite of less recombinant DDX3 available for interacting with ERα, the interaction band for ERα was comparable between full-length DDX3 and both truncated parts of DDX3. This suggests that full-length DDX3 might actually interact much more strongly with ERα, compared to the truncations. In summary, this data shows that DDX3 physically interacts with ERα, likely independent of estrogen binding. It is possible that the interaction is mediated by multiple interaction sites that involve both the N-and C-terminal domains of DDX3.

3.13. DDX3 knockdown reduces proliferation of T47D and MCF7 cells

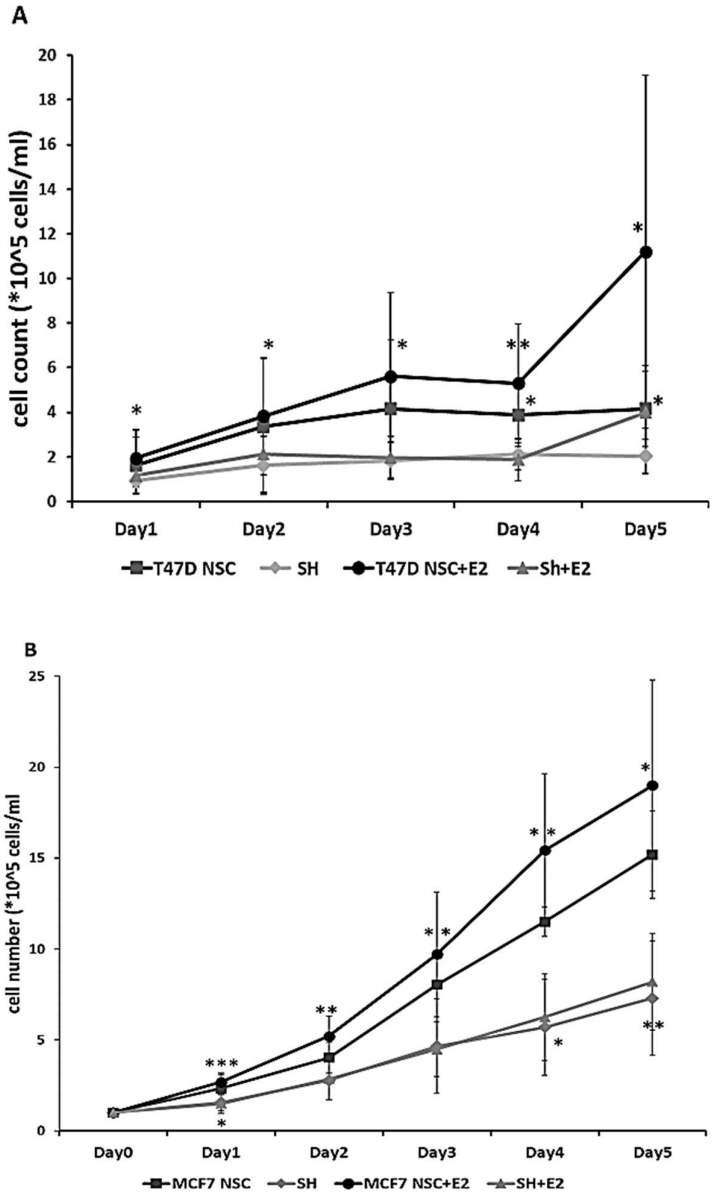

Figure 3.21: DDX3 knockdown significantly reduced cell proliferation

DDX3 knockdown was induced in T47D and MCF7 NSC and DDX3 knockdown ShDDX3 cells using 2µg/ml puromycin. Cells were seeded in indicated culture media in duplicates and manually counted for 5 consecutive days after trypsinization. a) T47D (NSC, ShDDX3 cells) cultured in replete medium, b) T47D (NSC, ShDDX3 cells) cultured in replete+E2 medium, c) MCF7 (NSC, ShDDX3 cells) cultured in replete medium, MCF7 (NSC, ShDDX3 cells) cultured in replete+E2 medium. Shown here is the average of 5 independent repeats. Statistical analysis was performed using paired t-test, with * $p \leq 0.05$, ** $p \leq 0.01$, and *** $p \leq 0.001$.

The effect of DDX3 knockdown on the proliferation of T47D and MCF7 cells was analysed by performing cell proliferation. DDX3 knockdown significantly reduced cell proliferation, both in the presence and absence of estrogen in both T47D and MCF7 cells (Figure 3.21). Cell proliferation was assessed by carrying out manual cell counts for five consecutive days in T47D NSC and DDX3 knockdown (ShDDX3) cells, in the presence and absence of estrogen (Figure 3.21a).

As expected, estrogen clearly enhanced NSC cells proliferation. DDX3 knockdown (shDDX3) cells proliferated 2-3-fold less than control (NSC) cells in the presence and absence of estrogen. Cell proliferation was significantly reduced for DDX3 knockdown (shDDX3) cells in comparison to NSC cells by day 4 and day 5 for T47D cells in estrogen untreated conditions (Figure 3.21a). Estrogen treated cells proliferated much faster and the effect of DDX3 knockdown on cell proliferation was more pronounced and compared to NSC cells, the cell proliferation was significantly reduced for estrogen treated DDX3 knockdown (shDDX3) cells from day 1 for both T47D and MCF7 cells.

Similar experiments were also performed for MCF7 cells, where DDX3 knockdown also significantly reduced cell proliferation in replete and replete + estrogen treated medium by 2-3-fold. MCF7 cells were less responsive to estrogen, however cell proliferation was significantly reduced for both estrogen treated and untreated cells (Figure 3.21b).

3.14. DDX3 knockdown reduced colony forming ability in T47D:

Cancer cells have the capability for a single cell to grow into a large colony through clonal expansion. The clonogenic assay is an in vitro quantitative technique that is employed to examine whether cancer stem cells can survive and generate colony growth in an anchorage-independent culture model. The 0.05% crystal violet solution is used in this assay to visualize the generated colonies. This method demonstrates that cancer cells can survive and generate colony growth in an anchorage-independent manner and fail to demonstrate contact inhibition.

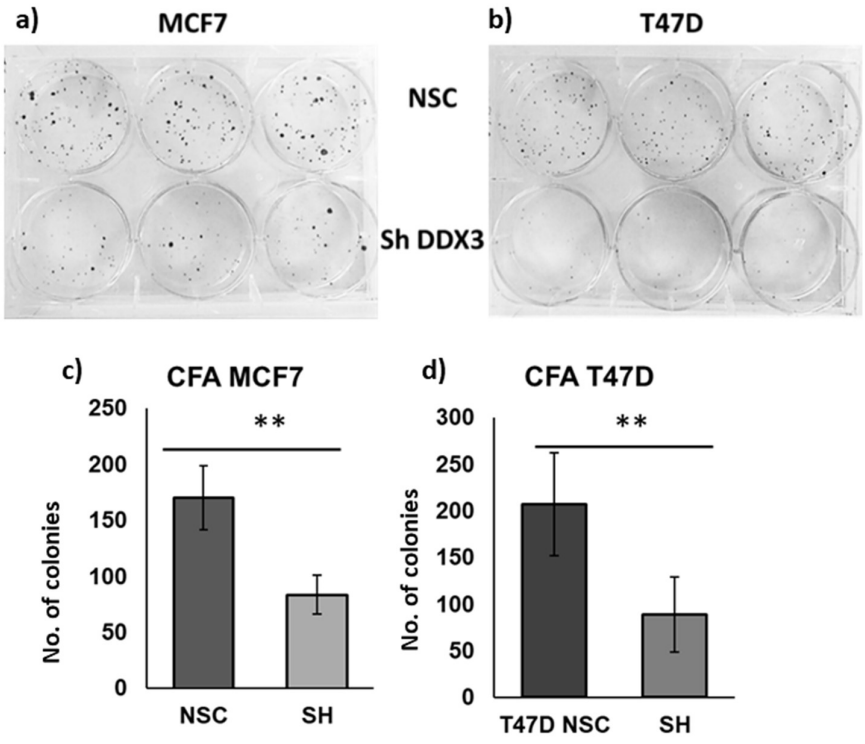

Figure 3.22: DDX3 knockdown reduced colony forming ability of breast cancer cells

DDX3 knockdown was induced in MCF7 and T47D cells using Doxycycline for 3 days, cells were then seeded in 6 well-plate and incubated for 15 days, with media replaced every third day. At the end of incubation, colonies were fixed using methanol and stained with 0.05%crystal violet. Excess stain was washed using tap water. Colonies were counted manually. The image shown here is from one experiment and the graph shows average of 6 independent experiments. Statistical analysis was performed using paired t-test. (p values: for MCF7 0.002, for T47D 0.004)

The effect of DDX3 knockdown on the clonogenic potential of breast cancer cells were studied using colony forming assays. DDX3 knockdown was induced in MCF7 and T47D cells and plated them at a low density in 6wp. The formation of individual colonies was observed. Colonies were fixed and stained with crystal violet after 14 days. DDX3 knockdown reduced the colony-forming ability of MCF7 (Figure 3.22a) and T47D (Figure 3.22b) cells by approximately 70%, further confirming a role for DDX3 in breast cancer cell proliferation and colony-forming potential. MCF7 cells generated larger colonies and showed tendency to aggregate together, whereas T47D cells generated smaller colonies. Figure 3.22c and d show the statistically significant reduction in colony forming ability of both MCF7 and T47D cells after DDX3 knockdown.

3.15. DDX3 knockdown sensitized T47D cells to tamoxifen treatment

Tamoxifen is an ERα antagonist used in the clinical treatment of pre-menopausal ER+ breast cancer patients and it has helped in reducing the mortality rate for ERα-positive breast cancer. However, development of tamoxifen resistance through various mechanisms is an ongoing and significant clinical problem (Clarke et al., 2001). The now retracted paper by Guo et al 2010 (Guo et al., 2010b) had showed that IKKε-mediated phosphorylation of ERα led to E2-independent cell proliferation and increased tamoxifen resistance (Guo et al., 2010b) (de Leeuw et al., 2011) (Boehm et al., 2007).

As DDX3 knockdown affected cell proliferation in MCF7 and T47D breast cancer cell lines, it was next investigated whether DDX3 plays a role in the development of tamoxifen resistance and whether the tamoxifen sensitivity can be restored by knockdown of DDX3. This might highlight DDX3 as a potential ERα-positive breast cancer treatment target.

To evaluate DDX3's role in breast cancer cell proliferation and tamoxifen sensitivity, MTT assays that measure the metabolic activity of proliferating cells were used. For these MTT assays, the T47D DDX3 knockdown cell line (ShDDX3) in comparison to their non-silencing control cells (NSC) were used in a 5-day proliferation assay. DDX3 knockdown was induced by treating the cells with 2μg/ml of doxycycline for three days and then seeding them in a 96-well plate. Cells were allowed to settle for 24-hours, and the medium was then replaced with treatment medium containing E2 and Tamoxifen.

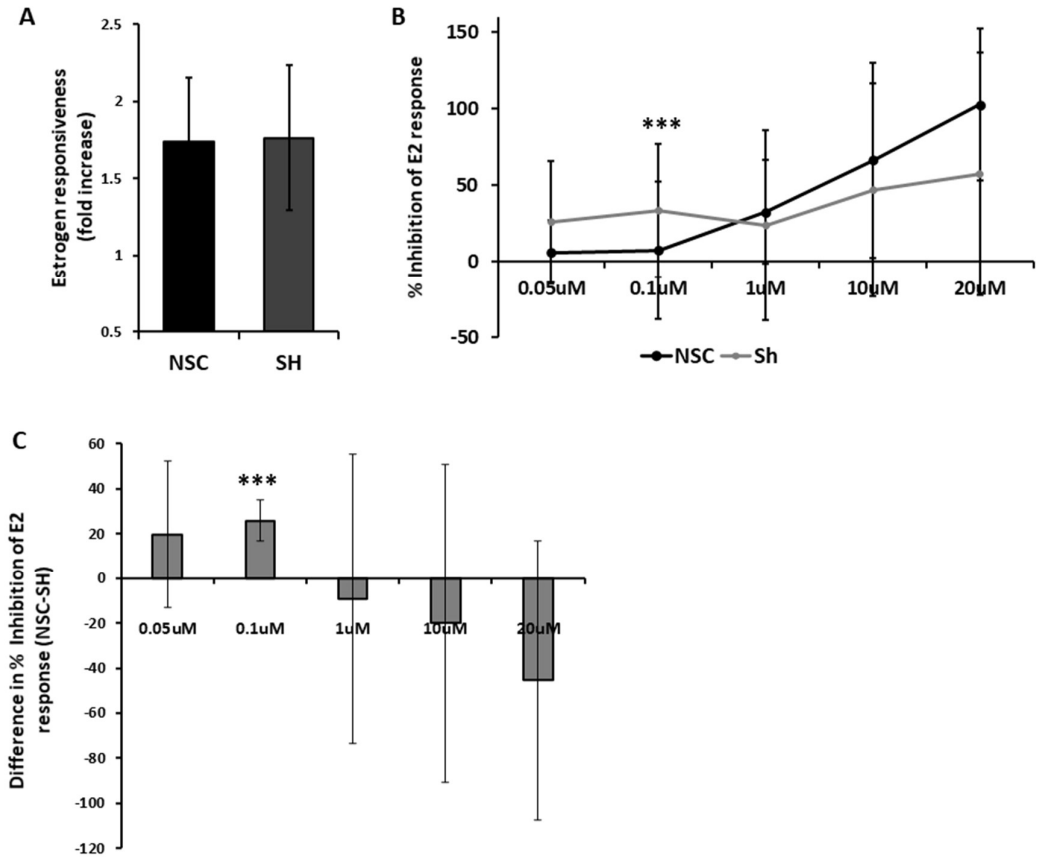

Figure 3.23: DDX3 knockdown sensitized T47D cells to tamoxifen treatment

DDX3 knockdown was induced in ShDDX3 cells by treating them with 2µg/ml doxycycline for 2 days. T47D ShDDX3 and NSC ells were then seeded at 1500 cells/well density in a 96 well-plate. After 24 hours the medium on the cells was replaced with treatment medium as indicated in the figure and cells were harvested after 5 days for MTT assay to measure cell viability. A: Estrogen responsiveness was calculated and compared between NSC and ShDDX3 cells by dividing treated absorbance values by untreated values for NSC and Sh cells (NSC+E2/NSC and SH+E2/SH). This was calculated for all the treatment conditions and used as a base value to calculate tamoxifen response.

The effect of DDX3 knockdown on tamoxifen sensitivity was calculated by using following equations:
(NSC+E2) – (tamoxifen+E2 treated) and (SH+E2) – (Tamoxifen treated).
E2 response fold difference = (NSC+E2)-(Tam+E2)
and for SH cells E2 response fold difference = (SH+E2)-(Tam+E2).
Percent inhibition of E2 response (figure b and c) was calculated using;
(Percent inhibition of E2 response= Difference between tamoxifen treadted-E2 treated con/ E2 treated con-1)*100.

To summarize the data from Figure 3.23b, %inhibition for each experiment was calculated by subtracting shDDX3 E2 response inhibition from NSC E2 response inhibition (data was treated as paired data), as depicted in figure 3.23 c. Shown here is the average of six independent experiments (+SD), paired-test was performed for statistical analysis and the t-test values were 0.24, 0.00094, 0.74, 0.53, 0.13 for 0.05µM to 20µM concentrations of tamoxifen, respectively. Results were therefore only considered statistically significant for 0.1uM tamoxifen with the paired t-test value of 0.00094 (***).

The estrogen responsiveness was first compared between NSC and shDDX3 cells. To this end, the fold increase in proliferation induced by E2 was calculated by dividing absorbance values for E2-treated cells by absorbance values for untreated cells, and then compared this between NSC and shDDX3 cells. The data indicated that there was no difference in the E2-responsiveness between NSC and shDDX3 cells (Figure 3.23a). This suggests that DDX3 knockdown does not affect the ability of cells to respond to E2. Instead, as seen in Figure 3.21a, shDDX3 cells proliferated less than NSC cells in the presence and absence of E2.

Next, the inhibition of E2-reponse for various tamoxifen concentrations (0.05 µM to 20 µM) was compared for T47D NSC and DDX3 knockdown (ShDDX3) cells (Figure 3.23b). shDDX3cells showed more inhibition of E2-response at lower concentrations of tamoxifen. At 0.05µM tamoxifen there was ~25% inhibition and at 0.1µM tamoxifen there was ~33% inhibition of E2 response for ShDDX3 cells, with more and statistically significant inhibition at 0.1µM tamoxifen. However, there was less inhibition of E2-response at higher concentrations of tamoxifen for ShDDX3 cells.

At higher concentrations of tamoxifen (from 1µM to 20µM) this effect was reversed, with NSC cells becoming more sensitive to inhibition by tamoxifen treatment in a dose dependent manner. At 1µM tamoxifen there was ~32% inhibition, with ~66% inhibition at 10uM tamoxifen and ~100% inhibition at 20µM tamoxifen. There was consistently more inhibition at higher tamoxifen concentrations in NSC cells compared to ShDDX3 cells. Figure 3.22c shows the– percent of E2- response inhibition for ShDDX3 cells compared to NSC cells for the same data.

DDX3 knockdown cells being more sensitive to tamoxifen treatment at lower concentrations indeed suggests that DDX3 knockdown increases tamoxifen sensitivity in breast cancer cells.

3.16. Chapter Conclusion

In conclusion, this work suggests a role for DDX3 in enhancing activation of ERα by collaborating with IKKε potentially by modulating IKKε mediated phosphorylation of ERα. The enzymatic function of DDX3 was not required for its effect on ERα activation. The regulation of ERα by DDX3 also affected downstream targets genes of ERα, as DDX3 knockdown reduced expression of ERα target genes. DDX3 likely also mediates its effect on ERα through enhancing its phosphorylation at S167, by physically interacting with ERα, as evident from this study. DDX3 mediated regulation of ERα resulted in reduced cell proliferation and colony forming ability in ShDDX3 cells (MCF7 and T47D cells) and rendered shDDX3 cells more sensitive to low-dose tamoxifen treatment. Lastly, to regulate ERα activity, DDX3 directly interacted with ERα.

Chapter 4. Results

4. Proteomics analysis of DDX3 knockdown in the T47D breast cancer cell line

Approach

In the previous chapter (chapter 3) it was demonstrated that DDX3 was essential for regulating ERα activity and estrogen responsiveness in breast cancer cell lines, potentially through phosphorylation of ERα. The regulation of ERα activity by DDX3 resulted in reduced ERα target gene and downstream protein expression.

To get a more global overview of the role played by DDX3 in ERα positive breast cancer, the effects of DDX3 knockdown on the proteome of the ERα positive breast cancer cell line T47D were investigated by using DDX3 knockdown T47D cells (shDDX3) and its matching non-silencing control cells (NSC) were used. DDX3 knockdown was induced by addition of doxycycline (2μg/ml) to the culture medium for 3 days under estrogen-replete (complete) and -deplete conditions.

Cells were harvested (6-8*10^6 cells) and lysates prepared for mass spectrometric analysis using the Filter Aided Sample Preparation (FASP) method (detailed protocol in Chapter 2). An Ultimate 3000 NanoLC system coupled to a Q-Exactive mass spectrometer was used for mass spectrometry-based analysis. Four replicates were analysed using label-free LC-MS/MS.

Protein identification and label-free quantification (LFQ) normalization of LC-MS/MS data was performed using MaxQuant. Thereafter, the Andromeda search algorithm incorporated in the MaxQuant software was used to correlate LC-MS/MS data against the Homo sapiens Uniprot reference proteome database and a contaminant sequence set provided by MaxQuant. Perseus v.1.5.6.0 was used for data analysis, processing and visualization. Normalised LFQ intensity values were used as the quantitative measurement of protein abundance for subsequent analysis. ANOVA-based multi-sample t-tests were performed using

a cut-off of $p < 0.05$ on the dataset to identify statistically significant differentially abundant proteins.

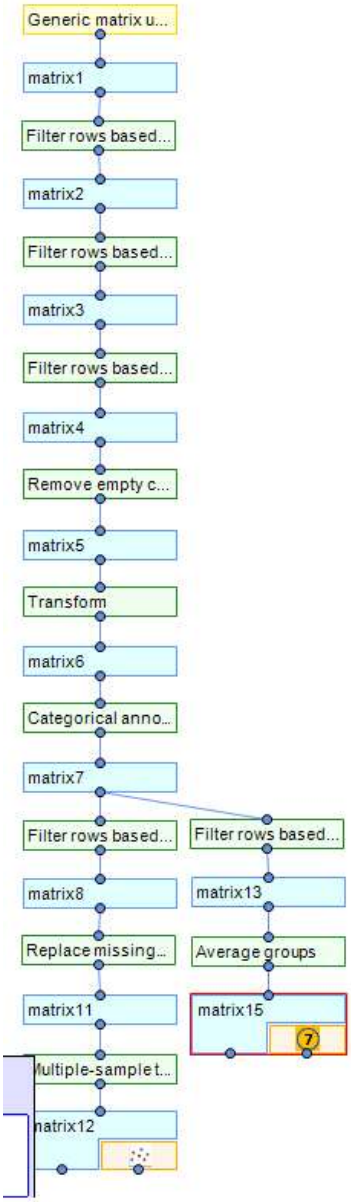

Figure 4.1: Perseus workflow

Perseus workflow used for filtering the proteomics data obtained from MaxQuant using the directions here: http://www.coxdocs.org/doku.php?id=perseus:user:use_cases:interactions.

This workflow filters for the removal of contaminants and peptides identified by site and performed statistical tests to identify significantly differentially expressed proteins.

Using Perseus v.1.5.6.0, an analysis to compare levels of proteins expressed in T47D NSC and ShDDX3 cells cultured in estrogen-replete medium was performed. A total of 425 proteins was detected that were present in both groups in the LC-MS/ MS analysis. Out of these, 52 significantly differentially expressed proteins were identified between T47D NSC and ShDDX3 cells (table 5.1), out of which 30 were more highly expressed in NSC cells, and 22 were more highly expressed in ShDDX3 cells. In addition, 13 proteins were uniquely expressed in T47D NSC and 4 proteins were uniquely expressed in T47D ShDDX3 cells.

4.1. Proteins suppressed in shDDX3 cells versus control NSC cells (complete medium)

UNIPROT ID	Fold change (SH/NSC)	p-value	Protein name
Proteins downregulated in shDDX3 cells compared to NSC control (complete medium)			
P14618	0.31	0.0169	Pyruvate kinase
P49327	0.32	0.0316	Fatty acid synthase
P00558	0.34	0.0045	Phosphoglycerate kinase 1
Q07020	0.35	0.0199	60S ribosomal protein
P22314	0.35	0.0050	Ubiquitin-like modifier-activating enzyme 1
P06576	0.35	0.0480	ATP synthase subunit beta, mitochondrial
P30101	0.36	0.0119	Protein disulfide-isomerase A3
P0CG12	0.38	0.0011	Chromosome transmission fidelity protein 8 homolog isoform 2
P07355	0.38	0.044	Annexin A2
P07900	0.38	0.0045	Heat shock protein HSP 90-alpha
P06733	0.39	0.0176	Alpha-enolase
P60709	0.4	0.0160	Actin, cytoplasmic 1
Q02790	0.43	0.0143	Peptidyl-prolyl cis-trans isomerase
P68363	0.43	0.0137	Tubulin alpha-1B chain -1A chain -1C chain
P09651	0.44	0.0456	Heterogeneous nuclear ribonucleoprotein A1
P23526	0.44	0.0129	Adenosylhomocysteinase OS
P11021	0.45	0.0269	78 kDa glucose-regulated protein
P04406	0.45	0.0107	Glyceraldehyde-3-phosphate dehydrogenase
P38646	0.45	0.0389	Stress-70 protein, mitochondrial
P11142	0.45	0.0360	Heat shock cognate 71 kDa protein
Q5VTE0	0.47	0.0106	Putative elongation factor 1-alpha-like 3 |Elongation factor 1-alpha 1
P08238	0.49	0.0246	Heat shock protein HSP 90-beta
P15531	0.51	0.0071	Nucleoside diphosphate kinase A
P25705	0.53	0.0376	ATP synthase subunit alpha, mitochondrial
P10809	0.54	0.0392	60 kDa heat shock protein, mitochondrial
P30041	0.56	0.0265	Peroxiredoxin-6
P21333	0.58	0.0018	Filamin-A
Q06830	0.61	0.0046	Peroxiredoxin-1
Q86UP2	0.76	0.0454	Kinectin
Unique proteins in NSC			
O00410	Unique		Importin-5
P05388	Unique		60S acidic ribosomal protein P0
P17987	Unique		T-complex protein 1 subunit alpha
P22234	Unique		Multifunctional protein ADE2

P29373	Unique	Cellular retinoic acid-binding protein 2
P40227	Unique	T-complex protein 1 subunit zeta
P40939	Unique	Trifunctional enzyme subunit alpha
P55060	Unique	Exportin-2
P63244	Unique	Guanine nucleotide-binding protein subunit beta-2-like 1
Q05639	Unique	Elongation factor 1-alpha 2
Q14974	Unique	Importin subunit beta-1
Q99536	Unique	Synaptic vesicle membrane protein VAT-1 homolog
Q9HCL2	Unique	Glycerol-3-phosphate acyltransferase 1, mitochondrial

Table 4.1: Proteins upregulated and uniquely expressed in NSC cells

Statistically differently expressed proteins based on ANOVA test which showed more than a 1.3- fold difference were included in this table. The top part of the table shows proteins upregulated in NSC cells (and downregulated in ShDDX3 cells) and the bottom part of the table shows proteins only expressed in NSC cells and absent in shDDX3 cells.

A STRING network analysis of the proteins was performed for the proteins that were more highly expressed in NSC and suppressed in shDDX3 cells, which showed a statistically significant enrichment of interactions (p-value 1.15e-09), that was present in NSC cells and absent from DDX3 knockdown shDDX3 cells. The high confidence protein networks were selected by setting the confidence threshold in STRING to 0.7 and only physical interactions were selected. This analysis showed enrichment of the following KEGG or Reactome pathways in NSC cells, that were reduced in expression in shDDX3 cells: Estrogen signalling pathway, HIF-1 signalling pathway, glycolysis, protein processing in endoplasmic reticulum, mitochondrial protein import, antigen processing and presentation.

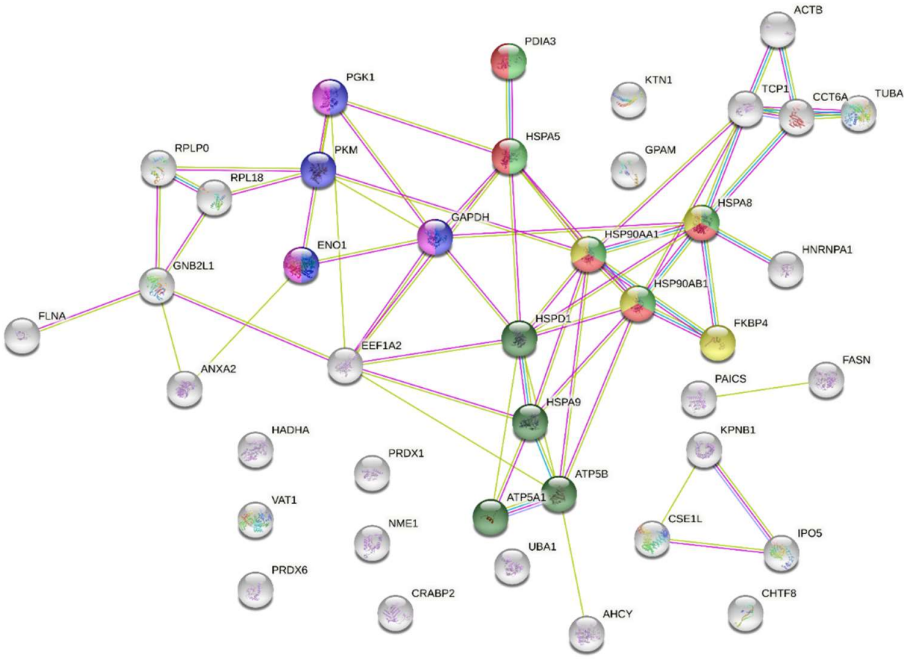

Figure 4.2: STRING analysis for proteins uniquely or more highly expressed in NSC cells compared to shDDX3 cells.

The network shows proteins based on physical interactions only with a confidence threshold of 0.7. Coloured proteins belong to the following enriched pathways: Glycolysis (blue), Protein processing in ER (Varešlija et al.), ESR-signalling (yellow), mitochondrial protein import (dark green), Antigen processing and presentation (light green), HIF-1α signalling (purple) (colour codes for associated pathways displayed in the table below)

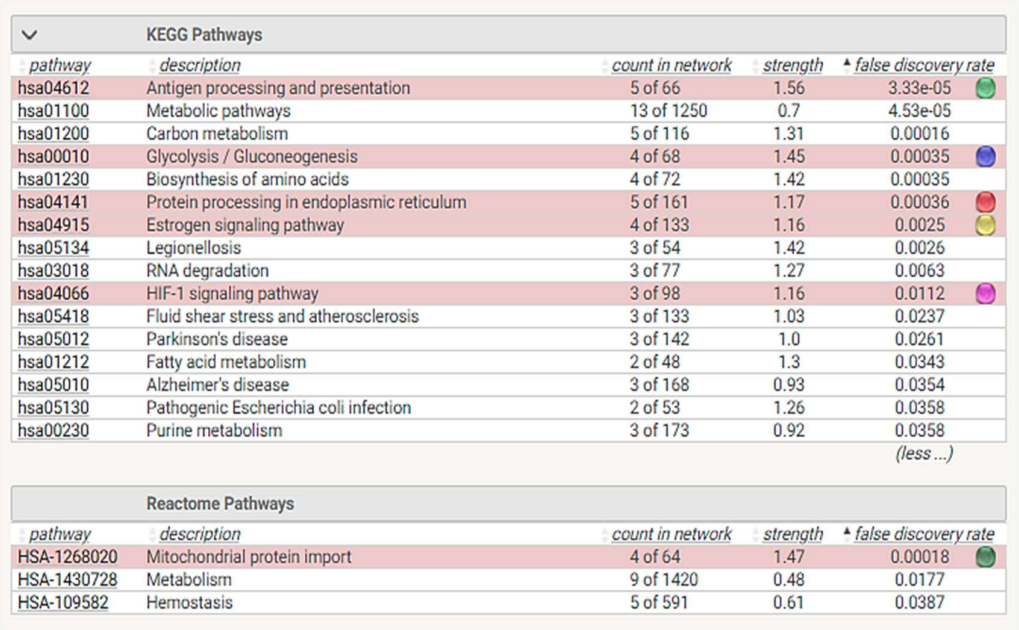

KEGG Pathways

pathway	description	count in network	strength	false discovery rate
hsa04612	Antigen processing and presentation	5 of 66	1.56	3.33e-05
hsa01100	Metabolic pathways	13 of 1250	0.7	4.53e-05
hsa01200	Carbon metabolism	5 of 116	1.31	0.00016
hsa00010	Glycolysis / Gluconeogenesis	4 of 68	1.45	0.00035
hsa01230	Biosynthesis of amino acids	4 of 72	1.42	0.00035
hsa04141	Protein processing in endoplasmic reticulum	5 of 161	1.17	0.00036
hsa04915	Estrogen signaling pathway	4 of 133	1.16	0.0025
hsa05134	Legionellosis	3 of 54	1.42	0.0026
hsa03018	RNA degradation	3 of 77	1.27	0.0063
hsa04066	HIF-1 signaling pathway	3 of 98	1.16	0.0112
hsa05418	Fluid shear stress and atherosclerosis	3 of 133	1.03	0.0237
hsa05012	Parkinson's disease	3 of 142	1.0	0.0261
hsa01212	Fatty acid metabolism	2 of 48	1.3	0.0343
hsa05010	Alzheimer's disease	3 of 168	0.93	0.0354
hsa05130	Pathogenic Escherichia coli infection	2 of 53	1.26	0.0358
hsa00230	Purine metabolism	3 of 173	0.92	0.0358

(less ...)

Reactome Pathways

pathway	description	count in network	strength	false discovery rate
HSA-1268020	Mitochondrial protein import	4 of 64	1.47	0.00018
HSA-1430728	Metabolism	9 of 1420	0.48	0.0177
HSA-109582	Hemostasis	5 of 591	0.61	0.0387

Table.4.2: Significantly enriched KEGG and Reactome pathways

KEGG and Reactome pathways showing pathways enriched with low false discovery rate. (Colour codes match with the STRING network above)

4.2. Three proteins affected by DDX3 knockdown are involved in the KEGG Estrogen Signalling Pathway

Next, KEGG Mapper analysis of the same protein list was performed. This software allows visualization of the submitted proteins in enriched KEGG pathways.

Due to the obvious connection to this project, the proteins involved in the Estrogen Signaling Pathway (KEGG), were looked in more detail.

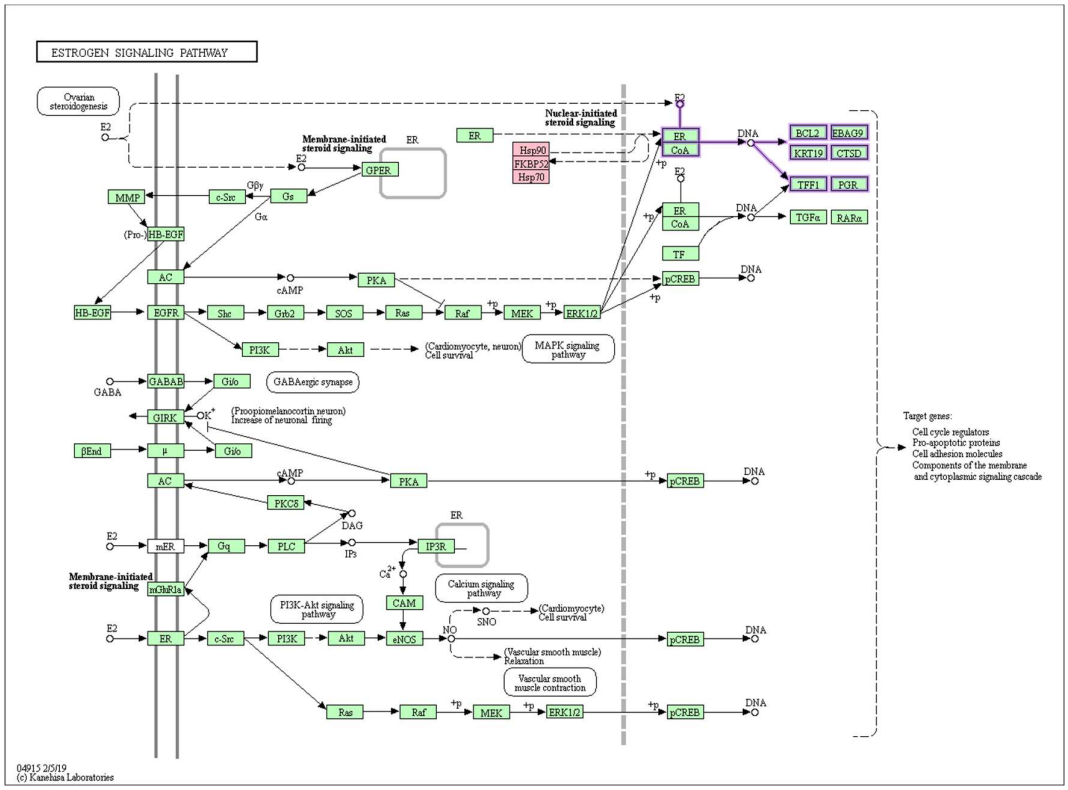

Figure 4.3: KEGG Pathway Map for Estrogen signalling

KEGG pathway showing enrichment of proteins involved in Estrogen signalling pathway. The proteins highlighted in light pink, Hsp90, Hsp70, FKBP52, were identified in the proteomics analysis as significantly downregulated in DDX3 knockdown cells compared to controls. The pathway maps and module maps that are experimentally characterized genes and proteins are coloured in green, as per KEGG convention. (Colour scheme- Pink: associated with cancers, Green: experimentally characterised genes and proteins involved in the protein interactome).

Interestingly, this analysis highlighted three connected proteins (Hsp90, Hsp70, FKBP52) that are involved in the ERα signalling pathway and that are significantly downregulated in DDX3 knockdown cells compared to controls.

HSP90 was previously shown to associate with ER and regulate ER-mediated cell proliferation (Gallerne et al., 2013). ERs remain in an inactive state trapped in multimolecular 68 chaperone complexes organized around HSP90, containing p23 (PTGES3), and immunophilins (FKBP4 or 69 FKPB5) (Obermann, 2018) (Dhamad et al., 2016). Hsp90 was shown to interact with unliganded steroid hormone receptors and to regulate human estrogen receptor (ER)'s ability to bind its ligands in vivo and vitro. It was shown to be essential for maintaining ER in a high affinity hormone-binding conformation (Fliss et al., 2000), and to play an essential role in dimerization of ERα/α and ERα/β, but not for the dimerization of ERβ/β (Powell et al., 2010). HSP90 is essential for ERα hormone binding (Fliss et al., 2000), dimer formation (Powell et al., 2010), and binding to the EREs.

HSP70 was also shown to interact with ERα in the cytoplasm and nucleus of MCF7 cells under normal cell culture conditions. The interaction between HSP70 and ERα was shown to be dependent on the presence of Estrogen. Under estrogen starvation, the HSP70-ERα interaction was only detected in the cytosol (and not in the nucleus) and estrogen treatment was shown not to affect this after starvation. This was an important observation.

The FK506-binding protein 4 (FKBP4, also known as FKBP52) has been reported to possess multiple functions in various kinds of cancers based on its interaction with different cellular targets (Federer-Gsponer et al., 2018). It has been described to have a potential role in tumorigenesis and as a putative tumour marker; and is shown to be upregulated in breast cancer. FKBP4 expression was shown to be associated with breast cancer progression and prognosis, especially of ER-negative breast cancer. Furthermore, FKBP4 depletion specifically was shown to reduce cell growth and proliferation of triple negative breast cancer

cells. Upregulated FKBP4 was also linked to worse survival in luminal A subtype patients (HR/ hormone receptor positive) patients (Xiong et al., 2020) FKBPs are components of steroid hormone receptor complexes and by regulating receptor function, they are known to impact anti-estrogen resistance resulting in phenotypic changes in breast cancer (Zgajnar et al., 2019).

4.3. DDX3 knockdown affected proteins that are involved in glycolysis:

DDX3 knockdown affected proteins mostly involved in glycolysis that are suppressed in ShDDX3 cells but highly expressed in NSC cells. STRING and KEGG mapper analysis also showed an enrichment of proteins associated with glycolysis in NSC cells that were downregulated in ShDDX3 cells. The four proteins linked to glycolysis were: PKM2, Pyruvate kinase muscle isozyme M2, which showed the highest fold differential expression in NSC cells and were suppressed in shDDX3 cells, and ENO1, PGK1, GAPDH (see table 4.1), which were highly expressed in NSC cells and reduced in ShDDX3 cells.

PKM2, is a rate-limiting glycolytic enzyme that catalyzes the final step in glycolysis. PKM2 was shown to be essential to achieve the nutrient demands of cancer cell proliferation contributing to tumorigenesis. PKM2 was also shown to translocate into the nucleus and interact directly with HIF-1α and promote transactivation of HIF-1 target genes by enhancing binding and recruitment of transcriptional coactivator p300. PKM2 transcription is also activated by HIF-1 creating a positive feedback loop, that essentially alters glucose metabolism in cancer cells (Luo and Semenza, 2011). In addition, nuclear PKM2 was also shown to act as a coactivator of β-catenin to induce the expression of c-Myc (Yang et al., 2011). Vice versa, in cancer cells, PKM2 was shown to be overexpressed, and this was driven by c-Myc (David et al., 2010).

PKM2 is clearly an interesting hit that warrants further analysis and might lead to an investigation about metabolic changes caused by DDX3 knockdown and how these affect cancer cell proliferation and survival.

4.4. Proteins suppressed in shDDX3 cells versus control NSC cells (deplete medium)

In the cells grown under estrogen-deplete conditions more proteins were detected that were present in both the groups (630), out of these 12 proteins were significantly differentially expressed between NSC and ShDDX3 cells. However, there were an additional 631 proteins that were only detected in NSC cells and 4 proteins that were uniquely detected in ShDDX3 cells. Thus, in total more proteins seemed to be affected by DDX3 knockdown when cells were grown under estrogen-deplete conditions.

Proteins downregulated in shDDX3 cells compared to NSC control (Deplete medium)			
Uniprot ID	Fold change (SH/NSC)	p-value	Protein IDs
P62316	0.44	0.007	SMD2_HUMAN
P06733	0.45	0.027	ENOA, ENOB, ENOG
P30040	0.70	0.0431	ERP29
+ an additional 631 proteins that were uniquely detected in NSC cells only (not listed here)			

Table 4.3: Proteins more highly expressed (3) in NSC cell and downregulated in ShDDX3 cells.

Proteins that were uniquely expressed (631- not shown here) in NSC cells in deplete medium, which were absent in ShDDX3 cells.

Next STRING analysis was carried out for highly and uniquely expressed protein in NSC cells that were highly downregulated or not expressed in shDDX3 cells when both cells were cultured in deplete medium. A lot of interactions and clusters came up, the p-value for the enrichment score was p= < 1.0e-16. The protein networks with high confidence were selected by setting the confidence threshold in STRING to 0.7 and selected only physical interactions. This analysis showed enrichment of the following KEGG pathways, which were affected by DDX3 knockdown:

Spliceosome, Ribosome, Protein processing in endoplasmic reticulum, RNA transport, antigen processing and presentation.

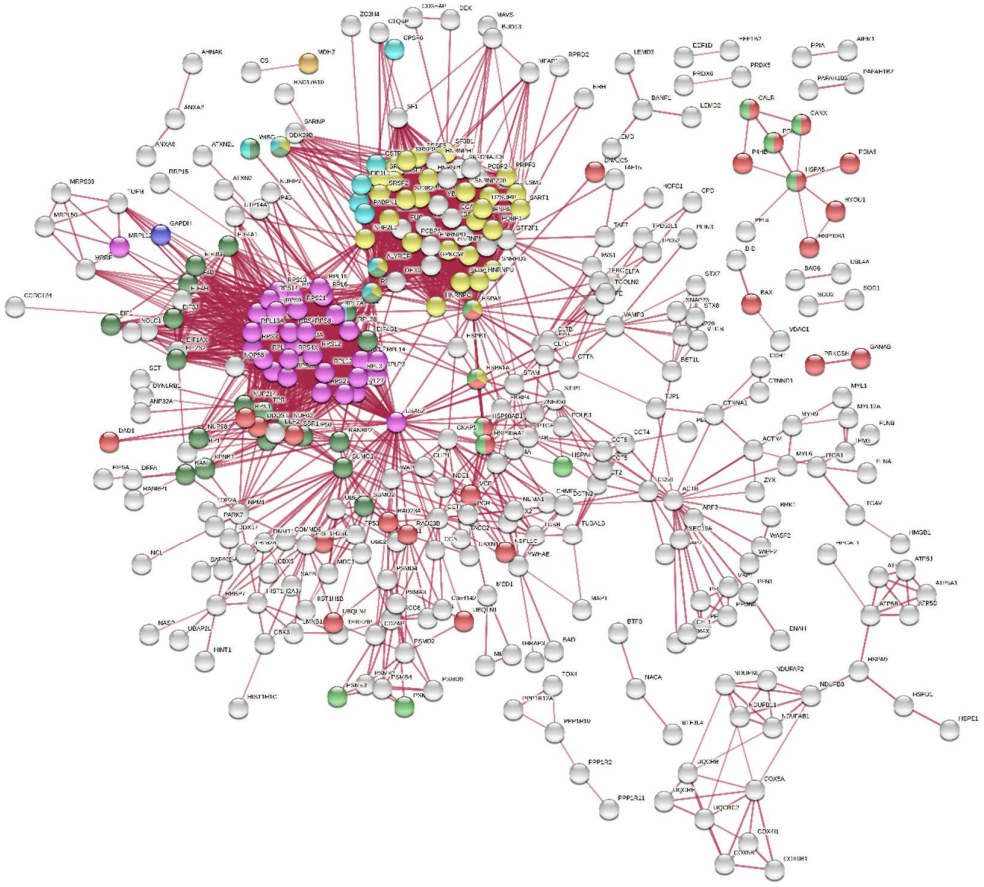

Figure 4.4: STRING analysis for significantly upregulated and uniquely expressed proteins in NSC cells grown in deplete medium

The network shows proteins based on physical interactions only. The network came up with a lot of interactions, so a more stringent interaction score for high confidence was applied (interaction score: high confidence 0.700) and disconnected nodes were hidden for this image. Coloured proteins belong to the following enriched KEGG pathways: Spliceosome (yellow), ribosome (purple), Protein processing in ER (Varešlija et al.). (Additional colour codes for associated pathways displayed in the table below).

KEGG Pathways				
pathway	description	count in network	strength	false discovery rate
hsa03040	Spliceosome	35 of 130	0.92	2.92e-17
hsa03010	Ribosome	31 of 130	0.87	3.32e-14
hsa04141	Protein processing in endoplasmic reticulum	30 of 161	0.76	1.94e-11
hsa05010	Alzheimer's disease	25 of 168	0.67	9.50e-08
hsa03013	RNA transport	24 of 159	0.67	1.25e-07
hsa05016	Huntington's disease	25 of 193	0.61	7.79e-07
hsa05012	Parkinson's disease	21 of 142	0.66	1.19e-06
hsa01200	Carbon metabolism	16 of 116	0.63	9.74e-05
hsa00190	Oxidative phosphorylation	16 of 131	0.58	0.00035
hsa04612	Antigen processing and presentation	11 of 66	0.71	0.00055
hsa01230	Biosynthesis of amino acids	11 of 72	0.68	0.0010
hsa04130	SNARE interactions in vesicular transport	7 of 33	0.82	0.0038
hsa01100	Metabolic pathways	64 of 1250	0.2	0.0042
hsa03015	mRNA surveillance pathway	11 of 89	0.58	0.0044
hsa04217	Necroptosis	15 of 155	0.48	0.0044
hsa04714	Thermogenesis	18 of 228	0.39	0.0100
hsa03050	Proteasome	7 of 43	0.7	0.0110
hsa05100	Bacterial invasion of epithelial cells	9 of 72	0.59	0.0111
hsa04932	Non-alcoholic fatty liver disease (NAFLD)	13 of 149	0.43	0.0188
hsa04530	Tight junction	14 of 167	0.42	0.0188
hsa00620	Pyruvate metabolism	6 of 39	0.68	0.0256
hsa05130	Pathogenic Escherichia coli infection	7 of 53	0.61	0.0256
hsa00010	Glycolysis / Gluconeogenesis	8 of 68	0.56	0.0256
hsa05168	Herpes simplex infection	14 of 181	0.38	0.0296
hsa05412	Arrhythmogenic right ventricular cardiomyopathy (ARVC)	8 of 72	0.54	0.0297
hsa04145	Phagosome	12 of 145	0.41	0.0316
hsa04260	Cardiac muscle contraction	8 of 76	0.52	0.0372

Table 4.4: Significantly enriched KEGG pathway

KEGG pathways showing enrichment with low false discovery rate. (Colour codes match with the STRING network above)

STRING analysis for NSC and ShDDX3 cells grown under deplete medium conditions showed more proteins that were differentially expressed/ detected in NSC cells, which were either reduced in expression or absent in ShDDX3 cells. Therefore, there was more enrichment of interactions, clusters, and pathways identified in NSC cells, which were reduced in ShDDX3 cells by DDX3 knockdown. Despite, the ER-signalling pathway was not enriched here in cells cultured in deplete medium, ER-signalling pathway only came up for the complete medium samples. This is likely because the ER-signalling pathway would only be functioning in the presence of estrogen in complete medium.

Two very prominent clusters that were enriched here are Spliceosome and Ribosome (purple and yellow) and they were also highly enriched KEGG pathways (this was not observed in complete medium samples). The OXPHOS pathway was also significantly enriched in the protein network associated with these proteins (not apparent in complete medium samples). On the other hand, the Antigen/ER processing pathway was enriched in NSC cells cultured in both complete and deplete medium and was absent in ShDDX3 cells analysis.

Enrichment of spliceosome, ribosome, protein processing in endoplasmic reticulum, RNA transport and mRNA surveillance pathways in NSC control cells (which was absent in shDDX3 cells) might suggest that DDX3 is required for cell survival and 'housekeeping functions' under estrogen depletion stress. It will need further investigation to identify how DDX3 regulates gene expression for these proteins and how this affects cellular function.

4.5. Proteins higher expressed in shDDX3 versus NSC cells (complete medium)

Next, the proteins that were higher expressed in DDX3 knockdown cells (shDDX3) compared to NSC controls were identified. A total of 425 proteins was detected that were present in both the groups. Out of these, 52 significantly differentially expressed proteins were identified between T47D NSC and ShDDX3 cells, of which 22 were more highly expressed in ShDDX3 cells and 30 were suppressed relative to NSC cells. In addition, 4 proteins were uniquely expressed in T47D ShDDX3 cells.

Uniprot ID+B1:C23	Fold change (Sh/NSC)	p-value	Protein name
Upregulated proteins in shDDX3 (complete medium) compared to control NSC			
P13987	+1.82	0.048	CD59 glycoprotein
Q9UPT8	+1.53	0.03	Zinc finger CCCH domain-containing protein 4
Q14676	+1.53	0.003	Mediator of DNA damage checkpoint protein 1
Q9P206	+1.49	0.001	Uncharacterized protein KIAA1522
P48634	+1.46	0.003	Protein PRRC2A
O43399	+1.43	0	Tumor protein D54
P60033	+1.42	0.032	CD81 antigen
Q09666	+1.37	0.02	Neuroblast differentiation-associated protein AHNAK
Q13428	+1.34	0.021	Treacle protein
P0CG12	+1.33	0.007	Chromosome transmission fidelity protein 8 homolog isoform 2
P23588	+1.33	0.032	Eukaryotic translation initiation factor 4B
Q13442	+1.32	0.037	28 kDa heat- and acid-stable phosphoprotein
Q9BQ61	+1.32	0.002	Uncharacterized protein C19orf43
Q02818	+1.31	0.039	Nucleobindin-1
Q15075	+1.3	0.047	Early endosome antigen 1
E9PAV3	+1.3	0.026	Nascent polypeptide-associated complex subunit alpha
Q8NFC6	+1.29	0.044	Biorientation of chromosomes in cell division protein 1-like 1
Q9UHR5	+1.29	0.028	SAP30-binding protein
Q9Y520	+1.26	0.014	Protein PRRC2C
P49790	+1.21	0.007	HUMAN Nuclear pore complex protein Nup153
O43169	+1.19	0.03	Cytochrome b5 type B
O14974	+1.17	0.013	Protein phosphatase 1 regulatory subunit 12A
Unique proteins in shDDX3			
P55061	Unique		HUMAN Bax inhibitor 1
Q9NYB0	Unique		Telomeric repeat-binding factor 2-interacting protein 1

Table 4.5 Proteins more highly expressed (22) and uniquely expressed (3) in shDDX3 cells in complete medium

Statistically differently expressed proteins based on ANOVA test were included in this table. The top part of the table shows proteins upregulated in shDDX3 cells and the bottom part of the table shows proteins only expressed in shDDX3 cells and absent in NSC cells.

The STRING analysis was performed on the proteins that were higher expressed in shDDX3 compared to NSC cells (Figure 4.5).

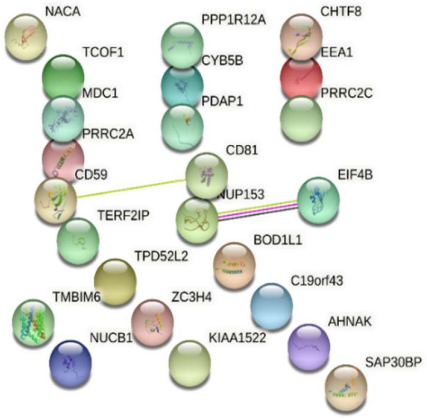

Protein Domains and Features (InterPro)				
domain	description	count in network	strength	false discovery rate
IPR009738	BAT2, N-terminal	2 of 3	2.74	0.00090
IPR033184	Protein PRRC2	2 of 3	2.74	0.00090
IPR036420	BRCT domain superfamily	2 of 25	1.81	0.0104
IPR001357	BRCT domain	2 of 26	1.8	0.0104

Figure 4.5: STRING analysis for proteins upregulated in shDDX3 cells compared to NSC cells, including unique proteins expressed in shDDX3 only

The network shows proteins based on full network (functional and physical interactions). (Interaction score: medium confidence 0.400). The table shows enriched protein domains (Interpro).

This STRING analysis showed no significant enrichment of interactions. However, 2 protein families were significantly enriched, namely the PRR2C proteins and the BRCT domain proteins (as shown in the STRING Interpro table in Figure 4.5).

PRRC2 (PRRC2A and PRRC2C) (Proline Rich Coiled-Coil 2A and C) proteins were enriched with a p-value of 0.0009. PRRC2A plays a role in the regulation of pre-mRNA splicing and PRRC2C was shown to be required for efficient formation of stress granules (Sakashita et al., 2004, Youn et al., 2018).

The other protein family that showed enrichment in shDDX3 cells compared to control NSC cells were the BRCT domain proteins (p-value 0.01), with MDC1 and TERF2IP falling into this category. MDC1 is 'Mediator of DNA damage checkpoint protein 1' and is required for checkpoint-mediated cell cycle arrest in response to DNA damage within both the S phase and G2/M phases of the cell cycle. It serves as a scaffold for the recruitment of DNA repair and signal transduction proteins to discrete foci of DNA damage marked by Serine139 phosphorylation of histone H2AX. MDC1 was also shown to be required for downstream events subsequent to the recruitment of these proteins (Stewart et al., 2003). These include phosphorylation and activation of the ATM, CHEK1 and CHEK2 kinases, and stabilization of TP53 and apoptosis. It was interesting to see this as DDX3 knockdown might induce DNA damage in ShDDX3 cells, as loss of DDX3 was shown to correlate with increased DNA damage accumulation in mammalian cancer cells (Chen et al., 2017).

TERF2IP, Telomeric repeat-binding factor 2-interacting protein 1; was shown to act both as a regulator of telomere function and as a transcription regulator. It is involved in the regulation of telomere length and protection as a component of the shelterin complex (telosome). In contrast to other components of the shelterin complex, it is dispensable for telomere capping and does not participate in the protection of telomeres against non-homologous end-joining (NHEJ)-mediated repair. Instead, it is required to negatively regulate telomere recombination and is essential for repressing homology-directed repair. TERF2IP was shown to be recruited to telomeric double-stranded 5'-TTAGGG-3' repeats via its interaction with TERF2. Independently of its function in telomeres, it also acts as a transcription regulator by being recruited to extratelomeric 5'-TTAGGG-3' sites. It also regulates gene expression by associating with the I-kappa-B-kinase (Enmark et al.) complex to act as a regulator of the NF-kappa-β signaling. It was shown to promote IKK-mediated phosphorylation of RELA/p65, leading to enhanced expression

of NF-kappa-β target genes. DDX3 was shown to suppress NF-κβ (p65/p50)-mediated transcriptional activity by interacting with the (NF)-κβ subunit p65 (Xiang et al., 2016).

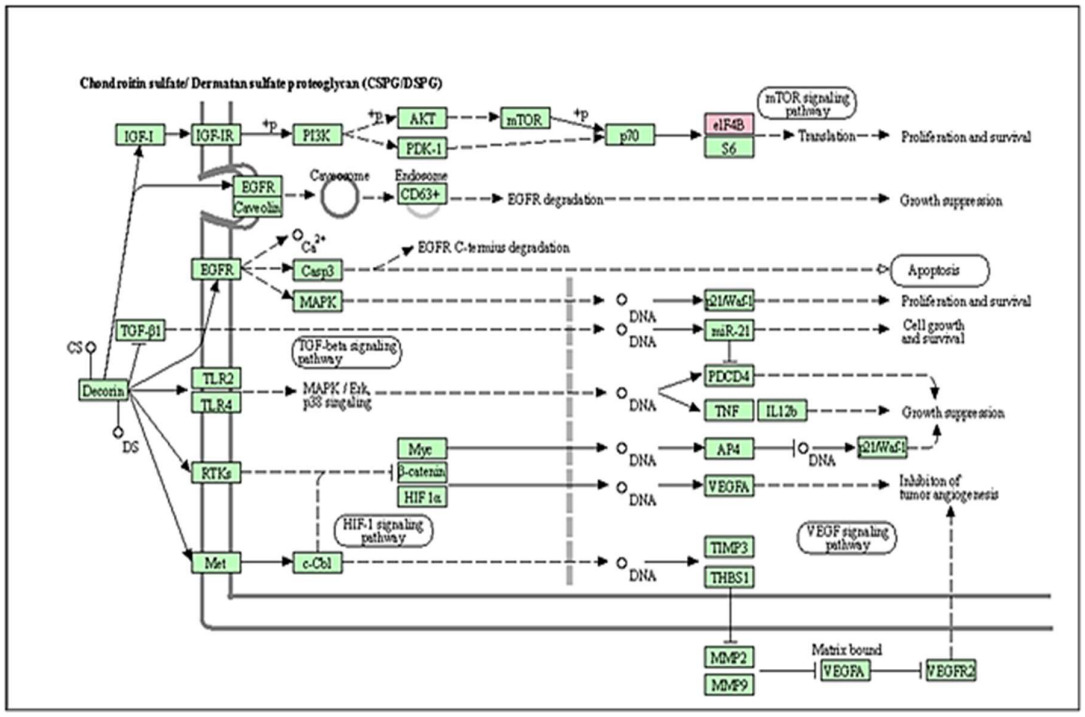

Figure 4.6: KEGG pathway showing eIF4B related signalling network

eIF4B was higher expressed in shDDX3 compared to NSC cells. eIF4B is associated with translation and cell proliferation and is linked to the mTOR signalling pathway.

Another interesting protein more highly expressed in shDDX3 cells when compared to NSC cells, was EIF4B, Eukaryotic translation initiation factor 4B; which is required for the binding of mRNA to ribosomes. eIF4B was shown to regulate translation of proliferative and pro-survival mRNAs (Figure 4.6). Moreover, eIF4B depletion in cancer cells was shown to attenuate proliferation, sensitizing them to stress-driven apoptosis (Shahbazian et al., 2010). It was therefore interesting to see eIF4B as one of the proteins upregulated in ShDDX3 cells.

4.6. Proteins higher expressed in shDDX3 versus NSC cells (deplete medium)

Next, the proteins higher expressed in ShDDX3 cells compared to NSC control cells in deplete medium were analysed. 459 proteins were identified in both the groups, 12 proteins were significantly different in both, and out of these 7 proteins were upregulated in ShDDX3 cells and an additional 4 were uniquely expressed in ShDDX3 deplete medium cells.

Upregulated proteins in ShDDX3 cells (deplete medium) compared to NSC			
P12830	+1.28	0.019	CADH1
P61604	+1.35	0.028	CH10
P82970	+1.77	0.014	HMGN5
P52815	+1.77	0.008	RM12
Q96CT7	+1.86	0.034	CC124
Q13070	+2.43	0.016	GAGE6, GAGE5, GAGE3
Q13068	+2.52	0.027	GAGE4, GG12I, GG12G, GG12F, GAGE7, GAGE1, GG12J, GG12H, GG12C
Proteins uniquely expressed in ShDDX3 cells (deplete medium)			
Q6IAA8	Unique		LTOR1
Q8WVC0	Unique		LEO1
Q9NUQ8	Unique		ABCF3
Q9Y5J9	Unique		TIM8B

Table 4.6: Proteins more highly expressed or uniquely detected in ShDDX3 cells grown in deplete medium

STRING analysis performed for these proteins did not show significant enrichment for networks or pathways. Of note, the small sets of proteins that were higher expressed in shDDX3 cells compared to NSC cells were quite different between samples from deplete medium versus complete medium (compare Table 6 and Table 5).

4.7. Proteins higher expressed under complete medium conditions versus deplete medium conditions in NSC control cells

Using Perseus, an analysis was carried out to identify proteins whose expression was influenced by estrogen depletion, to compare proteins expressed in NSC cells grown in complete medium versus NSC cells grown in estrogen-deplete medium. A total of 630 proteins was identified to be present in both sets of samples. There were 17 significantly different proteins between complete and deplete medium samples, out of these 7 proteins were upregulated in complete medium samples and 10 proteins were upregulated in deplete medium samples. 4 proteins were uniquely expressed in complete medium samples and 3 proteins were uniquely expressed in deplete medium samples.

Uniprot ID	Fold change Com/Dep	p-value	Protein IDs
Proteins higher expressed in complete medium (NSC)			
P42126	+4.97	0.045	ECI1
P00492	+2.44	0.001	HPRT
Q9UKK9	+1.77	0.005	NUDT5
P22692	+1.72	0.009	IBP4
O14745	+1.57	0.017	NHRF1
O95817	+1.42	0.028	BAG3
Q5JTV8	+1.19	0.012	TOIP1
Unique in Complete medium (NSC)			
P40227	Unique		TCPZ
P46109	Unique		CRKL
P55060	Unique		XPO2
Q99536	Unique		VAT1

Table 4.7: Proteins more highly expressed or uniquely detected in NSC cells grown in complete medium compared to NSC cells in deplete medium

In this comparison, 17 proteins were significantly different, out of which 7 were higher expressed in complete medium NSC cells and an additional 4 were uniquely expressed.

There was only a relatively small number of proteins that were differentially expressed. This was a bit surprising, and unexpected as more proteins should have been identified as differentially regulated by estrogen depletion even for NSC control cells. There was no significant enrichment of interactions or pathways when STRING analysis was performed on these proteins. At medium confidence level there were only SLC9A3R1, Na(+)/H(+) exchange regulatory cofactor NHERF1, and T-complex protein 1 subunit zeta, a molecular chaperone, that were connected; and 9 other disconnected protein nodes were identified (PPI enrichment p-value: 0.487). SLC9A3R1 was shown to play a role in the WNT signalling pathway and was shown to be induced by estrogen (Liu et al., 2015). NHERF1 inhibits Wnt signalling-mediated proliferation of cervical cancer. And downregulation of NHERF1 was shown to contribute to cervical cancer progression (Wang et al., 2018). NHERF1 was highly expressed in NSC cells which was interestingly highly downregulated in ShDDX3 cells. Suggesting that estrogen induced WNT signalling activation via SLC9A3R1 was significantly reduced by DDX3 knockdown. Furthermore, NHERF1 which is a regulator of Wnt-mediated cell proliferation in cervical cancer was also significantly reduced in DDX3 knockdown sh cells. This is a very interesting observation as Tamoxifen is shown to act as agonist or antagonist in tissue specific manner, and therefore might indicate a role of Wnt pathway modulation in tamoxifen driven increased risk of cervical and endometrial cancers.

Next, the proteins that were upregulated in cells grown in deplete medium compared to complete medium were identified and analysed (Table 4.7).

Uniprot ID	Fold change (Dep/ Com)	p-value	Protein IDs
Proteins upregulated in Deplete medium (NSC) compared to Complete medium (NSC)			
P16989	1.10	0.047	YBOX3
O60716	1.18	0.012	CTND1
Q86UP2	1.30	0.044	KTN1
P12830	1.35	0.000	CADH1, CADH3
P14314	1.36	0.010	GLU2B
P41208	1.37	0.044	CETN2, CETN1
Q14103	1.38	0.045	HNRPD
P07602	1.56	0.040	SAP
O14979	1.68	0.013	HNRDL
P30040	1.84	0.001	ERP29
Unique in Deplete medium (NSC)			
Q86U42	Unique		PABP2
Q9H1B7	Unique		I2BPL
Q9NYB0	Unique		TE2IP

Table 4.8: Upregulated or uniquely expressed proteins in deplete medium NSC cells compared to NSC cells grown in complete/ estrogen replete medium

STRING network analysis of these proteins showed a significant enrichment of interactions (p-value = 0.0267).

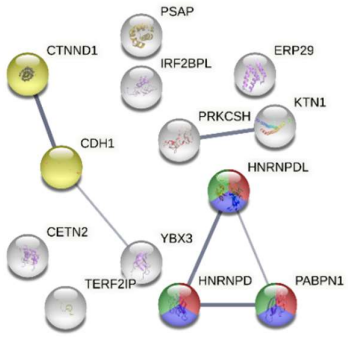

Figure 4.7: STRING analysis for proteins uniquely expressed or upregulated in deplete medium cultured NSC cells compared to complete medium-cultured NSC cells

Full network STRING analysis showing functional and physical protein association with medium confidence level (minimum interaction score 0.4 (PPI enrichment p-value:0.0267) (Colour coded according to the table below)

KEGG Pathways				
pathway	*description*	*count in network*	*strength*	*false discovery rate*
hsa04520	Adherens junction	2 of 71	1.63	0.0208

Protein Domains and Features (InterPro)				
domain	*description*	*count in network*	*strength*	*false discovery rate*
IPR000504	RNA recognition motif domain	3 of 228	1.3	0.0225
IPR035979	RNA-binding domain superfamily	3 of 241	1.27	0.0225
IPR012677	Nucleotide-binding alpha-beta plait domain superfamily	3 of 241	1.27	0.0225

Table 4.9: KEGG pathway and InterPro analysis

KEGG pathways and Interpro protein domains enriched with proteins uniquely expressed and upregulated in deplete medium compared to complete medium grown NSC control cells.

The STRING analysis revealed only a couple of protein networks, but among the enriched interactions and related pathways, CTNND1 and CDH1 came up with high confidence (adherenes junctions, false discovery rate 0.02). This is interesting as they play a role in adherenes junction formation and might be associated with the β-catenin network and cell migration pathways. CTNND1, was shown to bind and activate target genes of the Wnt signalling pathway (Tamai et al., 2004). CDH1 is Cadherin-1, a calcium-dependent cell adhesion protein. CDH1 is involved in regulating cell-cell adhesion, mobility, and proliferation of epithelial cells and has a potent invasion suppressor role (Onder et al., 2008).

Overall, more proteins differentially regulated by estrogen depletion in NSC control cells were expected to be identified, as lesser proteins were identified the results from this analysis were a bit surprising.

4.8. Proteins higher expressed under complete medium conditions versus deplete medium conditions in shDDX3 cells

Because relatively few differentially expressed proteins were detected in the complete medium versus deplete medium comparison in NSC control cells, next the same comparative analysis was carried out in ShDDX3 cells. A total of 436 proteins were identified in both groups. There were 24 significantly different proteins between complete vs deplete medium samples derived from shDDX3 cells (shown in the table below). However, an additional 571 proteins were uniquely expressed in complete medium samples and 577 proteins were uniquely expressed in deplete medium samples (not listed here). Thus, a much higher number of differentially expressed proteins was identified in the shDDX3 cells cultured in estrogen-replete versus -deplete conditions than in the NSC control cells discussed above.

Uniprot ID	Fold change ShDDX3 Complete/Deplete	p-value	Protein name
Q53FA7	+2.21	0.030	Quinone oxidoreductase PIG3
O95721	+1.55	0.039	Synaptosomal-associated protein 29
O95817	+1.49	0.042	HUMAN BAG family molecular chaperone regulator 3
Q9UFG5	+1.44	0.003	UPF0449 protein C19orf25
O43670	+1.42	0.027	BUB3-interacting and GLEBS motif-containing protein ZNF207
Q09666	+1.37	0.017	Neuroblast differentiation-associated protein AHNAK
Q9UHD8	+1.35	0.009	Septin-9
P48634	+1.33	0.036	Protein PRRC2A
Q9BQ61	+1.32	0.026	Uncharacterized protein C19orf43
Q99584	+1.30	0.044	Protein S100-A13
Q99700	+1.29	0.040	Ataxin-2
Q8NFC6	+1.28	0.028	Biorientation of chromosomes in cell division protein 1-like 1
Q9Y520	+1.25	0.046	Protein PRRC2C
+ an additional 571 proteins that were uniquely detected in complete medium grown cells only (not listed here).			

Table 4.10: Proteins higher expressed in complete medium grownShDDX3 cells compared to shDDX3 cells grown in deplete medium.

A total of 436 proteins were identified in both groups. There were 24 significantly different proteins between complete vs deplete medium samples derived from shDDX3 cells. However, an additional 571 proteins were uniquely expressed in complete medium samples and 577 proteins were uniquely expressed in deplete medium samples.

Next, the STRING analysis was performed for proteins higher and uniquely expressed in shDDX3 cells grown in complete medium compared to deplete medium.

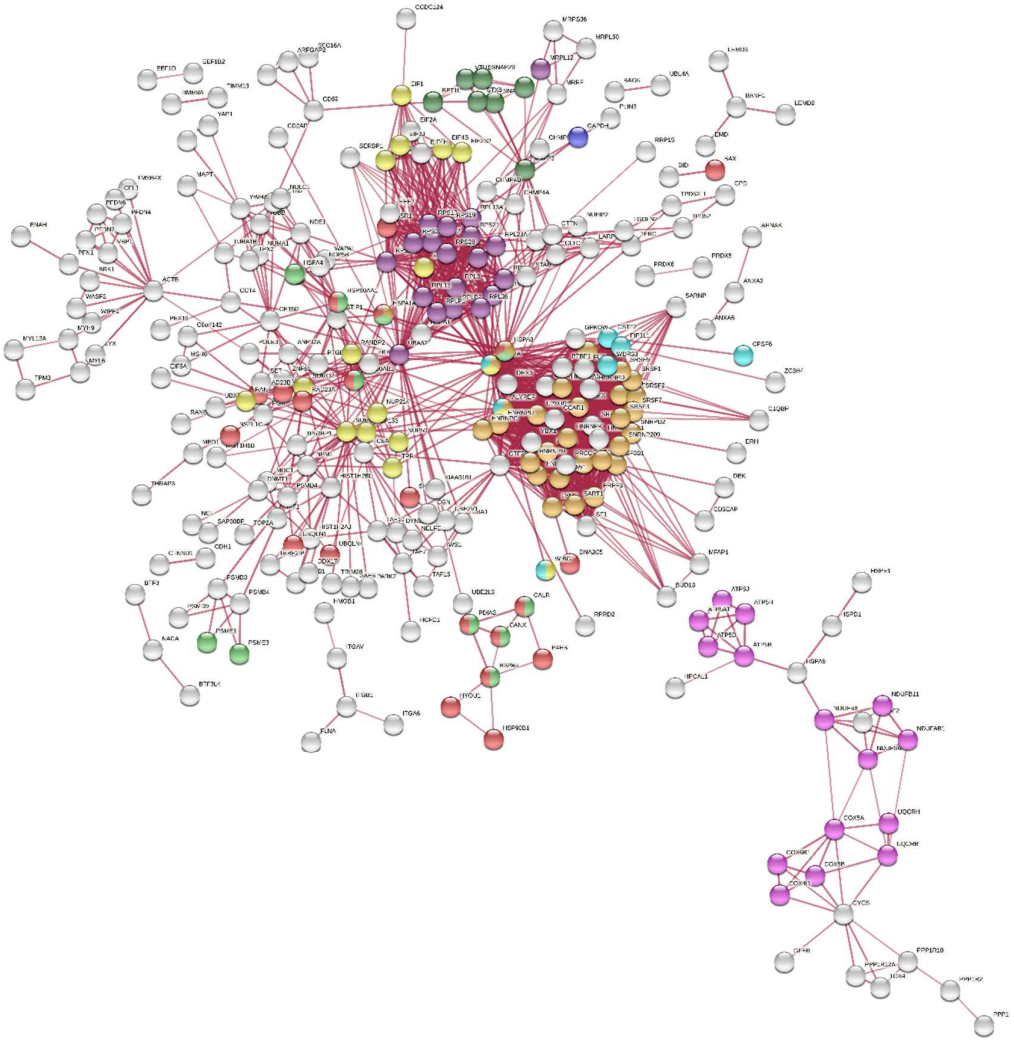

Figure 4.8: STRING analysis for proteins higher and uniquely expressed in shDDX3 cells grown in complete medium compared to deplete medium.

The network shows proteins based on physical interactions only. The network came up with lot of interactions, so a stringent interaction score was applied (high confidence 0.700) and disconnected nodes are not shown in the image. Coloured pathways: Spliceosome (dark yellow), ribosome (purple), Protein processing in ER (Varešlija et al.) antigen processing and presentation (light green), RNA transport (yellow), glycolysis (blue), oxidative phosphorylation (pink). (colour codes for associated pathways displayed in the table below) PPI enrichment p-value:< 1.0e-16.

KEGG Pathways				
pathway	description	count in network	strength	false discovery rate
hsa03040	Spliceosome	32 of 130	0.93	5.28e-16
hsa04130	SNARE interactions in vesicular transport	7 of 33	0.86	0.0023
hsa04612	Antigen processing and presentation	11 of 66	0.76	0.00026
hsa04141	Protein processing in endoplasmic reticulum	26 of 161	0.75	2.01e-09
hsa03010	Ribosome	19 of 130	0.7	2.18e-06
hsa05010	Alzheimer's disease	24 of 168	0.69	7.37e-08
hsa05216	Thyroid cancer	5 of 37	0.67	0.0498
hsa05012	Parkinson's disease	19 of 142	0.66	6.11e-06
hsa05130	Pathogenic Escherichia coli infection	7 of 53	0.66	0.0184
hsa00010	Glycolysis / Gluconeogenesis	8 of 68	0.61	0.0181
hsa00190	Oxidative phosphorylation	15 of 131	0.6	0.00038
hsa05016	Huntington's disease	22 of 193	0.59	6.94e-06
hsa03013	RNA transport	18 of 159	0.59	8.26e-05
hsa05412	Arrhythmogenic right ventricular cardiomyopathy (ARVC)	8 of 72	0.58	0.0210
hsa05100	Bacterial invasion of epithelial cells	8 of 72	0.58	0.0210
hsa01230	Biosynthesis of amino acids	8 of 72	0.58	0.0210
hsa05410	Hypertrophic cardiomyopathy (HCM)	8 of 81	0.53	0.0352
hsa01200	Carbon metabolism	11 of 116	0.51	0.0138
hsa05414	Dilated cardiomyopathy (DCM)	8 of 88	0.5	0.0488
hsa03015	mRNA surveillance pathway	8 of 89	0.49	0.0498

Table 4.11 : KEGG pathway analysis for proteins higher and uniquely expressed in shDDX3 cells grown in complete medium compared to deplete medium, showing enriched pathways.

STRING network analysis of these proteins showed a significant enrichment of interactions (p-value < 1.0e-16). However, even though more proteins came up as differentially expressed following estrogen depletion in shDDX3 cells, there were still no clusters that were clearly linked to ERα or an estrogen response. Instead, protein clusters linked to the KEGG pathways Ribosome

and Spliceosome, OXPHOS and Protein Processing in ER were enriched. This profile was strikingly similar to clusters/pathways emerging for the NSC/shDDX3 comparison in section 2/Figure 4.4.

4.9. Proteins higher expressed in deplete medium conditions versus complete medium conditions in shDDX3 cells

Next, analysis was carried out that identified proteins upregulated in ShDDX3 cells grown in deplete medium compared to shDDX3 cells grown in complete medium. There were 436 total proteins detected in both groups, out of these 26 were significantly differentially expressed, and 12 were upregulated in ShDDX3 deplete medium cells. An additional 577 proteins were uniquely detected in deplete medium samples only.

Uniprot ID	Fold change ShDDX3 Complete/Deplete	p-value	Protein name
Q8N128	-1.31	0.034	Protein FAM177A1
Q9UKV3	-1.31	0.008	Apoptotic chromatin condensation inducer in the nucleus
Q969E4	-1.42	0.031	Transcription elongation factor A protein-like 3
Q9Y6H1	-1.43	0.031	Coiled-coil-helix-coiled-coil-helix domain-containing protein 2, mitochondrial
P00167	-1.50	0.024	HUMAN Cytochrome b5
Q86UP2	-1.52	0.014	Kinectin OS
P12830	-1.56	0.016	Cadherin-1
Q01844	-1.69	0.038	RNA-binding protein EWS
Q9NP97	-1.70	0.045	Dynein light chain roadblock-type 1
P52815	-1.87	0.004	39S ribosomal protein L12, mitochondrial
P51858	-1.89	0.013	Hepatoma-derived growth factor
P82970	-2.09	0.003	High mobility group nucleosome-binding domain-containing protein 5
+ an additional 577 proteins that were uniquely detected in deplete medium grown cells only (not listed here).			

Table 4.12: Proteins upregulated in deplete medium in ShDDX3 cells

12 proteins were upregulated in shDDX3 cells, 577 proteins were uniquely detected only in shDDX3 cells.

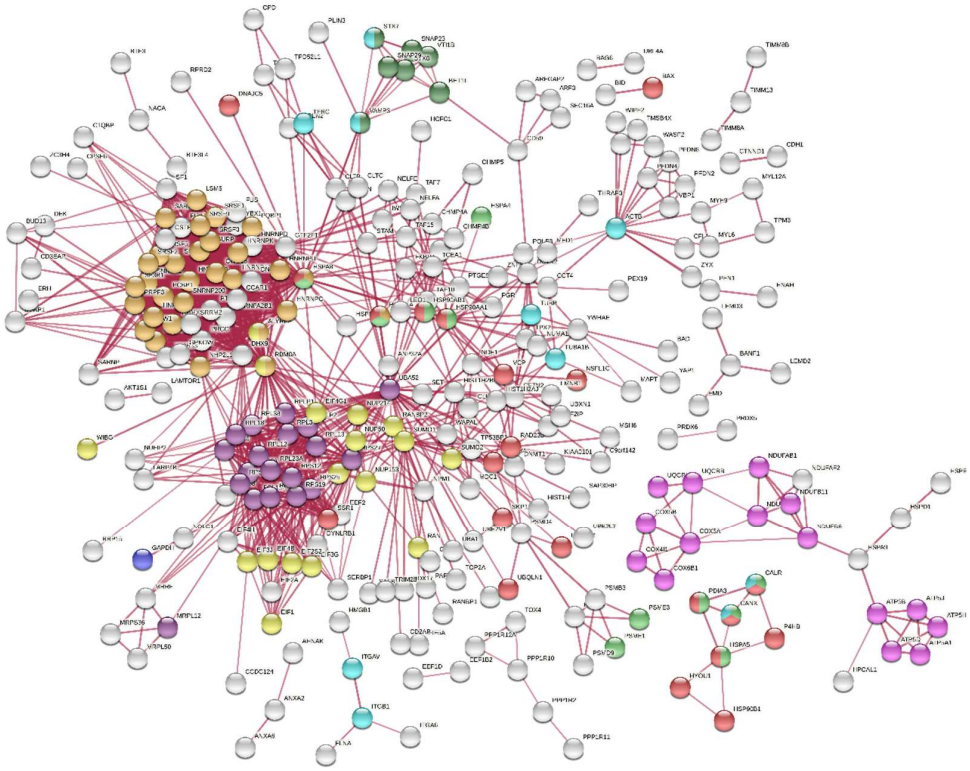

Figure 4.9: STRING analysis for significantly upregulated proteins and uniquely expressed in shDDX3 cells deplete medium compared to complete medium.

The network shows proteins based on physical interactions only. The network came up with lot of interactions, so a stringent interaction score was applied (high confidence 0.700) and disconnected nodes were hidden. Coloured pathways: Spliceosome (dark yellow), ribosome (purple), Protein processing in ER (Varešlija et al.). (colour codes for associated pathways displayed in the table below). (PPI enrichment p-value:< 1.0e-16).

KEGG Pathways				
pathway	description	count in network	strength	false discovery rate
hsa03040	Spliceosome	33 of 130	0.94	9.41e-17
hsa04130	SNARE interactions in vesicular transport	7 of 33	0.86	0.0024
hsa04612	Antigen processing and presentation	11 of 66	0.75	0.00028
hsa04141	Protein processing in endoplasmic reticulum	26 of 161	0.74	2.49e-09
hsa03010	Ribosome	19 of 130	0.7	2.54e-06
hsa05010	Alzheimer's disease	23 of 168	0.67	4.09e-07
hsa05130	Pathogenic Escherichia coli infection	7 of 53	0.65	0.0220
hsa05012	Parkinson's disease	18 of 142	0.64	3.04e-05
hsa00010	Glycolysis / Gluconeogenesis	8 of 68	0.6	0.0220
hsa03013	RNA transport	18 of 159	0.59	9.43e-05
hsa00190	Oxidative phosphorylation	15 of 131	0.59	0.00042
hsa05412	Arrhythmogenic right ventricular cardiomyopathy (ARVC)	8 of 72	0.58	0.0235

Table 4.13: KEGG pathway analysis for significantly upregulated and uniquely expressed proteins in ShDDX3 cells grown in deplete medium compared to complete medium.

KEGG pathway analysis showed enrichment of spliceosomes, antigen processing and presentation, protein processing in endoplasmic reticulum, and ribosome pathways, in ShDDX3 cells grown in deplete medium compared to complete medium. These pathways were also enriched in complete versus deplete and NSC versus Sh. It was difficult to understand why the pathways enriched in complete and deplete would be same as it was unexpected.

4.10. Chapter Conclusion

In conclusion, the most important and immediately relevant finding from this proteomics analysis is the enrichment of the KEGG Estrogen Signalling Pathway in the NSC controls versus ShDDX3 proteome comparison for the cells cultured in estrogen replete/ complete medium. HSP90, FKBP52 and HSP70 were clearly the most interesting hits. HSP90 expression was shown to be associated with poor overall survival in breast cancer (Dimas et al., 2018) and is an interesting clinical target. HSP70 high expression and FKBP4 were also shown to be associated with ER positive status (ER+) (Xiong et al., 2020). As HSP90 and HSP70 were downregulated in DDX3 knockdown cells, thus it will be interesting to follow up on their role in the ERα signalling pathway in conjunction with DDX3, which might unravel a novel role for DDX3 in regulating ERα signalling.

Chapter 5. Results

5. WNT pathway

DDX3 was shown to be a regulator of the Wnt–β-catenin pathway, where it acts as a regulatory subunit of CK1ε and influences β-catenin-dependent transcriptional activation. DDX3 binds to CK1ε, in a Wnt-dependent manner, and directly stimulates its kinase activity, promoting phosphorylation of the scaffold protein dishevelled (Dvl). This facilitates β-catenin translocating into the nucleus. In the nucleus, β-catenin can interact with two major transcription factors, the T-cell factor (TCF) bound to a consensus site (5'-T/A-T/A-CAAAG-3') (Behrens et al., 1996, Molenaar et al., 1996) and lymphocyte enhancer factor, accompanied with several transcriptional co-activators, such as BCL9, CBP, p300, and Pygo, to regulate transcription of multiple target genes (Behrens et al., 1996). Moreover, in colorectal cancer, DDX3 expression was shown to be correlated with nuclear β-catenin expression. It was also shown that up-regulation of DDX3 expression can contribute to induction of TCF4 reporter activity and the elevation of mRNA expression levels of TCF4-regulated downstream genes, such as c-MYC, AXIN2, CCND1 and BIRC5A (Zhao et al., 2016).

Venu Raman et al. showed that inhibition of DDX3 results in reduced Wnt signalling, and that DDX3 interfered with Wnt signalling at different levels. Whereas (Cruciat et al., 2013b) demonstrated that DDX3 inhibition had no effect on Wnt signalling activity after induction with β-catenin overexpression and DDX3's involvement in this pathway was independent of its helicase activity.

This suggests that DDX3 might have two potential mechanisms of Wnt pathway activation, via enhancing CK1ε-mediated activation of β-catenin and by directly interacting with β-catenin at the promoter level. Due to the important role of the Wnt pathway in breast cancer and the potential link with ERα, the role of DDX3 in the Wnt signalling pathway was investigated in the experimental settings used in this study (chapter 3).

5.1 DDX3's role in β-catenin and CK1ε mediated Wnt pathway activation:

To analyse the role of DDX3 in Wnt/β-catenin signalling in the breast cancer cell lines used for this project, Topflash reporter gene assay was established. The reporter plasmid Super 8x Topflash contains seven TCF binding sites upstream of a minimal promoter that drives firefly luciferase reporter expression. This Topflash promoter can therefore be used for quantifying β-catenin dependent transcriptional activity.

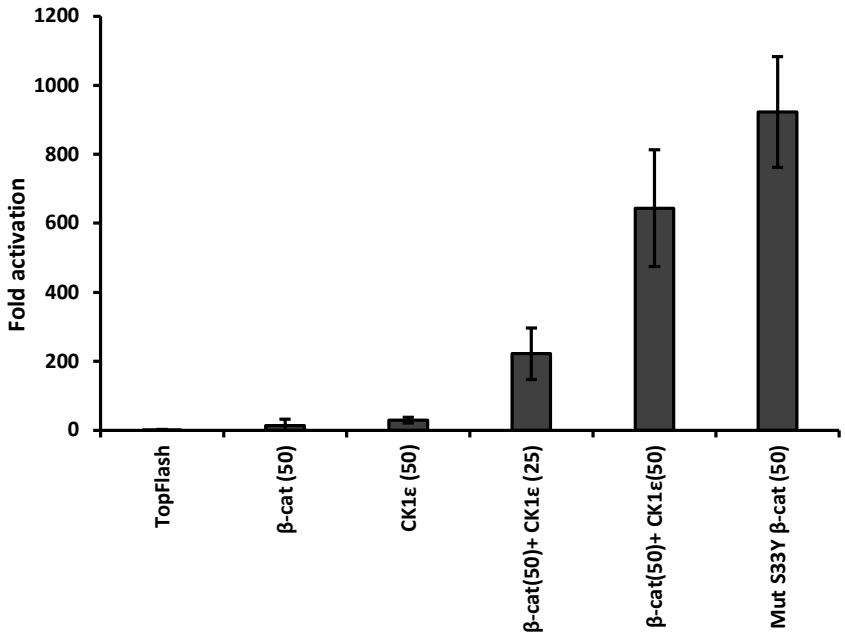

Figure 5.1: β-catenin and CK1ε enhance Topflash reporter activity

MCF7 cells were transfected with the TCF-dependent Topflash reporter construct (60ng/ml) and a Renilla luciferase control construct (for normalization) (20ng/ml). As indicated, expression constructs for wildtype or a constitutively active mutant β-catenin (S33Y) (50ng/ml), and/or CK1ε (25ng/ml or 50ng/ml) were co-transfected. An empty vector plasmid was used to adjust total DNA concentration to 230ng. 24h after transfection, samples were harvested using Passive Reporter Lysis buffer. Firefly luciferase and Renilla luciferase activities were then measured. Renilla luciferase values were used for normalisation. Shown here is one representative experiment of three independent experiments, depicting the mean of three triplicates with error bars showing $\pm$SD.

At first, MCF7 cells were used to test and establish the Topflash reporter assay. As expected, when β-catenin and CK1ε were overexpressed independently, TCF-dependent reporter gene activity was enhanced to some extent but co-expression of β-catenin and CK1ε caused dramatic increase in Topflash activity in a CK1ε dose-dependent manner, which was approximately 10-20 times higher than that induced by β-catenin or CK1ε on their own.

A mutant β-catenin expression construct (S33Y) was also tested in this assay. The S33Y mutant of β-catenin is not rapidly degraded by the β-catenin destruction complex (that is typically active in unstimulated cells), and thus accumulates to higher levels in cells. As expected, the constitutively active β-catenin mutant S33Y most strongly enhanced Topflash activity.

After establishing the assay setup, next the involvement of DDX3 in β-catenin mediated gene expression was investigated using MCF7cells as a model. This allowed to compare β-catenin mediated Topflash activity between non-silencing control (NSC) cells and cells with reduced DDX3 expression (ShDDX3 cells).

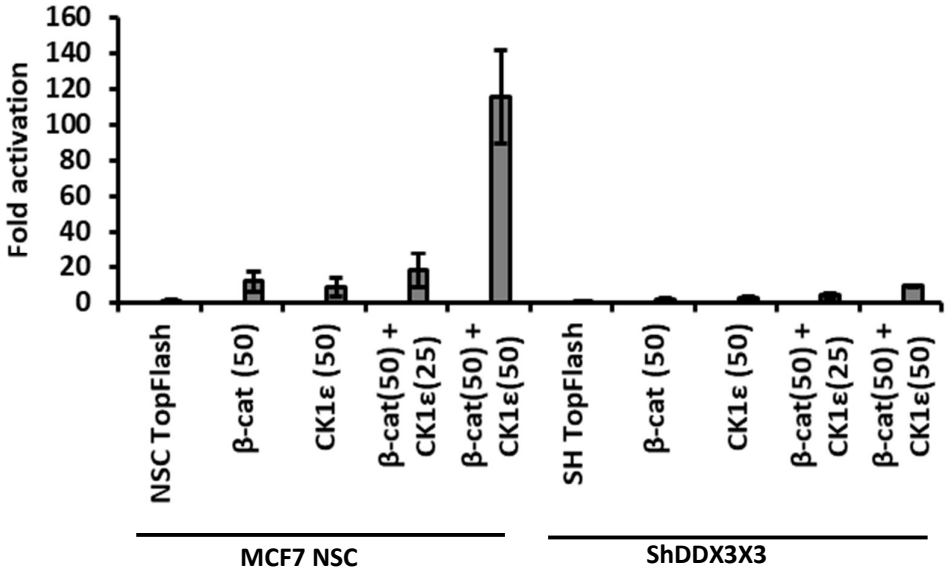

Figure 5.2: DDX3 enhances β-catenin- and CK1e-mediated Topflash reporter activity

DDX3 knockdown was induced in MCF7 NSC and ShDDX3 cells by adding doxycycline (2µg/ml) in the medium. MCF7 NSC and ShDDX3 cells were transfected with the TCF-dependent Topflash reporter construct (60ng/ml) and a Renilla luciferase control construct (for normalization) (20ng/ml). As indicated in the figure, the expression constructs for wildtype β-catenin (50ng/ml), and/or CK1ε (25ng/ml or 50ng/ml) were co-transfected. An empty vector plasmid was used to adjust total DNA concentration to 230ng. 24h after transfection, samples were harvested using Passive Reporter Lysis Buffer. Firefly luciferase and Renilla luciferase activities were then measured. Renilla luciferase values were used for normalisation. Shown here is one representative experiment of three independent experiments, depicting the mean of three triplicates with error bars showing SD

As previously seen, WT β-catenin and CK1ε activated the Topflash reporter to some extent, which was further enhanced by co-expression of both β-catenin and CK1ε. B-catenin and CK1e-mediated Topflash activity were strongly reduced in DDX3 knockdown cells (ShDDX3) compared to NSC cells.

To clarify whether this is mediated via DDX3's effect on CK1ε and/or direct effect on β-catenin, the effect of DDX3 knockdown on activity of the constitutively active S33Y mutant of β-catenin was tested.

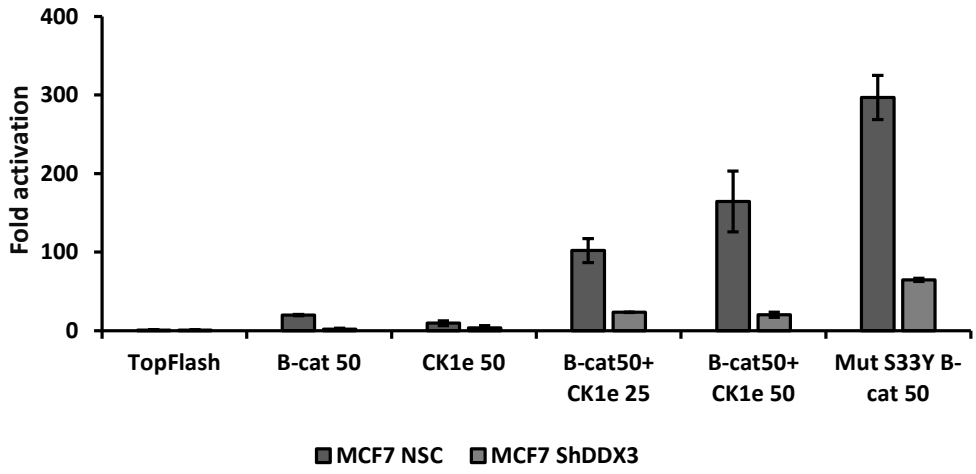

Figure 5.3: DDX3 knockdown affected β-catenin (WT and mutant) and CK1ε mediated Topflash reporter activity

DDX3 knockdown was induced in MCF7 NSC and ShDDX3 cells by adding doxycycline (2μg/ml) in the medium. MCF7 NSC and ShDDX3 cells were transfected with TCF-dependent Topflash reporter construct (60ng/ml) and a Renilla luciferase control construct (for normalization) (20ng/ml). As indicated in the figure, the expression constructs for wildtype β-catenin (50ng/ml) and/or a constitutively active mutant β-catenin (S33Y) (50ng/ml), and/or CK1ε (25ng/ml or 50ng/ml) were co-transfected. An empty vector plasmid was used to adjust total DNA concentration to 230ng.24h after transfection, samples were harvested using Passive Reporter Lysis Buffer. Firefly luciferase and Renilla luciferase activities were then measured. Renilla luciferase values were used for normalization. Shown here is one representative experiment of three independent experiments, depicting the mean of three triplicates with error bars showing ±SD.

As seen previously, S33Y β-catenin activated the Topflash reporter more strongly than WT β-catenin. The activity of the S33Y β-catenin mutant was also strongly reduced in DDX3 knockdown (shDDX3) cells compared to their NSC counterparts.

This suggests that DDX3 can indeed regulate the Wnt pathway through a direct effect on β-catenin-mediated transactivation at the promoter level.

Whether DDX3 affects levels of active β-catenin protein was investigated by performing western blot analysis on DDX3 knockdown (shDDX3) compared to NSC cells with an antibody that specifically recognizes the active non-phosphorylated form of β-catenin.

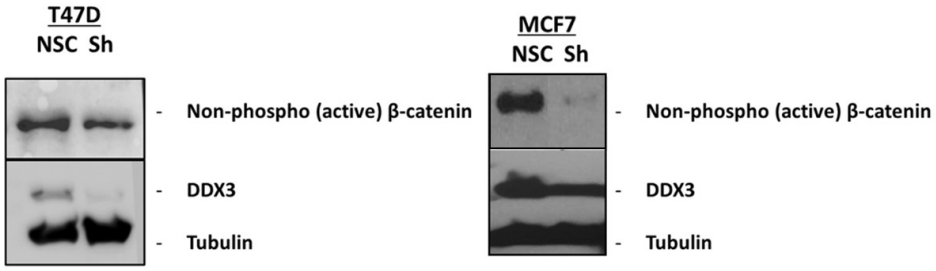

Figure 5.4: DDX3 knockdown reduced non-phospho (active) β-catenin expression in MCF7 and T47D breast cancer cell lines

DDX3 knockdown was induced in T47D and MCF7 NSC and ShDDX3 cells for three days by the addition of doxycycline (2μg/ml) in culture medium. Equal number of cells were harvested for both NSC and ShDDX3 for each cell type. Samples were prepared using Lamaelli sample buffer and subjected to SDS-PAGE analysis and immunodetection with indicated antibodies and a loading control tubulin. Shown here is one representative experiment out of two independent experiments.

This analysis demonstrated slightly reduced non-phosphorylated (active) β-catenin protein levels in ShDDX3 cells compared to their NSC counterparts. This suggests that DDX3 also regulates levels of active β-catenin protein, presumably via its effects on CK1ε mediated activation and stabilization of β-catenin.

5.2 Do WNT pathway components modulate ERα activity?

Interestingly, β-Catenin was suggested to be a positive regulator of Estrogen receptor-α function in breast cancer cells. From the experiments in the previous section, there was an evidence that DDX3 knockdown affects active β-Catenin levels as well as β-Catenin-mediated Topflash reporter activity.

Thus, the next aim was to determine whether DDX3's role in CK1ε / β-Catenin-mediated activation of the Wnt pathway could influence the ERα read-outs used in Chapter 3.

It was hypothesized that DDX3's regulation of WNT pathway components might indirectly regulate ERα activity in three different ways:

1. β-catenin leads to increased ERα protein levels, as has previously been demonstrated (Mayer et al 2011). The effects of DDX3 on β-catenin levels and activity could therefore lead to an increase in ERα levels which then enhances ERE reporter activity.
2. β-catenin (or β-catenin + DDX3) could directly interact with ERα at the promoter level to jointly drive transactivation of the ERE reporter
3. DDX3 enhances CK1ε activity, and CK1e (akin to CK2) could directly phosphorylate ERα leading to its activation.

To test these hypotheses, a very efficient readout system used in Chapter 3, namely the ERE-reporter gene assay in which any activation of ERα results in enhanced ERE activation was used. ERE reporter assays were used to understand the potential effects of CK1e/β-catenin on ERα protein levels and activity.

To first determine whether the effect of β-catenin on ERE-activation was mediated by increased ERα expression, its effects on endogenous versus overexpressed ERα was compared in ERE reporter assays in MCF7 cells.

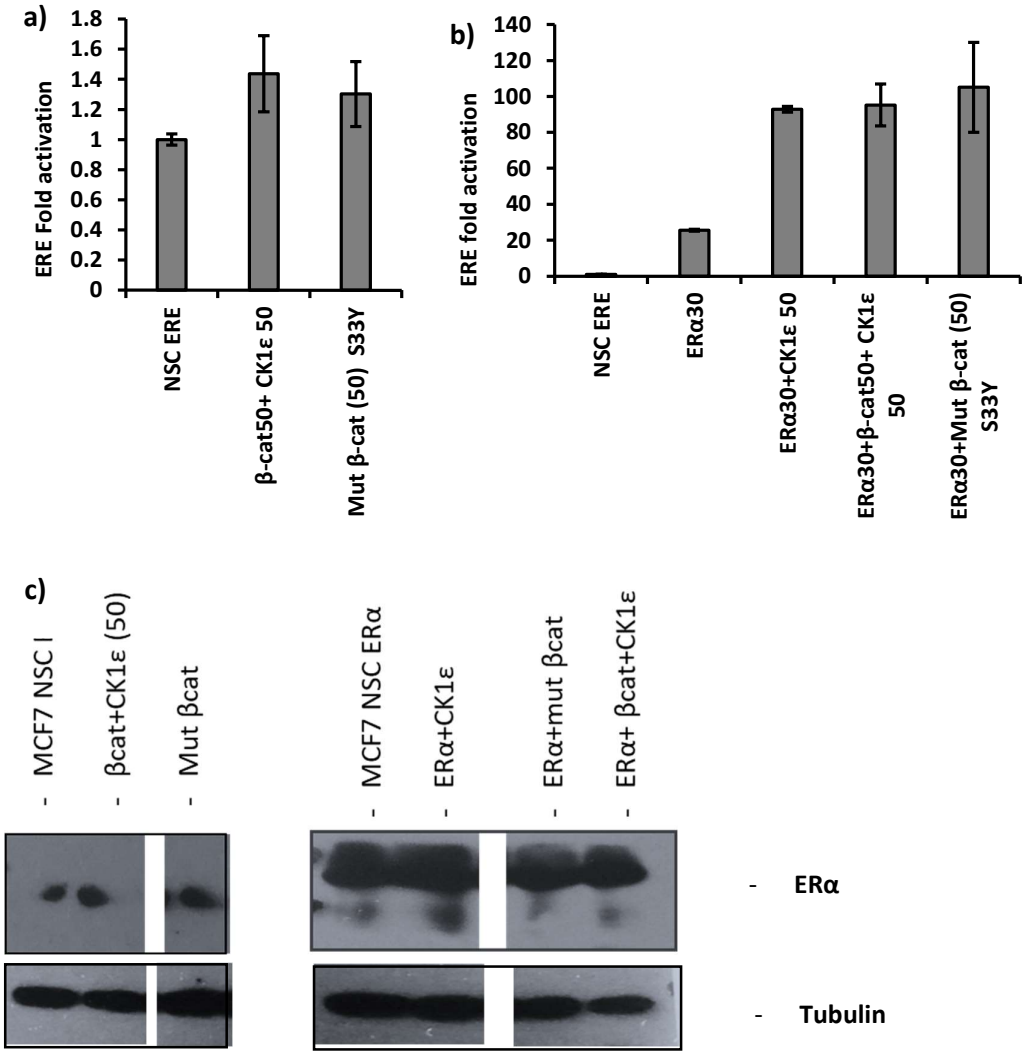

Figure5.5: a, b and c: CK1ε activated ERα mediated ERE activity

5.5 a & b) MCF7 cells were transfected with ERE reporter construct (60ng/ml) and a Renilla luciferase control construct (for normalization) (20ng/ml). As indicated in the figure, the expression constructs for Wild type β-catenin (50ng/ml) or a constitutively active mutant β-catenin (S33Y) (50ng/ml) and/or CK1ε (50ng/ml), and/or ERα were co-transfected, and an empty vector plasmid was used to adjust total DNA concentration to 230ng. 24h after transfection, samples were harvested using Passive Reporter Lysis Buffer. Firefly luciferase and Renilla luciferase activities were then measured. Renilla luciferase values were used for normalization. Each experiment was performed in triplicate. Shown here is one representative experiment of three independent experiments, with error bars showing ±SD 5.5 c) Western blot analysis was performed for the samples from ERE reporter assay with endogenous and overexpressed ERα, and/or CK1ε, and/or β-catenin (from Figure 5.5 a&b).

The basal ERE activation was very low in the absence of overexpressed ERα compared to overexpressed ERα (Figure 5.5a and b). CK1ε co-expressed with β-catenin or the constitutively active β-catenin S33Y mutant enhanced the weak ERE activity mediated by endogenous ERα ~1.5-fold (Figure 5.5a). Overexpression of ERα resulted in greatly increased ERE activity as seen before (chapter 3, section 1). CK1ε enhanced ERE activation mediated by overexpressed ERα by ~4.5-fold when compared to cells transfected with ERα alone. ERE activation did not increase further when β-catenin was also expressed alongside CK1ε and ERα. However, co-expressing mutant SY33 β-catenin with ERα enhanced ERE activity also by ~4.5-fold. This suggests that there might be a direct effect of β-catenin on ERα activity in enhancing ERα mediated ERE reporter activity.

The increase observed with CK1ε/ β-catenin expression on endogenous ERα activity was very small, so it is unlikely that an increase in endogenous ERα levels mediated by β-catenin plays a substantial role in the effects of DDX3, CK1ε and β-catenin in the presence of overexpressed ERα. However, to compare ERα protein levels directly, western blot analysis was also carried out on the lysates from the reporter assay. The levels of endogenous and over-expressed ERα were compared and the results for potential effects of β-catenin and CK1ε on ERα levels were analysed. It was difficult to consistently detect endogenous ERα because of the low expression levels; but there was no major increase in endogenous ERα expression in the presence of exogenous β-catenin or CK1ε. There was much more ERα in samples with overexpressed ERα (as expected) and no further increase in ERα levels was observed with over-expressed β-catenin/CK1ε. This suggests that the strong enhancement in ERE reporter assays observed with DDX3 or β-catenin/CK1ε co-expression is unlikely to be mediated via increased ERα levels.

As explained above, it is also possible that β-catenin acts together with ERα at the promoter level and /or that CK1ε affects ERα activity directly. To further test these possible mechanisms, ERE reporter assays were next performed in MCF7 NSC and ShDDX3 cells.

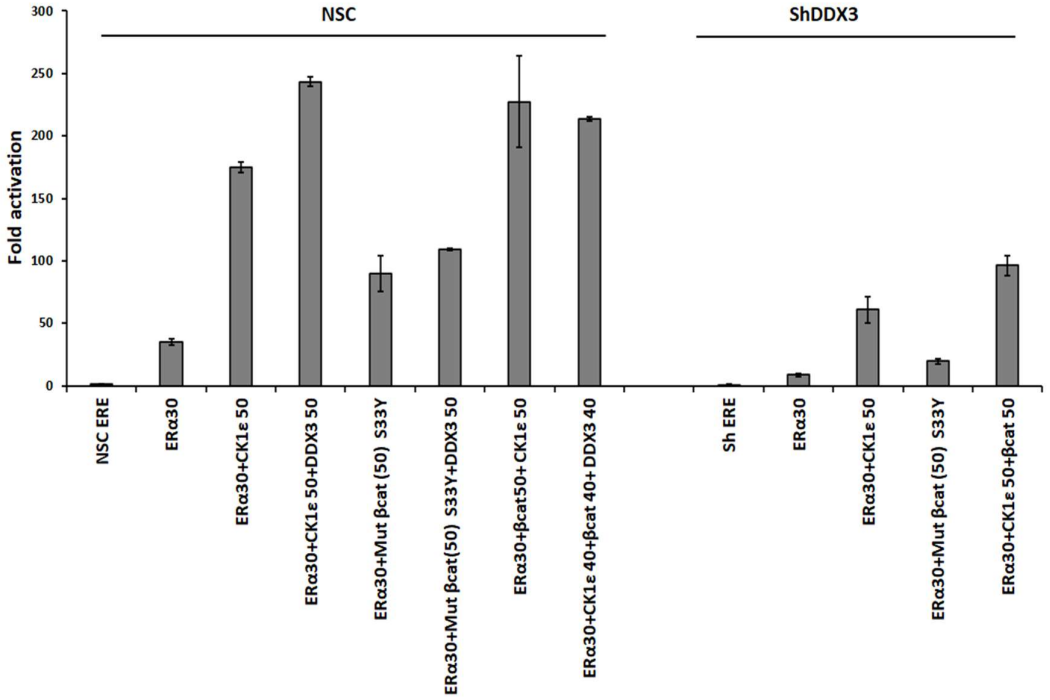

Figure 5.6: DDX3 knockdown affected WT-β-cat and CK1ε, and mutant β-cat (S33Y) mediated ERE activation

DDX3 knockdown was induced in MCF7 NSC and ShDDX3 cells by adding doxycycline (2μg/ml) in the medium. The cells were transfected with ERE reporter construct (60ng/ml) and a Renilla luciferase control construct (for normalization) (20ng/ml). As indicated in the figure, expression constructs for ERα (30ng/ml), CK1ε (50ng/ml), and/or wildtype β-catenin (50ng/ml) or a constitutively active mutant β-catenin (S33Y) (50ng/ml), were co-transfected and an empty vector plasmid was used to adjust total DNA concentration to 230ng. 24h after transfection, samples were harvested using Passive Reporter Lysis Buffer. Firefly luciferase and Renilla luciferase activities were then measured. Renilla luciferase values were used for normalization. Shown here is one representative experiment of three independent experiments, depicting the mean of three triplicates with error bars showing ±SD.

As seen previously (Figure 5.5) CK1ε enhanced ERα mediated ERE activation and this was further enhanced by DDX3. In this assay system there was higher level of ERE activation with CK1ε compared to S33Y β-catenin, which was opposite of effects the observed in the Topflash reporter assay, where mutant S33Y β-catenin activated more than β-catenin and CK1ε together. This might suggest that CK1ε has an additional, β-catenin-independent effect in activation of ERE activity (potentially directly on ERα activity via phosphorylating it).

When overexpressing ERα with mutant S33Y β-catenin, there was an enhancement of ERα activity compared to ERα alone, but no further increase with DDX3. This suggests that β-

catenin and ERα can act together at the promoter level to enhance ERE reporter activity, but that DDX3's main effect might be upstream of this.

ERE activity was overall reduced with DDX3 knockdown for all the conditions, including ERE activation mediated by S33Y β -catenin. This might be because of DDX3's direct effect on ERα rather than on β-catenin.

Based on this data it was still difficult to answer what part of the CK1 effect is β-catenin mediated and what effect is directly on ERα.

5.3 CK1ε has an independent effect on ERα activation:

The effects of DDX3 on IKKε-mediated ERα phosphorylation and activation were previously explored in Chapter 3. In addition, DDX3 was also shown to interact with IKKα, IKKβ and TBK1, kinases that are related to IKKε (de Leeuw et al., 2011). Therefore, in this study it was tested whether these kinases could also drive ERE activity or whether this was specific to IKKε, as they were also shown to interact with DDX3 (Fullam et al., 2018, Cruciat et al., 2013a). As DDX3 had also been shown to interact with CK1ε and to enhance its activity, CK1ε was also included in this study.

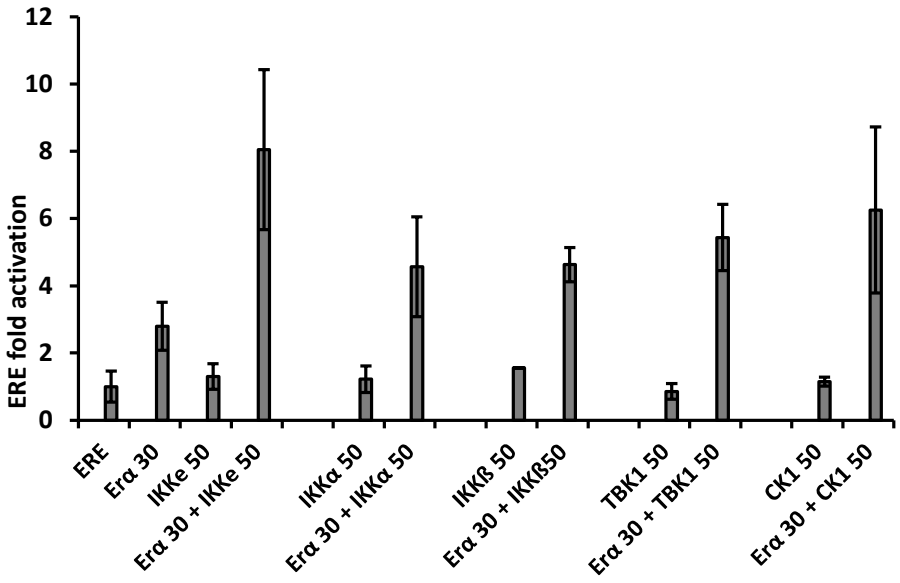

Figure 5.7: CK1ε activates ERE activity similar to IKKε and other related kinases

MCF7 cells were transfected with the ERE reporter construct (60ng/ml) and a Renilla luciferase control construct (for normalization) (20ng/ml). As indicated in the figure, expression constructs for ERα (30ng/ml), IKKε, IKKα, IKKβ, TBK1 and CK1ε (all at 50ng/ml) were co-transfected, and an empty vector plasmid was used to adjust total DNA concentration to 230ng. 24h after transfection, samples were harvested using Passive Reporter Lysis Buffer. Firefly luciferase and Renilla luciferase activities were then measured. Renilla luciferase values were used for normalization. Shown here is one representative experiment out of three independent experiments, depicting the mean of three triplicates with error bars showing ±SD.

In these experiments, it was observed that IKKα, IKKβ, TBK1, and CK1ε could all drive ERα-dependent ERE activity. In the Wnt pathway the kinases CK1ε and CK2 play important roles. The casein kinases (CK) are subdivided into either casein kinase 1 (CK1) or casein kinase 2 (CK2) families and they have high level of homology in their catalytic domains (Stöter M et al. 2005). CK2 was shown to be upregulated in most proliferating tissues and was shown to phosphorylate ERα at S167, at S282 and S559 and regulate interaction of ERα with estrogen response elements (ERE) in vitro. After confirming that, CK1ε activated β-catenin mediated ERα activation, there was a need to investigate if CK1ε could also phosphorylate ERα.

To further examine whether CK1ε can indeed phosphorylate ERα, a western blot analysis was carried out on lysates from MCF7 cells overexpressing ERα and CK1ε.

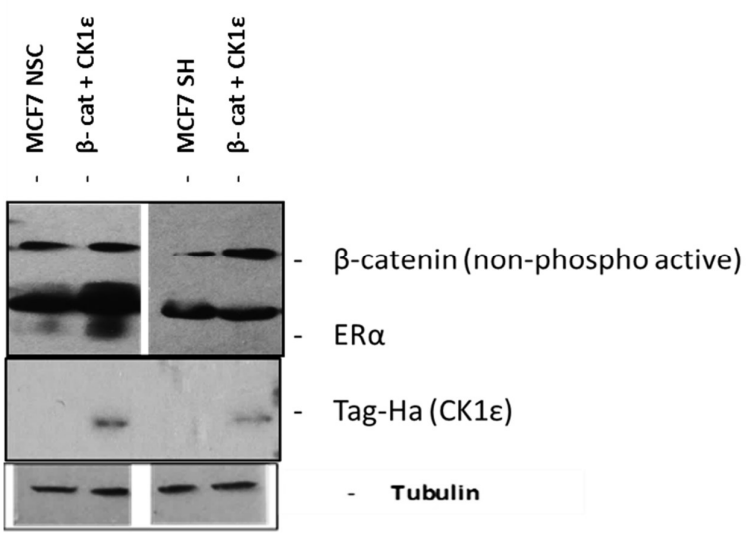

Figure 5.8: CK1ε increased ERα protein levels

Samples from the reporter assay performed in MCF7 NSC and Sh cells, were used to perform SDS-PAGE and western blot analysis to examine ERα and β-catenin protein levels, as indicated. Shown here is one representative experiment of two independent experiments.

The Western Blot shown in Figure 5.8 was initially carried out to examine total ERα protein levels in the presence of exogenous β-catenin and CK1ε expression. There was a slight increase in ERα levels when both of these were co-expressed in NSC cells compared to the control. The slight smearing/upshift of the ERα band was also noticed, indicating the possibility of phosphorylation of ERα by CK1ε (akin to that seen with CK2) (Williams et al., 2009). The NSC lysates overexpressing β-catenin and CK1ε showed smearing of the band which was not present in the matching DDX3 knockdown lysate, supporting the hypothesis that DDX3 may drive phosphorylation of ERα.

In this study, it was previously confirmed that DDX3 plays a role in the phosphorylation of ERα (chapter3). And since there was now an indication of CK1ε causing smearing of the ERα band indicative of phosphorylation (Figure 5.8), it was next investigated whether DDX3 also regulates CK1ε mediated phosphorylation of ERα.

5.4 CK1ε mediates phosphorylation of ERα:

To confirm these observations, over-expression experiments were carried out in MCF7 NSC and shDDX3 cells on a larger scale (6wp transfections) and ERα S167 phosphorylation was detected with a phospho-specific antibody to determine whether CK1ε could indeed phosphorylate ERα at this residue.

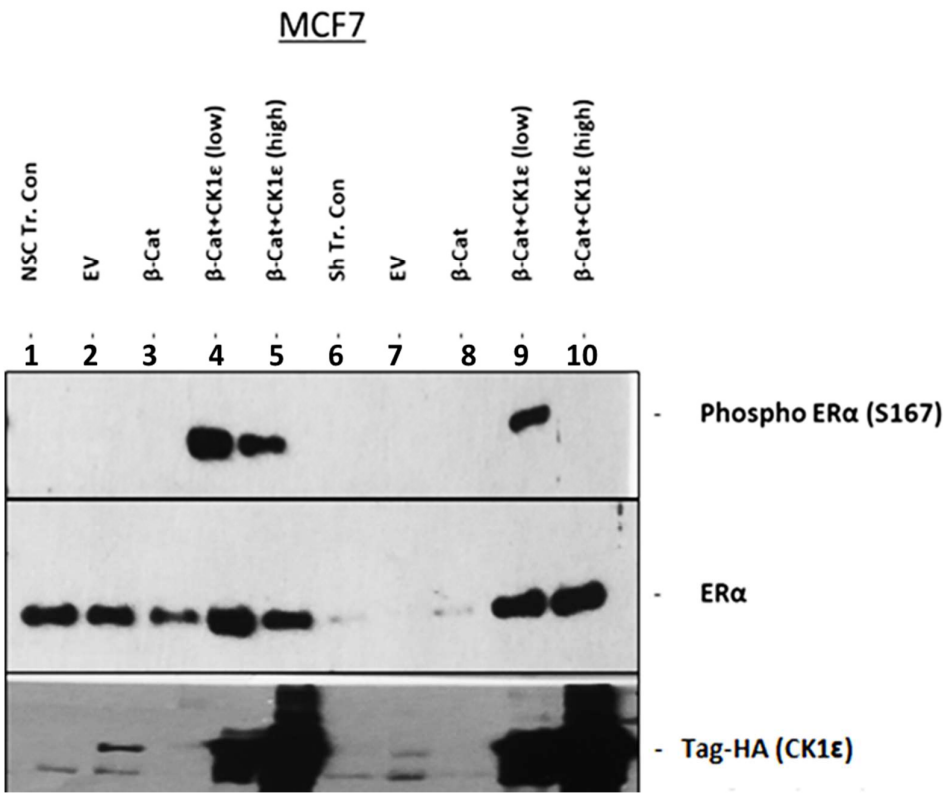

Figure 5.9: DDX3 knockdown reduced CK1ε mediated phosphorylation of ERα

DDX3 knockdown was induced in MCF7 NSC and Sh cells by adding doxycycline (1µg/ml) to the culture medium for 3 days. Cells were then seeded in a 12wp and transfected with β-catenin (2µg) and CK1ε (2µg and 4µg) expression constructs along with a matching Empty vector control (EV), as indicated. 24 hours post transfection, samples were prepared and subjected to SDS-PAGE and western blot analysis to examine phospho-ERα and β-catenin protein expression levels. Shown here is a representative experiment of two independent experiments.

In these experiments, it was observed that cells overexpressing low levels of CK1ε had higher levels of phosphorylated ERα (lane4), which was not detectable in the corresponding shDDX3 cells (lane 9). This suggests that DDX3 knockdown reduced CK1ε mediated phosphorylation of ERα at S167. There was no difference observed between NSC and ShDDX3 cells with the higher amount of CK1ε.

To better understand the relevance of CK1ε-mediated phosphorylation of ERα, the phosphorylation of ERα mediated by IKKε was compared with that mediated by CK1ε in HEK293T NSC and ShDDX3 cells.

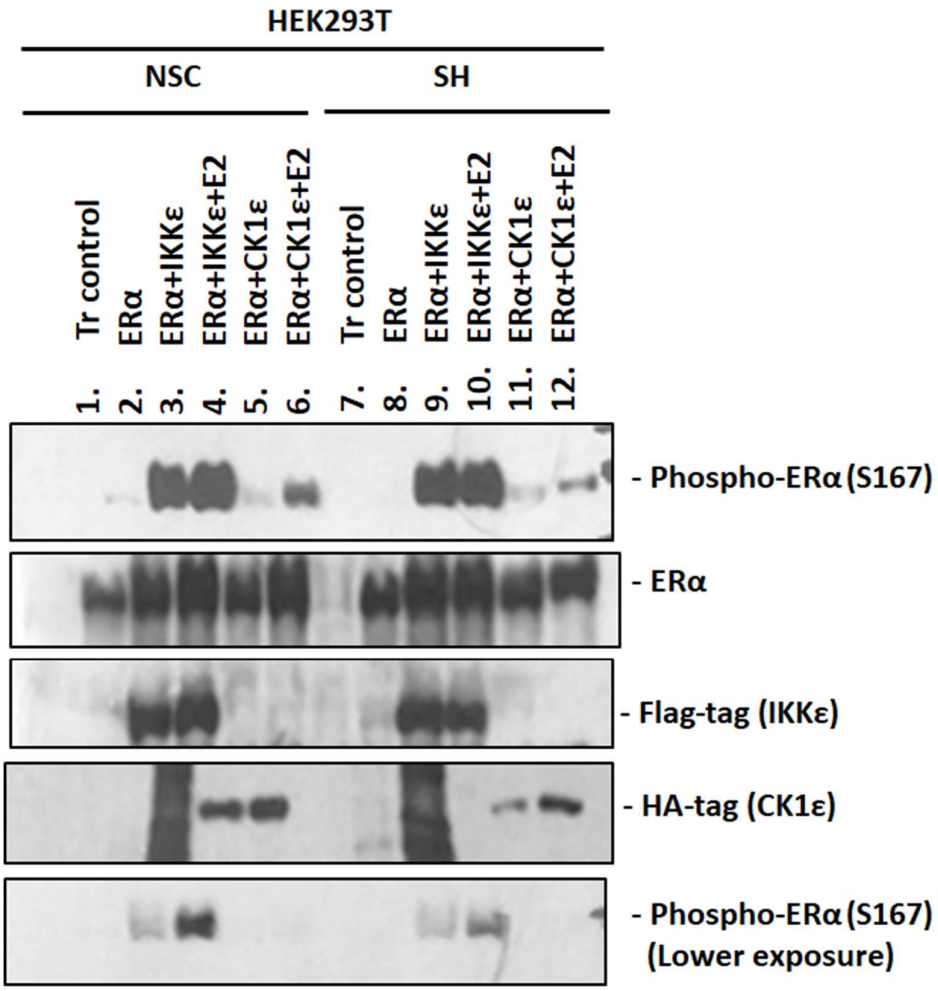

Figure 5.10: CK1ε and IKKε mediated phosphorylation of ERα

DDX3 knockdown was induced in HEK293T cells by addition of doxycycline (1µg/ml), the non-silencing control NSC cells and the DDX3 knockdown ShDDX3 cells were seeded in 12wp and transfected with indicated expression constructs for 24hr. Cells were stimulated where indicated with 25nM E2 (estradiol) for 8hr before harvesting. SDS-PAGE and Western blot analysis was performed on the lysates to examine phospho-ERα protein levels. Shown here is one representative experiment.

As seen previously, IKKε overexpression strongly phosphorylated ERα at S167, which was slightly enhanced with additional E2 stimulation (Figure 5.10: lane3, 4). CK1ε overexpression only led to a slight increase in phosphorylated ERα (lane 5), which was quite strongly enhanced by E2 stimulation (lane 6). CK1ε mediated phosphorylation of ERα was reduced in DDX3 knockdown (ShDDX3) cells for E2 stimulated cells (lane 6 vs lane 12). The lower exposure phospho-ERα (lower panel) showed reduced phospho-ERα level for E2 stimulated ShDDX3 cells compared to controls, confirming our initial observations that DDX3 might modulate IKKε mediated activation of ERα by phosphorylating it.

It would have been ideal to compare E2 stimulated IKKε and CK1ε overexpressing lysates with E2 induced ERα phosphorylation as a control, but it was mistakenly not included in the experiment. Nonetheless, it can be concluded from this experiment that DDX3 knockdown reduced CK1ε mediated phosphorylation of ERα.

5.5. Chapter conclusion

In conclusion, DDX3 knockdown reduced CK1ε mediated phosphorylation of ERα, indicating that DDX3 might has a role in CK1ε-mediated regulation of ERα. CK1ε-mediated phosphorylation was much weaker compared to IKKε, indicating that it is not as good as IKKε at phosphorylating ERα.

It was also evident that CK1ε has a β-catenin-independent effect on the ERα /ERE system by directly phosphorylating ERα, supporting the effects observed in ERE reporter assays where there was stronger enhancement of ERE activity with CK1ε overexpression compared to mutant S33Y β-catenin over-expression.

Chapter 6. Discussion

6.1 Effects of DDX3 on ERα activity

This work focuses on the investigation of DDX3's potential role in ERα activation. Previous studies from the Dr Schroeder's lab showed that DDX3 interacts with IKKε (Schroder et al., 2008), in an interaction that ultimately facilitates activation of the transcription factor IRF3 and expression of the anti-viral cytokine IFNβ. The hypothesis for this project was that DDX3 and IKKε might have a similar collaborative effect on ERα activation in the context of ER+ breast cancer. This hypothesis was inspired by a now retracted paper by Guo et al., 2010, in which it was suggested that IKKε mediates ERα phosphorylation and enhances estrogen-independent ERα activity and cell proliferation. In this study, IKKε was shown to phosphorylate ERα at S167 in an estrogen-independent manner and contribute to tamoxifen resistance (Guo et al., 2010b) (now retracted paper). Other DEAD-box-helicases' such as DDX5 and DDX317, had already been shown to physically and functionally interact with nuclear receptors, including ERα (Clark et al., 2008) (Fuller-Pace and Nicol, 2012, Wortham et al., 2009), making it conceivable that DDX3 also might have a similar function further warranting an investigation of a potential involvement of DDX3 in ERα activation.

In this study, the hypothesis that DDX3 and IKKε collaborate to regulate ERα activity, was tested, which is akin to their role in IRF3 activation. DDX3 and IKKε were previously both independently shown to be breast cancer oncogenes, but this study is the first demonstrating the collaborative role of DDX3 and IKKε in enhancing ERα activity. When DDX3 and IKKε were independently co-expressed with ERα there was a slight enhancement of ERα activity in ERE reporter gene assays, but when DDX3 and IKKε were jointly co-expressed there was further enhancement of ERα activity.

The data presented in this study suggested that there is a direct interaction between DDX3 and ERα (which was tested and confirmed in this study), and DDX3 might directly enhance ERα activity, contributing to the enhancement of IKKε mediated effect on ERα activation. On comparing ERα activation in complete and estrogen depleted medium it was evident that DDX3 and IKKε mediated activation was enhanced in the absence of estrogen, suggesting that DDX3 mediated enhancement whether ERα activity is independent of presence/ absence of estrogen.

6.1.1 Enzymatic activity of DDX3 is not required for activating ERα

The enzymatic function (ATPase and RNA unwinding) of DDX3 is essential for most of the cellular processes controlled by DDX3. However, this study demonstrated that the enzymatic activity of DDX3 is not essential for its effect on ERα activity. The ATPase and helicase deficient mutant of DDX3 K230E was able to drive ERα activation at least as potently as the wild-type. K230E mediated activation of ERα seemed even higher compared to wild-type DDX3, but this might be due to its higher expression levels compared to wild-type DDX3. The results presented here clearly demonstrate that DDX3's effect on ERα activation is independent of its ATPase and helicase activity, similar to DDX5/17 that were shown to affect nuclear receptor activity independent of their enzymatic activity (Fuller-Pace and Nicol, 2012).

DDX3's role in IRF3 activation and IFNβ induction was also independent of its enzymatic activity, where it was proposed to act as a multifunctional adaptor molecule. Based on this, we had hypothesized that this might also be true for DDX3's role in ERα activation. So, this finding was not completely unexpected based on previous findings from the MU Host-Pathogen Interaction lab and our hypothesis.

RK-33, an inhibitor of DDX3's ATPase activity, was suggested to supress proliferation of cancer cells, including breast cancer cells, however recently questions have emerged about its

specificity for DDX3. The findings that DDX3 regulates ERα activity in the presence and absence of estrogen and independent of its enzymatic activity is an important novel finding, as DDX3's effect on ERα would not be suppressed by RK-33 or other inhibitors that target its enzymatic activity. The findings of this study are also important from a clinical point of view, as any inhibitor of DDX3 that targets its enzymatic activity could potentially even make DDX3 more available for pathways that are driven by DDX3's ATPase-independent effects. However, this will require further evaluation.

6.1.2 Endogenous DDX3 mediates ERα activity in T47D cells

This study demonstrated that DDX3 modulates estrogen responses of Breast cancer cell lines by regulating ERα activation due to ligand-independent effect of DDX3 on ERα. As ERα positive breast cancer cells are dependent on estrogens for their proliferation, we investigated whether DDX3 was essential for estrogen responses of T47D and MCF7 cells and demonstrated that DDX3 knockdown reduced estrogen-dependent as well as basal ERα activity in T47D cells. The results suggest that DDX3 not only plays role in estrogen-independent activation of ERα as hypothesized originally, but also regulates ligand-stimulated ERα activity. In a now retracted paper, it was suggested that IKKε mediated phosphorylation drives estrogen-independent ERα activity and renders the cells non-responsive to tamoxifen treatment (Guo et al, 2010). This highlights the potential importance of this pathway from a clinical point of view. So, if DDX3 contributes to IKKε-mediated and estrogen-independent activation of ERα, this would implicate a novel role for DDX3 in breast cancer oncogenesis and tamoxifen resistance.

These results confirmed that endogenous DDX3 plays a role in mediating ERα activity in T47D and MCF7 cells and indicate that estrogen stimulation is not able to overcome defects caused by DDX3 knockdown. This is potentially the first study showing that endogenous DDX3 is

required for ERα activity. It is possible that DDX3's role in mediating S167 phosphorylation might also affect estrogen-stimulated ERα activity.

It was shown that p68, a DEAD-box helicase requires the DNA binding domain of ERα and depends on the ligand binding/AF2 domain of ERα and was also recruited to the ERα -responsive promoter upon estrogen stimulation and leads to ERα target gene expression (Wortham et al., 2009). So, it is possible that DDX3 might also function in similar way in activation of ERα.

6.1.3 Hypoxia enhanced DDX3 expression and ERα activity

DDX3 was shown to be highly expressed in breast cancer cells, and functions as an important regulator of tumour cell growth, proliferation. HIF1α was shown to be a transcriptional activator of DDX3 in breast cancer cells upregulating DDX3 expression in hypoxic conditions (Botlagunta et al., 2011). Chemically induced hypoxia (cobalt chloride: CoCl2) was shown to induce DDX3 mRNA expression, and this study also demonstrated that the DDX3 promoter contains HREs (HIF-response elements) suggesting that DDX3 expression is directly controlled by HIF1α. Hypoxia is one of the major characteristics of tumours, including breast tumours. Therefore, hypoxia-related DDX3 upregulation might be associated with a more aggressive phenotype in breast cancer. This caught our attention as there is a possibility that increased DDX3 expression under hypoxic conditions (such as in clinical scenario) would lead to increased ERα activity based on this study's initial results. It was then essential to answer the question, whether hypoxia induced upregulation of DDX3 expression enhances ERα activity.

The data for DMOG (Dimethyloxalylglycine) treated T47D NSC and ShDDX3 cells, showed a slight enhancement of ERα activity in DMOG-induced hypoxia in NSC cells as well as a slight increase in DDX3 expression. Interestingly, DDX3 knockdown seemed to reduce this hypoxia-mediated effect on ERα activity. However, these are preliminary results that need confirmation, as it was

difficult to get consistent results. HIF1α is known to be a highly unstable proteins so it is possible that we might have lost the detection window after HIF-1α mediated upregulation of DDX3 that would result in ERα activity enhancement. There was slight enhancement of ERα activity in DMOG induced hypoxia in the studies and it was difficult to get consistent results. And the western blot analysis indicated slight increase in DDX3 expression, but the results need confirmation as DMOG-time point experiments done to test HIF1α and DDX3 expression were not successful (not shown in this study). Another approach that could be tried to investigate further could be using a hypoxic chamber/ incubator, as it is difficult to control chemically induced hypoxia. It would be also interesting to further investigate HIF1α-mediated DDX3 upregulation's role in estrogen responsiveness and cell proliferation.

To summarise, this data provides some indication that Hypoxia indeed leads to upregulation of DDX3 expression and that this could result in increased ERα activity, but this would need to be confirmed in more stringent system, such as using hypoxic chamber/ incubator.

6.1.4 Effects on Phosphorylation of ERα

IKKε was previously suggested to phosphorylate ERα at S167, leading to estrogen-independent ERα activity and increased cell proliferation in the absence of estrogen (in a now retracted paper) (Guo et al., 2010b). This work confirmed that IKKε can indeed phosphorylate ERα at S167, thus backing up this aspect of the retracted study. DDX3 overexpression and knockdown also affected ERα phosphorylation, supporting the initial hypothesis that DDX3 and IKKε collaborate to enhance ERα activation.

It is also possible that this effect might not only be limited to IKKε and can also be driven by other kinases, such as IKKα and CK1. For example, CK1ε's effect on ERα phosphorylation was also tested in this study, which will be discussed here later.

6.1.5 DDX3 directly interacts with ERα and regulates its activity

DEAD-box helicases are known to be able to interact with nuclear receptors and regulate their activity. We wanted to explore whether DDX3 physically interacted with ERα in MCF7 and T47D breast cancer cell lines. This data shows the direct interaction between DDX3 and ERα, which is confirmed by two different techniques (IPs and pulldowns). It was important to have solid evidence for this, to confidently support that the effects observed in ERE reporter gene assays and on ERα target gene expression are not indirect or unspecific. The effects of normal culture conditions versus estrogen-deplete and estrogen stimulation-post depletion conditions on the DDX3- ERα interaction, were also tested to understand whether estrogen had any effect on this interaction. In this data there was a slight indication that DDX3 and ERα interacted more in complete/normal medium, but it was difficult to get consistent results, as protein interaction experiments are very sensitive, and it was difficult to control all the parameters/ factors involved. There doesn't seem to be a dramatic increase or loss of the interaction with estrogen

(depletion), but more subtle effects might have been missed in the experiments that might potentially still be physiologically relevant.

Next the regions of DDX3 were explored to map the interaction sites on DDX3, and therefore DDX3 truncation mutants were tested in both assay setups (co-IPs (data not shown) and pulldowns. In the experiments presented here, both parts of DDX3 (1-408 and 409-662) truncations could bind to ERα in both complete and estrogen depleted conditions. However, the interaction with full-length DDX3 was stronger. From the ERE reporter assay data performed in MCF7 cells it was also evident that DDX3 truncations could also activate ERα activity. The ERE-reporter data from MCF7 knockdown cells suggests that none of the truncations are able to drive ERα activation. This indicated the possibility of multiple interaction sites on DDX3 contributing to the overall functional interaction of DDX3 and ERα that might contribute to ERα activation.

It is also possible that there might be some technical artifacts leading to non-specific interaction. In the ERE reporter gene assays demonstrated in chapter 3, there was an unexpected activation by 139-408 and 139-572. Based on the work done by previous lab members (Gu et al 2013), these two truncation mutants were shown not to interact with IKKε. This might suggest that the DDX3 effect we see on ERα activity could partly be IKKε- independent and partly IKKε-dependent.

The interaction sites on ERα were not investigated in this study, due to time constraints. To further characterize the interaction between DDX3 and ERα, mapping of interaction sites on ERα is warranted to understand whether DDX3 interacts with the AF1 and/or AF2 domain of ERα, which could potentially help to answer whether DDX3-mediated ERα regulation is estrogen-dependent or estrogen-independent. It is also possible that DDX3 and ERα interact at multiple

sites and further characterisation of this interaction could help in understanding DDX3's exact mechanism(s) for regulating ERα activity.

6.1.6 DDX3 affects ERα target gene expression

This study also tests the effects of DDX3 knockdown on expression of previously identified ERα target genes, namely NRIP1, PS2, EGR3, ABCA3, GREB1 were previously shown to be direct downstream targets of ERα(Varešlija et al., 2016). NRIP1, GREB1, and ABCA3 genes were shown to be ER responsive. GREB1 is an estrogen receptor regulated tumour promoter gene. GREB1 mRNA was shown to correlate with ER Status in breast cancer patients and is a predictor of patient survival and responses to tamoxifen treatment. GREB1 was shown to be the most sensitive ER-regulated gene in response to E2 stimulation in breast cancer patients. Overexpression of GREB1 was shown to promote cell proliferation and the clonogenic ability of breast cancer cells (Liu et al., 2012b) . NRIP1 is another a putative ERα target gene that is upregulated by Estrogen and is associated with ER+ status of breast cancer cells (Lin et al., 2004). PS2 is an Estrogen-dependent gene that functions as growth factor in breast cancer cells. EGR3 is shown to be an estrogen responsive gene and its expression was associated with biomarker for treatment resistance. (Varešlija et al., 2016)

Work presented here has shown that DDX3 knockdown reduced expression of these ERα target genes. This data therefore confirmed that endogenous DDX3 plays a role in regulating ERα target gene expression and there was clear suppression of ERα target gene expression in DDX3 knockdown MCF7 and T47D cells.

6.1.7 Effects of DDX3 knockdown on breast cancer cell proliferation

Cell proliferation assays performed in two different breast cancer cell lines, demonstrated that DDX3 knockdown affected proliferation and colony formation ability of T47D and MCF7 cells in the presence and absence of estrogen. It is interesting that this was the case for both MCF7 (wild-type p53) and T47D (p53 inactivating mutation) cells, because DDX3 was previously shown to regulate p53 stability and to have opposite effects of cell proliferation in p53 wild-type and p53 deficient cells. The effects observed on cell proliferation were similar between MCF7 cells and T47D cells, thus suggesting that DDX3's role in regulating p53 does not play a major role in this context.

The effect of DDX3 knockdown on tamoxifen sensitivity were also investigated in this work. Tamoxifen is an ERα antagonist used in the clinical treatment of pre-menopausal ER+ breast cancer patients. However, development of tamoxifen resistance is an ongoing and significant clinical problem. The now retracted paper by Guo et al 2010 had showed that IKKε-mediated phosphorylation of ERα led to E2-independent cell proliferation and increased tamoxifen resistance. Thus, it was essential to evaluate DDX3's role in breast cancer cell proliferation and tamoxifen sensitivity using an MTT assay. The data from this study demonstrated that, DDX3 knockdown cells were more sensitive to tamoxifen treatment at lower concentrations, suggesting that DDX3 knockdown might indeed increase tamoxifen sensitivity in breast cancer cells. The unexpected finding in this study was reversal of response with higher tamoxifen concentrations. This will need further evaluation of this as it could pose a problem if DDX3 is to be targeted therapeutically. Study done on RK-33 (DDX3 inhibitor) in lung cancer, showed that DDX3 knockdown sensitized the to radiation therapy. Findings from study fall in line with this, as DDX3 knockdown resulted in sensitivity to tamoxifen at lower concentrations

It would have been useful to complement the MTT assays and cell proliferation assays with assays that also quantify cell death e.g., using cell death markers such as cleaved caspases, etc to confirm this finding. It is important to point out that cell proliferation and cell death might also be affected by other pathways that were shown to be regulated by DDX3, but it is not possible to dissect these effects in proliferation assays. It would also be interesting to perform similar study with ERα degraders (such as Fulvestrant) and inhibitors for DDX3.

Tamoxifen is an ERα antagonist used in the clinical treatment of pre-menopausal ER+ breast cancer patients. However, development of tamoxifen resistance is an ongoing and significant clinical problem. The now retracted paper by Guo et al 2010 had showed that IKKε-mediated phosphorylation of ERα led to E2-independent cell proliferation and increased tamoxifen resistance. DDX3's role in breast cancer cell proliferation and tamoxifen sensitivity was evaluated using MTT assay. In this data, DDX3 knockdown cells were more sensitive to tamoxifen treatment at lower concentrations, suggesting that DDX3 knockdown increases tamoxifen sensitivity in breast cancer cells. It would have been more useful to also look at cell growth and cell death by using different techniques; like flow-cytometry, looking at increased cell death markers such as caspases, etc to confirm this finding.

6.1.8 Mechanism of DDX3 in regulation of ERα activity

DDX3 could act in two different ways:

1. DDX3 might enhance ERα activation at S167 via mediating its phosphorylation by IKKε, IKKα, CK1ε and potentially other kinases driving estrogen-independent activity of ERα.
2. It is also possible that DDX3 might interact directly with ERα at the promoter level and regulate ERα -dependent transcriptional activity by acting as a transcriptional co-factor, similar to other DEAD-box helicases- DDX17/5.

This might explain why DDX3 affected both estrogen-independent and estrogen dependent signalling and cell proliferation.

This work provides evidence that DDX3 directly physically interacts with ERα. The attempts to probe for IKKε in the interaction experiments to demonstrate the tethering of IKKε to ERα via DDX3, but this was not successful at endogenous levels. However, in over-expression co-IPs performed in HEK239T cells, there was an indication of IKKε's involvement in this interaction (preliminary data not shown here).

DDX3 mutants that lack the nuclear export site and accumulate in nucleus were also tested in interaction assays, to understand if nuclear-expressed DDX3 would have a stronger or weaker effect on ERE read-outs and interaction with ERα, however the results were inconclusive. Another approach to answer this question about DDX3's role as transcriptional cofactor is by testing DDX3's effects on phospho-mimetic ERα, such as S167D and S118D mutants of ERα. In this assay system, S167D and S118D would drive ERE independent of needing phosphorylation at these residues. If DDX3 would still enhance this, that might be evidence that it can also act directly at promoter level.

In summary, this study provides the strong evidence for a role for DDX3 in regulating ERα activity, by regulating estrogen responsiveness of breast cancer cell lines and expression of ERα target genes, through direct physical interaction and phosphorylation. However, it will be interesting to follow-up on regions of DDX3 and ERα involved in this interaction using phosphomimetics approach.

6.2 Proteomics analysis of DDX3 knockdown in T47D cells

Next, the effects of DDX3 knockdown on the proteome of the ERα positive breast cancer cell line T47D were investigated, to get a more global overview of the gene expression changes of ERα target genes.

Using Perseus and subsequent STRING network analysis, differentially expressed proteins and their associated interactomes for different groups were compared. DDX3 knockdown resulted in more downregulated proteins than upregulated proteins in general, which was expected. More proteins were differentially expressed following DDX3 knockdown under deplete medium conditions, which is reminiscent of to the previously described requirement for DDX3 for protein expression/translation initiation under cellular stress conditions. (Oh et al., 2016).

6.2.1 Downregulated proteins ERα KEGG pathway:

Interestingly, the proteins downregulated in DDX3 knockdown cells under estrogen-replete conditions showed significant enrichment of the KEGG Estrogen Signalling Pathway. KEGG analysis pathway showed involvement of HSP90 and 70 along with FKBP52. HSP90 is linked to ERα's ligand binding ability and regulates cell proliferation. HSP70 was also shown to interact with ERα in the nucleus and in the cytoplasm in MCF7 cells in an estrogen-dependent manner. This is an important observation and requires further investigation, as this work focused on estrogen response and interaction between ERα and DDX3. So, it is possible that DDX3 knockdown might affect either nuclear or cytoplasmic estrogen-dependent signalling pathways, warranting further investigation.

Surprisingly, when comparing the proteomes of cells cultured in replete versus estrogen deplete medium, no clear links to estrogen or ERα signalling pathways were observed. This could be because, DDX3 is more of a positive regulator of gene expression, so the upregulated proteins might be upregulated to compensate for loss of DDX3. It is possible that this is due to the stringent tests applied to filter raw data. Applying less stringent statistical tests (e.g. T-test as opposed to ANOVA) could generate a list of more proteins that have more subtle expression differences and by comparing them in heat-map clustering. It is possible that this approach might reveal links to estrogen pathways.

6.2.2 Technical limitations

Compared to the whole proteome of human cells, only a fraction of proteins were detected in LC-MS/MS analysis, fewer than 500-600 proteins were detected in the samples. There can be various reasons for this like sample processing, settings, run-time on the MS machine, and critical thresholds applied for detection of peptides in the LC-MS/MS run. This means that differentially regulated effects/pathways might have been excluded because only a small proportion of the overall proteome was detected in the LC-MS/MS analysis.

Also, for extracting and filtering data for differentially expressed proteins from MaxQuant using Perseus stringent filtering parameters and statistical tests (ANOVA) were applied. These criteria could be loosened to obtain more hits, which would have the advantage of getting more proteins affected by DDX3 knockdown that can reveal additional pathways and network clusters, but it also means that the data generated using such non-stringent parameters may not be very accurate.

In summary, this data highlights the interesting finding about the role of Hsp90/70/FKBP4 in estrogen receptor signalling pathway which could provide an alternative explanation for DDX3's effect on ERα activity. Follow up work on elucidating the relevance of this observation and to try and identify more ERα/estrogen-regulated proteins in the dataset is warranted.

6.3 DDX3's role in the Wnt pathway

The Wnt pathway was shown to be deregulated in several types of cancers, including breast cancer. Genetic mutation-driven activation of Wnt signalling was shown to be a key factor in breast cancer metastasis (Hau CS et al, 2019) and was shown to be associated with EMT and stem phenotype (Li SH, et al. 2011).

The role of DDX3 as a scaffold protein in the Wnt signalling pathway was first identified in 2013 (Crucial et al 2013). DDX3 was shown to interact with the kinase CK1ε, which is involved in regulation of the Wnt pathway. DDX3 was later shown to mediate CK1ε's interaction with Wnt pathway protein dishevelled and mediate its phosphorylation, resulting in inactivation of the B-catenin degradation complex.

Therefore, in the TOPFLASH assay system, it was first confirmed that DDX3 does actually affect β-catenin and CK1ε mediated activation of Wnt pathway. This study established that DDX3 indeed enhances β-catenin and CK1ε-mediated Wnt activation. Study by (Pugh et al., 2012) had shown that mutant DDX3 leads to transactivation of a TCF promoter and enhances cell viability. Therefore, whether DDX3 could also affect transcriptional activity of a constitutively active β-catenin mutant was investigated next and it was determined that DDX3 knockdown reduced TOPFLASH reporter activity induced by the mutant β-catenin.

Interestingly, cross-talk between β-catenin and ERα in human breast cancer cells had been suggested. β-catenin knockdown was shown to result in reduced ERα mRNA and/or protein levels in MCF7 and T-47D and BT-474 breast cancer cells. Previous studies reported a significant reduction of estrogen-induced expression of ERα target genes such as PS2 and GREB1 (Nibedita Gupta and Doris Mayer, 2011; (Varešlija et al., 2016).. They showed that, upon E2 treatment, β-Catenin translocated to the nucleus but did not physically interact with ERα. β-Catenin

knockdown resulted in reduced ERα mRNA and protein Levels, as well as reduced ERα transcriptional activity and cell growth.

This needed further investigation whether DDX3 might potentially contribute to ERα activation via its effects on β-Catenin levels and activity. It was hypothesized that DDX3's regulation of WNT pathway components might indirectly regulate ERα activity in three different ways:

1. β-catenin leads to increased ERα protein levels, as has previously been demonstrated in the paper by Mayer et al (Mayer et al 2011). The effects of DDX3 on β-catenin levels and activity could therefore lead to an increase in ERα levels which then enhances ERE reporter activity.

   However, it was found that the increase of endogenous ERα activity induced by CK1ε/ β-catenin overexpression was very small, and similarly there were only subtle effects on ERα expression levels in the experiments. So, this is unlikely to cause the rather large effects of DDX3 overexpression/knockdown on ERE reporter activity. However, some effects of CK1ε and β-catenin overexpression on the ERE reporter activity were observed, which were more pronounced in the presence of overexpressed ERα. This suggests that the strong enhancement in ERE reporter assays observed with DDX3 or β-catenin/CK1ε co-expression is unlikely to be mediated via increased endogenous ERα levels.

2. β-catenin (or β-catenin + DDX3) could directly interact with ERα at the promoter level to jointly drive transactivation of the ERE reporter.

   It is possible that β-catenin acts along with ERα at the promoter level and /or that CK1ε affects ERα activity directly (see below) (Kim et al., 2010). However, in the experiments presented here, higher levels of ERE activation with CK1ε compared to S33Y β-catenin

were observed, suggesting that CK1ε might have an additional β-catenin-independent effect (potentially directly on ERα activity via phosphorylating it, see below). As mutant S33Y β-catenin could enhance ERE activity it is evident that B-catenin can directly regulate ERE reporter activity, independent of any effects of CK1ε on ERα.

3. DDX3 enhances CK1ε activity, and CK1ε (akin to CK2) could directly phosphorylate ERα leading to its activation.

   As it was demonstrated earlier in this study, DDX3 can affect IKKε-mediated ERα phosphorylation and activation, CK1ε overexpression also caused increased ERE activity, it was next investigated whether CK1ε's effect on ERα activity could also be mediated via phosphorylation of ERα by CK1ε (rather than through β-catenin). This data indeed provide evidence that CK1ε can phosphorylate ERα, and this can be mediated by DDX3. DDX3 knockdown reduced CK1ε mediated phosphorylation of ERα. CK1ε-mediated phosphorylation was however much weaker compared to IKKε, indicating that it is not as good as IKKε at phosphorylating ERα. It was also evident that CK1ε might have β-catenin-independent effect on the ERα /ERE system in ERE reporter gene assays because its overexpression led to stronger enhancement of ERE activity compared to mutant S33Y β-catenin over-expression.

In summary, the current study provides evidence:

1. That Wnt pathway components can indeed affect ERα /ERE activity.

2. That CK1ε can phosphorylate ERα at S167, albeit not as well as IKKε.

3. Therefore, these findings may potentially contribute to DDX3's effect on ERα / ERE but is unlikely to be the full explanation.

6.3.1 Limitations/open questions

It was fairly clear from this data that CK1ε can phosphorylate ERα when overexpressed, but we don't know the physiological relevance of this, as we cannot be sure whether this actually happens in cells under physiological conditions/endogenous levels. It was also unclear why the effect of DDX3 knockdown on CK1ε-mediated phosphorylation of ERα was only seen under E2-stimulation. This will require further analysis in future.

Based on this data it was still difficult to answer what part of the CK1ε's effect is β-catenin mediated and what effect is directly on ERα. It was not possible from the data to completely confirm/rule out the role of Wnt pathway/ β -catenin on ERE reporter and ERα -target gene expression. It is important to check the findings of this study again in future to make sure it was not just an artefact of the overexpression system and/or ERE reporter gene assay. Use of siRNA or shRNA to knockdown β-catenin and of inhibitors to block WNT pathway activity to test effects on ERE activity would shed light on the role of the endogenous Wnt pathway components in mediating effects of DDX3 on ERα activity.

6.4 Summary

In summary, this work demonstrates that DDX3 and IKKε collaborate in ERα mediated ERE activation, potentially in DDX3's ATPase-Helicase independent manner. This effect of DDX3 is likely due to direct interaction with ERα, leading to phosphorylation of ERα at S167 which results in estrogen-independent activation of ERα that drives ER target gene expression and increased cell proliferation.

This work demonstrates, that DDX3 also modulated IKKε and CK1ε regulated phosphorylation of ERα. As DDX3 has been shown to be a regulatory subunit of CK1 in Wnt activation it is possible that DDX3 facilitates cell proliferation and migration in more than one way. This work elucidates a molecular mechanism of ERα activation by DDX3X highlighting its oncogenic role in breast cancer and resistance to anti-endocrine treatment for ERα breast cancer, thus revealing a novel role for DDX3 in ERα+ breast cancer.

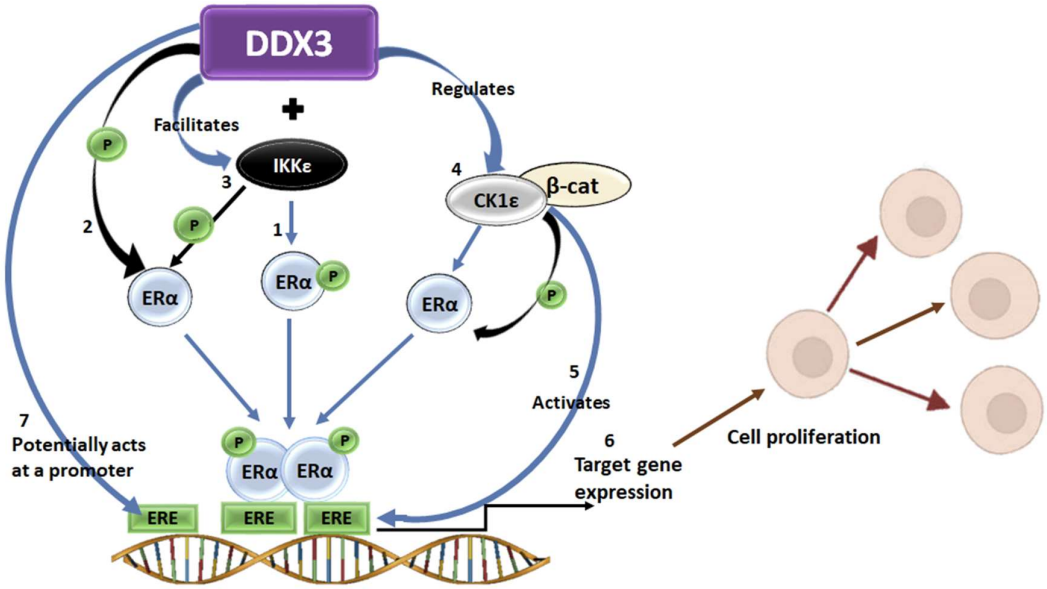

Figure 6.1: Schematic representation of findings of this study:

DDX3 regulates ERα activity in more than one way: DDX3 and IKKε, jointly activate ER mediated ERE activity (1). This effect of DDX3 is through direct interaction between DDX3 and ER, which results in E2-indepndent phosphorylation of ER (2). DDX3 also affects IKK mediated- E2- independent phosphorylation of ER (3). DDX3 is a regulatory subunit of CK1 in wnt pathway and also regulate CK1 and B-cat mediated phosphorylation of ER (4) and ERE activity (5). This leads to estrogen independent activation of ER, leading to ER target gene expression, cell proliferation, resistance to anti-endocrine treatment (6). It is possible that DDX3 might also act at ERE promoter (7) like other DEAD-box helicases, DDX5 and DDX17, both of which have been shown to regulate activity of ERα and other nuclear receptors independent of their RNA helicase activity (Wortham et al., 2009, Clark et al., 2008, Fuller-Pace, 2006)

6.5 Conclusion

This work demonstrated the role for the DEAD-box helicase DDX3 in activation and function of Estrogen receptor alpha (ERα). DDX3 activated ERα by interacting directly with ERα and promoting its phosphorylation at S167 by IKKε and/or other kinases. DDX3 mediated phosphorylation led to increased ERα activity, enhanced ERα target gene expression, and affected protein network associated with ERα. This work elucidated an additional molecular mechanism for DDX3's oncogenic role in breast cancer, which might also be involved in mediating resistance to anti-endocrine treatment in ERα expressing breast cancer.

References

ADLI, M. & BALDWIN, A. S. 2006. IKK-i/IKKepsilon controls constitutive, cancer cell-associated NF-kappaB activity via regulation of Ser-536 p65/RelA phosphorylation. *J Biol Chem,* 281**,** 26976-84.

AIHARA, H., KUMAR, N. & THOMPSON, C. C. 2014. Diagnosis, surveillance, and treatment strategies for familial adenomatous polyposis: rationale and update. *Eur J Gastroenterol Hepatol,* 26**,** 255-62.

ALAO, J. P. 2007. The regulation of cyclin D1 degradation: roles in cancer development and the potential for therapeutic invention. *Mol Cancer,* 6**,** 24.

AMIT, S., HATZUBAI, A., BIRMAN, Y., ANDERSEN, J. S., BEN-SHUSHAN, E., MANN, M., BEN-NERIAH, Y. & ALKALAY, I. 2002. Axin-mediated CKI phosphorylation of beta-catenin at Ser 45: a molecular switch for the Wnt pathway. *Genes Dev,* 16**,** 1066-76.

ARAO, Y., HAMILTON, K. J., COONS, L. A. & KORACH, K. S. 2013. Estrogen receptor α L543A,L544A mutation changes antagonists to agonists, correlating with the ligand binding domain dimerization associated with DNA binding activity. *J Biol Chem,* 288**,** 21105-21116.

ARIUMI, Y. 2014. Multiple functions of DDX3 RNA helicase in gene regulation, tumorigenesis, and viral infection. *Front Genet,* 5**,** 423.

ARIUMI, Y., KUROKI, M., ABE, K., DANSAKO, H., IKEDA, M., WAKITA, T. & KATO, N. 2007. DDX3 DEAD-box RNA helicase is required for hepatitis C virus RNA replication. *J Virol,* 81**,** 13922-6.

BAI, Y. & GIGUÉRE, V. 2003. Isoform-selective interactions between estrogen receptors and steroid receptor coactivators promoted by estradiol and ErbB-2 signaling in living cells. *Mol Endocrinol,* 17**,** 589-99.

BEHRENS, J., VON KRIES, J. P., KUHL, M., BRUHN, L., WEDLICH, D., GROSSCHEDL, R. & BIRCHMEIER, W. 1996. Functional interaction of beta-catenin with the transcription factor LEF-1. *Nature,* 382**,** 638-42.

BOEHM, J. S., ZHAO, J. J., YAO, J., KIM, S. Y., FIRESTEIN, R., DUNN, I. F., SJOSTROM, S. K., GARRAWAY, L. A., WEREMOWICZ, S., RICHARDSON, A. L., GREULICH, H., STEWART, C. J., MULVEY, L. A., SHEN, R. R., AMBROGIO, L., HIROZANE-KISHIKAWA, T., HILL, D. E., VIDAL, M., MEYERSON, M., GRENIER, J. K., HINKLE, G., ROOT, D. E., ROBERTS, T. M., LANDER, E. S., POLYAK, K. & HAHN, W. C. 2007. Integrative Genomic Approaches Identify IKBKE as a Breast Cancer Oncogene. *Cell,* 129**,** 1065-1079.

BOL, G. M., RAMAN, V., VAN DER GROEP, P., VERMEULEN, J. F., PATEL, A. H., VAN DER WALL, E. & VAN DIEST, P. J. 2013. Expression of the RNA Helicase DDX3 and the Hypoxia Response in Breast Cancer. *PLoS ONE,* 8**,** e63548.

BOL, G. M., XIE, M. & RAMAN, V. 2015. DDX3, a potential target for cancer treatment. *Mol Cancer,* 14**,** 188.

BOTLAGUNTA, M., KRISHNAMACHARY, B., VESUNA, F., WINNARD, P. T., JR., BOL, G. M., PATEL, A. H. & RAMAN, V. 2011. Expression of DDX3 is directly modulated by hypoxia inducible factor-1 alpha in breast epithelial cells. *PLoS One,* 6**,** e17563.

BOTLAGUNTA, M., VESUNA, F., MIRONCHIK, Y., RAMAN, A., LISOK, A., WINNARD, P., JR., MUKADAM, S., VAN DIEST, P., CHEN, J. H., FARABAUGH, P., PATEL, A. H. & RAMAN, V. 2008. Oncogenic role of DDX3 in breast cancer biogenesis. *Oncogene,* 27**,** 3912-22.

CADIGAN, K. M. & WATERMAN, M. L. 2012. TCF/LEFs and Wnt signaling in the nucleus. *Cold Spring Harb Perspect Biol,* 4.

CECCONI, F. & LEVINE, B. 2008. The role of autophagy in mammalian development: cell makeover rather than cell death. *Dev Cell,* 15**,** 344-357.

CHANG, P. C., CHI, C. W., CHAU, G. Y., LI, F. Y., TSAI, Y. H., WU, J. C. & WU LEE, Y. H. 2006. DDX3, a DEAD box RNA helicase, is deregulated in hepatitis virus-associated hepatocellular carcinoma and is involved in cell growth control. *Oncogene,* 25**,** 1991-2003.

CHAO, C. H., CHEN, C. M., CHENG, P. L., SHIH, J. W., TSOU, A. P. & LEE, Y. H. 2006. DDX3, a DEAD box RNA helicase with tumor growth-suppressive property and transcriptional regulation activity of the p21waf1/cip1 promoter, is a candidate tumor suppressor. *Cancer Res,* 66**,** 6579-88.

CHEANG, M. C., CHIA, S. K., VODUC, D., GAO, D., LEUNG, S., SNIDER, J., WATSON, M., DAVIES, S., BERNARD, P. S., PARKER, J. S., PEROU, C. M., ELLIS, M. J. & NIELSEN, T. O. 2009. Ki67 index, HER2 status, and prognosis of patients with luminal B breast cancer. *J Natl Cancer Inst,* 101**,** 736-50.

CHEN, W. & ROYER, W. E., JR. 2010. Structural insights into interferon regulatory factor activation. *Cell Signal,* 22**,** 883-7.

CHEN, W. J., WANG, W. T., TSAI, T. Y., LI, H. K. & LEE, Y. W. 2017. DDX3 localizes to the centrosome and prevents multipolar mitosis by epigenetically and translationally modulating p53 expression. *Sci Rep,* 7**,** 9411.

CHEUNG, E., ACEVEDO, M. L., COLE, P. A. & KRAUS, W. L. 2005. Altered pharmacology and distinct coactivator usage for estrogen receptor-dependent transcription through activating protein-1. *Proc Natl Acad Sci U S A,* 102**,** 559-64.

CHOI, Y. J. & LEE, S. G. 2012. The DEAD-box RNA helicase DDX3 interacts with DDX5, co-localizes with it in the cytoplasm during the G2/M phase of the cycle, and affects its shuttling during mRNP export. *J Cell Biochem,* 113**,** 985-96.

CLARK, E. L., COULSON, A., DALGLIESH, C., RAJAN, P., NICOL, S. M., FLEMING, S., HEER, R., GAUGHAN, L., LEUNG, H. Y., ELLIOTT, D. J., FULLER-PACE, F. V. & ROBSON, C. N. 2008. The RNA helicase p68 is a novel androgen receptor coactivator involved in splicing and is overexpressed in prostate cancer. *Cancer Res,* 68**,** 7938-46.

CLARKE, R., LIU, M. C., BOUKER, K. B., GU, Z., LEE, R. Y., ZHU, Y., SKAAR, T. C., GOMEZ, B., O'BRIEN, K., WANG, Y. & HILAKIVI-CLARKE, L. A. 2003. Antiestrogen resistance in breast cancer and the role of estrogen receptor signaling. *Oncogene,* 22**,** 7316-39.

CLARKE, R., SKAAR, T. C., BOUKER, K. B., DAVIS, N., LEE, Y. R., WELCH, J. N. & LEONESSA, F. 2001. Molecular and pharmacological aspects of antiestrogen resistance. *J Steroid Biochem Mol Biol,* 76**,** 71-84.

CLEVERS, H. & NUSSE, R. 2012. Wnt/beta-catenin signaling and disease. *Cell,* 149**,** 1192-205.

CORDIN, O., BANROQUES, J., TANNER, N. K. & LINDER, P. 2006. The DEAD-box protein family of RNA helicases. *Gene,* 367**,** 17-37.

COTTON, A. M., PRICE, E. M., JONES, M. J., BALATON, B. P., KOBOR, M. S. & BROWN, C. J. 2015. Landscape of DNA methylation on the X chromosome reflects CpG density, functional chromatin state and X-chromosome inactivation. *Hum Mol Genet,* 24**,** 1528-39.

CRUCIAT, C.-M., DOLDE, C., DE GROOT, R. E. A., OHKAWARA, B., REINHARD, C., KORSWAGEN, H. C. & NIEHRS, C. 2013a. RNA Helicase DDX3 Is a Regulatory Subunit of Casein Kinase 1 in Wnt–β-Catenin Signaling. *Science,* 339**,** 1436-1441.

CRUCIAT, C. M., DOLDE, C., DE GROOT, R. E., OHKAWARA, B., REINHARD, C., KORSWAGEN, H. C. & NIEHRS, C. 2013b. RNA helicase DDX3 is a regulatory subunit of casein kinase 1 in Wnt-β-catenin signaling. *Science,* 339**,** 1436-41.

D'SOUZA, A., SPICER, D. & LU, J. 2018. Overcoming endocrine resistance in metastatic hormone receptor-positive breast cancer. *J Hematol Oncol,* 11**,** 80.

DAGO, D. N., SCAFOGLIO, C., RINALDI, A., MEMOLI, D., GIURATO, G., NASSA, G., RAVO, M., RIZZO, F., TARALLO, R. & WEISZ, A. 2015. Estrogen receptor beta impacts hormone-induced alternative mRNA splicing in breast cancer cells. *BMC Genomics,* 16**,** 367.

DAVID, C. J., CHEN, M., ASSANAH, M., CANOLL, P. & MANLEY, J. L. 2010. HnRNP proteins controlled by c-Myc deregulate pyruvate kinase mRNA splicing in cancer. *Nature,* 463**,** 364-8.

DE FERRARI, G. V. & MOON, R. T. 2006. The ups and downs of Wnt signaling in prevalent neurological disorders. *Oncogene,* 25**,** 7545-53.

DE LEEUW, R., NEEFJES, J. & MICHALIDES, R. 2011. A role for estrogen receptor phosphorylation in the resistance to tamoxifen. *Int J Breast Cancer,* 2011**,** 232435.

DHAMAD, A. E., ZHOU, Z., ZHOU, J. & DU, Y. 2016. Systematic Proteomic Identification of the Heat Shock Proteins (Hsp) that Interact with Estrogen Receptor Alpha (ERalpha) and Biochemical Characterization of the ERalpha-Hsp70 Interaction. *PLoS One,* 11**,** e0160312.

DIMAS, D. T., PERLEPE, C. D., SERGENTANIS, T. N., MISITZIS, I., KONTZOGLOU, K., PATSOURIS, E., KOURAKLIS, G., PSALTOPOULOU, T. & NONNI, A. 2018. The Prognostic Significance of

Hsp70/Hsp90 Expression in Breast Cancer: A Systematic Review and Meta-analysis. *Anticancer Res,* 38**,** 1551-1562.

DUTERTRE, M., GRATADOU, L., DARDENNE, E., GERMANN, S., SAMAAN, S., LIDEREAU, R., DRIOUCH, K., DE LA GRANGE, P. & AUBOEUF, D. 2010a. Estrogen regulation and physiopathologic significance of alternative promoters in breast cancer. *Cancer Res,* 70**,** 3760-70.

DUTERTRE, M. & SMITH, C. L. 2003. Ligand-independent interactions of p160/steroid receptor coactivators and CREB-binding protein (CBP) with estrogen receptor-alpha: regulation by phosphorylation sites in the A/B region depends on other receptor domains. *Mol Endocrinol,* 17**,** 1296-314.

DUTERTRE, M., VAGNER, S. & AUBOEUF, D. 2010b. Alternative splicing and breast cancer. *RNA Biol,* 7**,** 403-11.

EECKHOUTE, J., KEETON, E. K., LUPIEN, M., KRUM, S. A., CARROLL, J. S. & BROWN, M. 2007. Positive cross-regulatory loop ties GATA-3 to estrogen receptor alpha expression in breast cancer. *Cancer Res,* 67**,** 6477-83.

EGELAND, N. G., LUNDE, S., JONSDOTTIR, K., LENDE, T. H., CRONIN-FENTON, D., GILJE, B., JANSSEN, E. A. & SOILAND, H. 2015. The Role of MicroRNAs as Predictors of Response to Tamoxifen Treatment in Breast Cancer Patients. *Int J Mol Sci,* 16**,** 24243-75.

ENMARK, E., PELTO-HUIKKO, M., GRANDIEN, K., LAGERCRANTZ, S., LAGERCRANTZ, J., FRIED, G., NORDENSKJÖLD, M. & GUSTAFSSON, J. A. 1997. Human estrogen receptor beta-gene structure, chromosomal localization, and expression pattern. *J Clin Endocrinol Metab,* 82**,** 4258-65.

FAIRMAN-WILLIAMS, M. E., GUENTHER, U. P. & JANKOWSKY, E. 2010. SF1 and SF2 helicases: family matters. *Curr Opin Struct Biol,* 20**,** 313-24.

FEDERER-GSPONER, J. R., QUINTAVALLE, C., MULLER, D. C., DIETSCHE, T., PERRINA, V., LORBER, T., JUSKEVICIUS, D., LENKIEWICZ, E., ZELLWEGER, T., GASSER, T., BARRETT, M. T., RENTSCH, C. A., BUBENDORF, L. & RUIZ, C. 2018. Delineation of human prostate cancer

evolution identifies chromothripsis as a polyclonal event and FKBP4 as a potential driver of castration resistance. *J Pathol,* 245**,** 74-84.

FITZGERALD, K. A., MCWHIRTER, S. M., FAIA, K. L., ROWE, D. C., LATZ, E., GOLENBOCK, D. T., COYLE, A. J., LIAO, S. M. & MANIATIS, T. 2003. IKKepsilon and TBK1 are essential components of the IRF3 signaling pathway. *Nat Immunol,* 4**,** 491-6.

FLISS, A. E., BENZENO, S., RAO, J. & CAPLAN, A. J. 2000. Control of estrogen receptor ligand binding by Hsp90. *J Steroid Biochem Mol Biol,* 72**,** 223-30.

FLOOR, S. N., CONDON, K. J., SHARMA, D., JANKOWSKY, E. & DOUDNA, J. A. 2016. Autoinhibitory Interdomain Interactions and Subfamily-specific Extensions Redefine the Catalytic Core of the Human DEAD-box Protein DDX3. *J Biol Chem,* 291**,** 2412-21.

FULLAM, A., GU, L., HOHN, Y. & SCHRODER, M. 2018. DDX3 directly facilitates IKKalpha activation and regulates downstream signalling pathways. *Biochem J,* 475**,** 3595-3607.

FULLAM, A. & SCHRÖDER, M. 2013. DExD/H-box RNA helicases as mediators of anti-viral innate immunity and essential host factors for viral replication. *Biochim Biophys Acta,* 1829**,** 854-65.

FULLER-PACE, F. V. 2006. DExD/H box RNA helicases: multifunctional proteins with important roles in transcriptional regulation. *Nucleic Acids Res,* 34**,** 4206-15.

FULLER-PACE, F. V. & NICOL, S. M. 2012. DEAD-box RNA helicases as transcription cofactors. *Methods Enzymol,* 511**,** 347-67.

GALLERNE, C., PROLA, A. & LEMAIRE, C. 2013. Hsp90 inhibition by PU-H71 induces apoptosis through endoplasmic reticulum stress and mitochondrial pathway in cancer cells and overcomes the resistance conferred by Bcl-2. *Biochim Biophys Acta,* 1833**,** 1356-66.

GAO, C. & CHEN, Y. G. 2010. Dishevelled: The hub of Wnt signaling. *Cell Signal,* 22**,** 717-27.

GEISSLER, R., GOLBIK, R. P. & BEHRENS, S. E. 2012. The DEAD-box helicase DDX3 supports the assembly of functional 80S ribosomes. *Nucleic Acids Res,* 40**,** 4998-5011.

GHONCHEH, M., POURNAMDAR, Z. & SALEHINIYA, H. 2016. Incidence and Mortality and Epidemiology of Breast Cancer in the World. *Asian Pac J Cancer Prev,* 17**,** 43-6.

GIRALDI, T., GIOVANNELLI, P., DI DONATO, M., CASTORIA, G., MIGLIACCIO, A. & AURICCHIO, F. 2010. Steroid signaling activation and intracellular localization of sex steroid receptors. *J Cell Commun Signal,* 4**,** 161-72.

GIULIANO, M., SCHIFP, R., OSBORNE, C. K. & TRIVEDI, M. V. 2011. Biological mechanisms and clinical implications of endocrine resistance in breast cancer. *Breast,* 20 Suppl 3**,** S42-9.

GOLDHIRSCH, A., WOOD, W. C., COATES, A. S., GELBER, R. D., THÜRLIMANN, B. & SENN, H. J. 2011. Strategies for subtypes--dealing with the diversity of breast cancer: highlights of the St. Gallen International Expert Consensus on the Primary Therapy of Early Breast Cancer 2011. *Ann Oncol,* 22**,** 1736-47.

GREEN, S., KUMAR, V., KRUST, A., WALTER, P. & CHAMBON, P. 1986. Structural and functional domains of the estrogen receptor. *Cold Spring Harb Symp Quant Biol,* 51 Pt 2**,** 751-8.

GRUBER, C. J., TSCHUGGUEL, W., SCHNEEBERGER, C. & HUBER, J. C. 2002. Production and actions of estrogens. *N Engl J Med,* 346**,** 340-52.

GU, L., FULLAM, A., BRENNAN, R. & SCHRÖDER, M. 2013. Human DEAD box helicase 3 couples IκB kinase ε to interferon regulatory factor 3 activation. *Mol Cell Biol,* 33**,** 2004-15.

GUO, J.-P., SHU, S.-K., ESPOSITO, N. N., COPPOLA, D., KOOMEN, J. M. & CHENG, J. Q. 2010a. IKK-επσιλον Phosphorylation of Estrogen Receptor α Ser-167 and Contribution to Tamoxifen Resistance in Breast Cancer. *Journal of Biological Chemistry,* 285**,** 3676-3684.

GUO, J. P., SHU, S. K., ESPOSITO, N. N., COPPOLA, D., KOOMEN, J. M. & CHENG, J. Q. 2010b. IKKepsilon phosphorylation of estrogen receptor alpha Ser-167 and contribution to tamoxifen resistance in breast cancer. *J Biol Chem,* 285**,** 3676-3684.

GUO, S. & SONENSHEIN, G. E. 2004. Forkhead box transcription factor FOXO3a regulates estrogen receptor alpha expression and is repressed by the Her-2/neu/phosphatidylinositol 3-kinase/Akt signaling pathway. *Mol Cell Biol,* 24**,** 8681-90.

HALL, J. M., MCDONNELL, D. P. & KORACH, K. S. 2002. Allosteric regulation of estrogen receptor structure, function, and coactivator recruitment by different estrogen response elements. *Mol Endocrinol,* 16**,** 469-86.

HALLS, C., MOHR, S., DEL CAMPO, M., YANG, Q., JANKOWSKY, E. & LAMBOWITZ, A. M. 2007. Involvement of DEAD-box proteins in group I and group II intron splicing. Biochemical characterization of Mss116p, ATP hydrolysis-dependent and -independent mechanisms, and general RNA chaperone activity. *J Mol Biol,* 365**,** 835-55.

HERBST, A., JURINOVIC, V., KREBS, S., THIEME, S. E., BLUM, H., GOKE, B. & KOLLIGS, F. T. 2014. Comprehensive analysis of beta-catenin target genes in colorectal carcinoma cell lines with deregulated Wnt/beta-catenin signaling. *BMC Genomics,* 15**,** 74.

HSU, P. P., KANG, S. A., RAMESEDER, J., ZHANG, Y., OTTINA, K. A., LIM, D., PETERSON, T. R., CHOI, Y., GRAY, N. S., YAFFE, M. B., MARTO, J. A. & SABATINI, D. M. 2011. The mTOR-regulated phosphoproteome reveals a mechanism of mTORC1-mediated inhibition of growth factor signaling. *Science,* 332**,** 1317-22.

HUA, H., ZHANG, H., KONG, Q. & JIANG, Y. 2018. Mechanisms for estrogen receptor expression in human cancer. *Exp Hematol Oncol,* 7**,** 24.

HUANG, J., LI, X., HILF, R., BAMBARA, R. A. & MUYAN, M. 2005. Molecular basis of therapeutic strategies for breast cancer. *Curr Drug Targets Immune Endocr Metabol Disord,* 5**,** 379-96.

HUANG, P., CHANDRA, V. & RASTINEJAD, F. 2010. Structural overview of the nuclear receptor superfamily: insights into physiology and therapeutics. *Annu Rev Physiol,* 72**,** 247-72.

HUDERSON, B. P., DUPLESSIS, T. T., WILLIAMS, C. C., SEGER, H. C., MARSDEN, C. G., POUEY, K. J., HILL, S. M. & ROWAN, B. G. 2012. Stable inhibition of specific estrogen receptor α (ERα) phosphorylation confers increased growth, migration/invasion, and disruption of estradiol signaling in MCF-7 breast cancer cells. *Endocrinology,* 153**,** 4144-59.

HUTTI, J. E., SHEN, R. R., ABBOTT, D. W., ZHOU, A. Y., SPROTT, K. M., ASARA, J. M., HAHN, W. C. & CANTLEY, L. C. 2009. Phosphorylation of the Tumor Suppressor CYLD by the Breast Cancer Oncogene IKKε Promotes Cell Transformation. *Molecular Cell,* 34**,** 461-472.

ISHAQ, M., HU, J., WU, X., FU, Q., YANG, Y., LIU, Q. & GUO, D. 2008. Knockdown of cellular RNA helicase DDX3 by short hairpin RNAs suppresses HIV-1 viral replication without inducing apoptosis. *Mol Biotechnol,* 39**,** 231-8.

JANKOWSKY, E. & FAIRMAN, M. E. 2007. RNA helicases--one fold for many functions. *Curr Opin Struct Biol,* 17**,** 316-24.

JENNY, F. H. & BASLER, K. 2016. Drosophila DDX3/Belle Exerts Its Function Outside of the Wnt/Wingless Signaling Pathway. *PLoS One,* 11**,** e0166862.

KANG, J. I., KWON, Y. C. & AHN, B. Y. 2012. Modulation of the type I interferon pathways by culture-adaptive hepatitis C virus core mutants. *FEBS Lett,* 586**,** 1272-8.

KIM, S. Y., DUNN, I. F., FIRESTEIN, R., GUPTA, P., WARDWELL, L., REPICH, K., SCHINZEL, A. C., WITTNER, B., SILVER, S. J., ROOT, D. E., BOEHM, J. S., RAMASWAMY, S., LANDER, E. S. & HAHN, W. C. 2010. CK1epsilon is required for breast cancers dependent on beta-catenin activity. *PLoS One,* 5**,** e8979.

KUMAR, V., GREEN, S., STACK, G., BERRY, M., JIN, J. R. & CHAMBON, P. 1987. Functional domains of the human estrogen receptor. *Cell,* 51**,** 941-51.

LA ROSA, P., PESIRI, V., LECLERCQ, G., MARINO, M. & ACCONCIA, F. 2012. Palmitoylation regulates 17beta-estradiol-induced estrogen receptor-alpha degradation and transcriptional activity. *Mol Endocrinol,* 26**,** 762-74.

LAHN, B. T. & PAGE, D. C. 1997. Functional coherence of the human Y chromosome. *Science,* 278**,** 675-80.

LE ROMANCER, M., POULARD, C., COHEN, P., SENTIS, S., RENOIR, J. M. & CORBO, L. 2011. Cracking the estrogen receptor's posttranslational code in breast tumors. *Endocr Rev,* 32**,** 597-622.

LEE, H. R., KIM, T. H. & CHOI, K. C. 2012. Functions and physiological roles of two types of estrogen receptors, ERα and ERβ, identified by estrogen receptor knockout mouse. *Lab Anim Res,* 28**,** 71-6.

LEFEBVRE, L. & SOL, D. 2008. Brains, lifestyles and cognition: Are there general trends? *Brain, Behavior and Evolution,* 72**,** 135-144.

LI, H., LIU, L., DAVID, M. L., WHITEHEAD, C. M., CHEN, M., FETTER, J. R., SPERL, G. J., PAMUKCU, R. & THOMPSON, W. J. 2002. Pro-apoptotic actions of exisulind and CP461 in SW480

colon tumor cells involve beta-catenin and cyclin D1 down-regulation. *Biochem Pharmacol,* 64**,** 1325-36.

LI, X., HUANG, J., FLUHARTY, B. R., HUANG, Y., NOTT, S. L. & MUYAN, M. 2008. What are comparative studies telling us about the mechanism of ERbeta action in the ERE-dependent E2 signaling pathway? *J Steroid Biochem Mol Biol,* 109**,** 266-72.

LIKHITE, V. S., STOSSI, F., KIM, K., KATZENELLENBOGEN, B. S. & KATZENELLENBOGEN, J. A. 2006. Kinase-specific phosphorylation of the estrogen receptor changes receptor interactions with ligand, deoxyribonucleic acid, and coregulators associated with alterations in estrogen and tamoxifen activity. *Mol Endocrinol,* 20**,** 3120-32.

LIN, C. Y., STRÖM, A., VEGA, V. B., KONG, S. L., YEO, A. L., THOMSEN, J. S., CHAN, W. C., DORAY, B., BANGARUSAMY, D. K., RAMASAMY, A., VERGARA, L. A., TANG, S., CHONG, A., BAJIC, V. B., MILLER, L. D., GUSTAFSSON, J. A. & LIU, E. T. 2004. Discovery of estrogen receptor alpha target genes and response elements in breast tumor cells. *Genome Biol,* 5**,** R66.

LIN, C. Y., VEGA, V. B., THOMSEN, J. S., ZHANG, T., KONG, S. L., XIE, M., CHIU, K. P., LIPOVICH, L., BARNETT, D. H., STOSSI, F., YEO, A., GEORGE, J., KUZNETSOV, V. A., LEE, Y. K., CHARN, T. H., PALANISAMY, N., MILLER, L. D., CHEUNG, E., KATZENELLENBOGEN, B. S., RUAN, Y., BOURQUE, G., WEI, C. L. & LIU, E. T. 2007. Whole-genome cartography of estrogen receptor alpha binding sites. *PLoS Genet,* 3**,** e87.

LINDER, P. & JANKOWSKY, E. 2011. From unwinding to clamping - the DEAD box RNA helicase family. *Nat Rev Mol Cell Biol,* 12**,** 505-16.

LIU, H., MA, Y., HE, H. W., WANG, J. P., JIANG, J. D. & SHAO, R. G. 2015. SLC9A3R1 stimulates autophagy via BECN1 stabilization in breast cancer cells. *Autophagy,* 11**,** 2323-34.

LIU, H., ZHANG, J., WANG, S., PANG, Z., WANG, Z., ZHOU, W. & WU, M. 2012a. Screening of autoantibodies as potential biomarkers for hepatocellular carcinoma by using T7 phase display system. *Cancer Epidemiol,* 36**,** 82-8.

LIU, M., WANG, G., GOMEZ-FERNANDEZ, C. R. & GUO, S. 2012b. GREB1 functions as a growth promoter and is modulated by IL6/STAT3 in breast cancer. *PLoS One,* 7**,** e46410.

LIU, X. & SHI, H. 2015. Regulation of Estrogen Receptor α Expression in the Hypothalamus by Sex Steroids: Implication in the Regulation of Energy Homeostasis. *Int J Endocrinol,* 2015**,** 949085.

LONG, X. & NEPHEW, K. P. 2006. Fulvestrant (ICI 182,780)-dependent interacting proteins mediate immobilization and degradation of estrogen receptor-alpha. *J Biol Chem,* 281**,** 9607-15.

LUO, W. & SEMENZA, G. L. 2011. Pyruvate kinase M2 regulates glucose metabolism by functioning as a coactivator for hypoxia-inducible factor 1 in cancer cells. *Oncotarget,* 2**,** 551-6.

MA, X. M. & BLENIS, J. 2009. Molecular mechanisms of mTOR-mediated translational control. *Nat Rev Mol Cell Biol,* 10**,** 307-18.

MAGGI, A. 2011. Liganded and unliganded activation of estrogen receptor and hormone replacement therapies. *Biochim Biophys Acta,* 1812**,** 1054-60.

MEDUNJANIN, S., HERMANI, A., DE SERVI, B., GRISOUARD, J., RINCKE, G. & MAYER, D. 2005. Glycogen synthase kinase-3 interacts with and phosphorylates estrogen receptor alpha and is involved in the regulation of receptor activity. *J Biol Chem,* 280**,** 33006-14.

MEDZHITOV, R., PRESTON-HURLBURT, P. & JANEWAY, C. A., JR. 1997. A human homologue of the Drosophila Toll protein signals activation of adaptive immunity. *Nature,* 388**,** 394-7.

MERRELL, K. W., CROFTS, J. D., SMITH, R. L., SIN, J. H., KMETZSCH, K. E., MERRELL, A., MIGUEL, R. O., CANDELARIA, N. R. & LIN, C. Y. 2011. Differential recruitment of nuclear receptor coregulators in ligand-dependent transcriptional repression by estrogen receptor-α. *Oncogene,* 30**,** 1608-14.

MOLENAAR, M., VAN DE WETERING, M., OOSTERWEGEL, M., PETERSON-MADURO, J., GODSAVE, S., KORINEK, V., ROOSE, J., DESTREE, O. & CLEVERS, H. 1996. XTcf-3 transcription factor mediates beta-catenin-induced axis formation in Xenopus embryos. *Cell,* 86**,** 391-9.

NAKAMURA, Y., NISHISHO, I., KINZLER, K. W., VOGELSTEIN, B., MIYOSHI, Y., MIKI, Y., ANDO, H., HORII, A. & NAGASE, H. 1991. Mutations of the adenomatous polyposis coli gene in

familial polyposis coli patients and sporadic colorectal tumors. *Princess Takamatsu Symp,* 22**,** 285-92.

NG, L. F., KAUR, P., BUNNAG, N., SURESH, J., SUNG, I. C. H., TAN, Q. H., GRUBER, J. & TOLWINSKI, N. S. 2019. WNT Signaling in Disease. *Cells,* 8.

NOTT, S. L., HUANG, Y., LI, X., FLUHARTY, B. R., QIU, X., WELSHONS, W. V., YEH, S. & MUYAN, M. 2009. Genomic responses from the estrogen-responsive element-dependent signaling pathway mediated by estrogen receptor alpha are required to elicit cellular alterations. *J Biol Chem,* 284**,** 15277-88.

NUSSE, R., VAN OOYEN, A., COX, D., FUNG, Y. K. & VARMUS, H. 1984. Mode of proviral activation of a putative mammary oncogene (int-1) on mouse chromosome 15. *Nature,* 307**,** 131-6.

OBERMANN, W. M. J. 2018. A motif in HSP90 and P23 that links molecular chaperones to efficient estrogen receptor alpha methylation by the lysine methyltransferase SMYD2. *J Biol Chem,* 293**,** 16479-16487.

OH, S., FLYNN, R. A., FLOOR, S. N., PURZNER, J., MARTIN, L., DO, B. T., SCHUBERT, S., VAKA, D., MORRISSY, S., LI, Y., KOOL, M., HOVESTADT, V., JONES, D. T., NORTHCOTT, P. A., RISCH, T., WARNATZ, H. J., YASPO, M. L., ADAMS, C. M., LEIB, R. D., BREESE, M., MARRA, M. A., MALKIN, D., LICHTER, P., DOUDNA, J. A., PFISTER, S. M., TAYLOR, M. D., CHANG, H. Y. & CHO, Y. J. 2016. Medulloblastoma-associated DDX3 variant selectively alters the translational response to stress. *Oncotarget,* 7**,** 28169-82.

ONDER, T. T., GUPTA, P. B., MANI, S. A., YANG, J., LANDER, E. S. & WEINBERG, R. A. 2008. Loss of E-cadherin promotes metastasis via multiple downstream transcriptional pathways. *Cancer Res,* 68**,** 3645-54.

OSHIUMI, H., SAKAI, K., MATSUMOTO, M. & SEYA, T. 2010. DEAD/H BOX 3 (DDX3) helicase binds the RIG-I adaptor IPS-1 to up-regulate IFN-beta-inducing potential. *Eur J Immunol,* 40**,** 940-8.

OWSIANKA, A. M. & PATEL, A. H. 1999. Hepatitis C virus core protein interacts with a human DEAD box protein DDX3. *Virology,* 257**,** 330-40.

PIKE, A. C., BRZOZOWSKI, A. M. & HUBBARD, R. E. 2000. A structural biologist's view of the oestrogen receptor. *J Steroid Biochem Mol Biol,* 74**,** 261-8.

POLAKIS, P. 2002. Casein kinase 1: a Wnt'er of disconnect. *Curr Biol,* 12**,** R499-R501.

POWELL, E., WANG, Y., SHAPIRO, D. J. & XU, W. 2010. Differential requirements of Hsp90 and DNA for the formation of estrogen receptor homodimers and heterodimers. *J Biol Chem,* 285**,** 16125-34.

PUGH, T. J., WEERARATNE, S. D., ARCHER, T. C., POMERANZ KRUMMEL, D. A., AUCLAIR, D., BOCHICCHIO, J., CARNEIRO, M. O., CARTER, S. L., CIBULSKIS, K., ERLICH, R. L., GREULICH, H., LAWRENCE, M. S., LENNON, N. J., MCKENNA, A., MELDRIM, J., RAMOS, A. H., ROSS, M. G., RUSS, C., SHEFLER, E., SIVACHENKO, A., SOGOLOFF, B., STOJANOV, P., TAMAYO, P., MESIROV, J. P., AMANI, V., TEIDER, N., SENGUPTA, S., FRANCOIS, J. P., NORTHCOTT, P. A., TAYLOR, M. D., YU, F., CRABTREE, G. R., KAUTZMAN, A. G., GABRIEL, S. B., GETZ, G., JÄGER, N., JONES, D. T., LICHTER, P., PFISTER, S. M., ROBERTS, T. M., MEYERSON, M., POMEROY, S. L. & CHO, Y. J. 2012. Medulloblastoma exome sequencing uncovers subtype-specific somatic mutations. *Nature,* 488**,** 106-10.

RADI, M., FALCHI, F., GARBELLI, A., SAMUELE, A., BERNARDO, V., PAOLUCCI, S., BALDANTI, F., SCHENONE, S., MANETTI, F., MAGA, G. & BOTTA, M. 2012. Discovery of the first small molecule inhibitor of human DDX3 specifically designed to target the RNA binding site: towards the next generation HIV-1 inhibitors. *Bioorg Med Chem Lett,* 22**,** 2094-8.

RAJBHANDARI, P., FINN, G., SOLODIN, N. M., SINGARAPU, K. K., SAHU, S. C., MARKLEY, J. L., KADUNC, K. J., ELLISON-ZELSKI, S. J., KARIAGINA, A., HASLAM, S. Z., LU, K. P. & ALARID, E. T. 2012. Regulation of estrogen receptor α N-terminus conformation and function by peptidyl prolyl isomerase Pin1. *Mol Cell Biol,* 32**,** 445-57.

ROBINSON, S. P. & JORDAN, V. C. 1987. Reversal of the antitumor effects of tamoxifen by progesterone in the 7,12-dimethylbenzanthracene-induced rat mammary carcinoma model. *Cancer Res,* 47**,** 5386-90.

ROGATSKY, I., TROWBRIDGE, J. M. & GARABEDIAN, M. J. 1999. Potentiation of human estrogen receptor alpha transcriptional activation through phosphorylation of serines 104 and 106 by the cyclin A-CDK2 complex. *J Biol Chem,* 274**,** 22296-302.

SAFE, S. 2001. Transcriptional activation of genes by 17 beta-estradiol through estrogen receptor-Sp1 interactions. *Vitam Horm,* 62**,** 231-52.

SAKASHITA, E., TATSUMI, S., WERNER, D., ENDO, H. & MAYEDA, A. 2004. Human RNPS1 and its associated factors: a versatile alternative pre-mRNA splicing regulator in vivo. *Mol Cell Biol,* 24**,** 1174-87.

SAND, P., LUCKHAUS, C., SCHLURMANN, K., GÖTZ, M. & DECKERT, J. 2002. Untangling the human estrogen receptor gene structure. *J Neural Transm (Vienna),* 109**,** 567-83.

SANTEN, R. J., LOBENHOFER, E. K., AFSHARI, C. A., BAO, Y. & SONG, R. X. 2005. Adaptation of estrogen-regulated genes in long-term estradiol deprived MCF-7 breast cancer cells. *Breast Cancer Res Treat,* 94**,** 213-23.

SATO, M., SUEMORI, H., HATA, N., ASAGIRI, M., OGASAWARA, K., NAKAO, K., NAKAYA, T., KATSUKI, M., NOGUCHI, S., TANAKA, N. & TANIGUCHI, T. 2000. Distinct and essential roles of transcription factors IRF-3 and IRF-7 in response to viruses for IFN-alpha/beta gene induction. *Immunity,* 13**,** 539-48.

SCHRÖDER, M. 2010. Human DEAD-box protein 3 has multiple functions in gene regulation and cell cycle control and is a prime target for viral manipulation. *Biochem Pharmacol,* 79**,** 297-306.

SCHRODER, M., BARAN, M. & BOWIE, A. G. 2008. Viral targeting of DEAD box protein 3 reveals its role in TBK1/IKK-epsilon-mediated IRF activation. *Embo J,* 17**,** 17.

SCHRÖDER, M., BARAN, M. & BOWIE, A. G. 2008. Viral targeting of DEAD box protein 3 reveals its role in TBK1/IKKepsilon-mediated IRF activation. *Embo j,* 27**,** 2147-57.

SHAH, Y. M. & ROWAN, B. G. 2005. The Src kinase pathway promotes tamoxifen agonist action in Ishikawa endometrial cells through phosphorylation-dependent stabilization of estrogen receptor (alpha) promoter interaction and elevated steroid receptor coactivator 1 activity. *Mol Endocrinol,* 19**,** 732-48.

SHAHBAZIAN, D., PARSYAN, A., PETROULAKIS, E., HERSHEY, J. & SONENBERG, N. 2010. eIF4B controls survival and proliferation and is regulated by proto-oncogenic signaling pathways. *Cell Cycle,* 9**,** 4106-9.

SIEUWERTS, A. M., LYNG, M. B., MEIJER-VAN GELDER, M. E., DE WEERD, V., SWEEP, F. C., FOEKENS, J. A., SPAN, P. N., MARTENS, J. W. & DITZEL, H. J. 2014. Evaluation of the ability of adjuvant tamoxifen-benefit gene signatures to predict outcome of hormone-naive estrogen receptor-positive breast cancer patients treated with tamoxifen in the advanced setting. *Mol Oncol,* 8**,** 1679-89.

SOULAT, D., BÜRCKSTÜMMER, T., WESTERMAYER, S., GONCALVES, A., BAUCH, A., STEFANOVIC, A., HANTSCHEL, O., BENNETT, K. L., DECKER, T. & SUPERTI-FURGA, G. 2008. The DEAD-box helicase DDX3X is a critical component of the TANK-binding kinase 1-dependent innate immune response. *Embo j,* 27**,** 2135-46.

STAMOS, J. L. & WEIS, W. I. 2013. The beta-catenin destruction complex. *Cold Spring Harb Perspect Biol,* 5**,** a007898.

STEWART, G. S., WANG, B., BIGNELL, C. R., TAYLOR, A. M. & ELLEDGE, S. J. 2003. MDC1 is a mediator of the mammalian DNA damage checkpoint. *Nature,* 421**,** 961-6.

STUNNENBERG, M., GEIJTENBEEK, T. B. H. & GRINGHUIS, S. I. 2018. DDX3 in HIV-1 infection and sensing: A paradox. *Cytokine Growth Factor Rev,* 40**,** 32-39.

SUN, M., SONG, L., ZHOU, T., GILLESPIE, G. Y. & JOPE, R. S. 2011. The role of DDX3 in regulating Snail. *Biochim Biophys Acta,* 1813**,** 438-47.

TAMAI, K., ZENG, X., LIU, C., ZHANG, X., HARADA, Y., CHANG, Z. & HE, X. 2004. A mechanism for Wnt coreceptor activation. *Mol Cell,* 13**,** 149-56.

TAMRAZI, A., CARLSON, K. E., DANIELS, J. R., HURTH, K. M. & KATZENELLENBOGEN, J. A. 2002. Estrogen receptor dimerization: ligand binding regulates dimer affinity and dimer dissociation rate. *Mol Endocrinol,* 16**,** 2706-19.

TANNER, N. K., CORDIN, O., BANROQUES, J., DOÈRE, M. & LINDER, P. 2003. The Q motif: a newly identified motif in DEAD box helicases may regulate ATP binding and hydrolysis. *Mol Cell,* 11**,** 127-38.

THOMAS, R. S., SARWAR, N., PHOENIX, F., COOMBES, R. C. & ALI, S. 2008. Phosphorylation at serines 104 and 106 by Erk1/2 MAPK is important for estrogen receptor-alpha activity. *J Mol Endocrinol,* 40**,** 173-84.

THOMPSON, M. R., KAMINSKI, J. J., KURT-JONES, E. A. & FITZGERALD, K. A. 2011. Pattern recognition receptors and the innate immune response to viral infection. *Viruses,* 3**,** 920-40.

TSUKAMOTO, A. S., GROSSCHEDL, R., GUZMAN, R. C., PARSLOW, T. & VARMUS, H. E. 1988. Expression of the int-1 gene in transgenic mice is associated with mammary gland hyperplasia and adenocarcinomas in male and female mice. *Cell,* 55**,** 619-25.

VAREŠLIJA, D., MCBRYAN, J., FAGAN, A., REDMOND, A. M., HAO, Y., SIMS, A. H., TURNBULL, A., DIXON, J. M., P, Ó. G., HUDSON, L., PURCELL, S., HILL, A. D. & YOUNG, L. S. 2016. Adaptation to AI Therapy in Breast Cancer Can Induce Dynamic Alterations in ER Activity Resulting in Estrogen-Independent Metastatic Tumors. *Clin Cancer Res,* 22**,** 2765-77.

VENKATARAMANAN, S., CALVIELLO, L., WILKINS, K. & FLOOR, S. N. 2020. DDX3X and DDX3Y are redundant in protein synthesis. *bioRxiv***,** 2020.09.30.319376.

WANG, Q., QIN, Q., SONG, R., ZHAO, C., LIU, H., YANG, Y., GU, S., ZHOU, D. & HE, J. 2018. NHERF1 inhibits beta-catenin-mediated proliferation of cervical cancer cells through suppression of alpha-actinin-4 expression. *Cell Death Dis,* 9**,** 668.

WANG, Z., LUO, Z., ZHOU, L., LI, X., JIANG, T. & FU, E. 2015. DDX5 promotes proliferation and tumorigenesis of non-small-cell lung cancer cells by activating beta-catenin signaling pathway. *Cancer Sci,* 106**,** 1303-12.

WARNER, M., NILSSON, S. & GUSTAFSSON, J. A. 1999. The estrogen receptor family. *Curr Opin Obstet Gynecol,* 11**,** 249-54.

WEBB, P., NGUYEN, P., VALENTINE, C., LOPEZ, G. N., KWOK, G. R., MCINERNEY, E., KATZENELLENBOGEN, B. S., ENMARK, E., GUSTAFSSON, J. A., NILSSON, S. & KUSHNER, P. J. 1999. The estrogen receptor enhances AP-1 activity by two distinct mechanisms with different requirements for receptor transactivation functions. *Mol Endocrinol,* 13**,** 1672-85.

WILKINS, K. & LAFRAMBOISE, T. 2011. Losing balance: Hardy-Weinberg disequilibrium as a marker for recurrent loss-of-heterozygosity in cancer. *Hum Mol Genet,* 20**,** 4831-9.

WILLIAMS, C. C., BASU, A., EL-GHARBAWY, A., CARRIER, L. M., SMITH, C. L. & ROWAN, B. G. 2009. Identification of four novel phosphorylation sites in estrogen receptor alpha: impact on receptor-dependent gene expression and phosphorylation by protein kinase CK2. *BMC Biochem,* 10**,** 36.

WORTHAM, N. C., AHAMED, E., NICOL, S. M., THOMAS, R. S., PERIYASAMY, M., JIANG, J., OCHOCKA, A. M., SHOUSHA, S., HUSON, L., BRAY, S. E., COOMBES, R. C., ALI, S. & FULLER-PACE, F. V. 2009. The DEAD-box protein p72 regulates ERalpha-/oestrogen-dependent transcription and cell growth, and is associated with improved survival in ERalpha-positive breast cancer. *Oncogene,* 28**,** 4053-64.

WULLSCHLEGER, S., LOEWITH, R. & HALL, M. N. 2006. TOR signaling in growth and metabolism. *Cell,* 124**,** 471-84.

XIANG, N., HE, M., ISHAQ, M., GAO, Y., SONG, F., GUO, L., MA, L., SUN, G., LIU, D., GUO, D. & CHEN, Y. 2016. The DEAD-Box RNA Helicase DDX3 Interacts with NF-kappaB Subunit p65 and Suppresses p65-Mediated Transcription. *PLoS One,* 11**,** e0164471.

XIONG, H., CHEN, Z., ZHENG, W., SUN, J., FU, Q., TENG, R., CHEN, J., XIE, S., WANG, L., YU, X. F. & ZHOU, J. 2020. FKBP4 is a malignant indicator in luminal A subtype of breast cancer. *J Cancer,* 11**,** 1727-1736.

YAGER, J. D. & DAVIDSON, N. E. 2006. Estrogen carcinogenesis in breast cancer. *N Engl J Med,* 354**,** 270-82.

YANG, Q., DEL CAMPO, M., LAMBOWITZ, A. M. & JANKOWSKY, E. 2007. DEAD-box proteins unwind duplexes by local strand separation. *Mol Cell,* 28**,** 253-63.

YANG, W., XIA, Y., JI, H., ZHENG, Y., LIANG, J., HUANG, W., GAO, X., ALDAPE, K. & LU, Z. 2011. Nuclear PKM2 regulates beta-catenin transactivation upon EGFR activation. *Nature,* 480**,** 118-22.

YAŞAR, P., AYAZ, G., USER, S. D., GÜPÜR, G. & MUYAN, M. 2017. Molecular mechanism of estrogen-estrogen receptor signaling. *Reprod Med Biol,* 16**,** 4-20.

YEDAVALLI, V. S., NEUVEUT, C., CHI, Y. H., KLEIMAN, L. & JEANG, K. T. 2004. Requirement of DDX3 DEAD box RNA helicase for HIV-1 Rev-RRE export function. *Cell,* 119**,** 381-92.

YEDAVALLI, V. S., ZHANG, N., CAI, H., ZHANG, P., STAROST, M. F., HOSMANE, R. S. & JEANG, K. T. 2008. Ring expanded nucleoside analogues inhibit RNA helicase and intracellular human immunodeficiency virus type 1 replication. *J Med Chem,* 51**,** 5043-51.

YEN, W. L. & KLIONSKY, D. J. 2008. How to live long and prosper: autophagy, mitochondria, and aging. *Physiology (Bethesda),* 23**,** 248-62.

YI, P., BHAGAT, S., HILF, R., BAMBARA, R. A. & MUYAN, M. 2002. Differences in the abilities of estrogen receptors to integrate activation functions are critical for subtype-specific transcriptional responses. *Mol Endocrinol,* 16**,** 1810-27.

YI, P., WANG, Z., FENG, Q., PINTILIE, G. D., FOULDS, C. E., LANZ, R. B., LUDTKE, S. J., SCHMID, M. F., CHIU, W. & O'MALLEY, B. W. 2015. Structure of a biologically active estrogen receptor-coactivator complex on DNA. *Mol Cell,* 57**,** 1047-1058.

YOUN, J. Y., DUNHAM, W. H., HONG, S. J., KNIGHT, J. D. R., BASHKUROV, M., CHEN, G. I., BAGCI, H., RATHOD, B., MACLEOD, G., ENG, S. W. M., ANGERS, S., MORRIS, Q., FABIAN, M., COTE, J. F. & GINGRAS, A. C. 2018. High-Density Proximity Mapping Reveals the Subcellular Organization of mRNA-Associated Granules and Bodies. *Mol Cell,* 69**,** 517-532 e11.

ZGAJNAR, N. R., DE LEO, S. A., LOTUFO, C. M., ERLEJMAN, A. G., PIWIEN-PILIPUK, G. & GALIGNIANA, M. D. 2019. Biological Actions of the Hsp90-binding Immunophilins FKBP51 and FKBP52. *Biomolecules,* 9.

ZHANG, M. H., MAN, H. T., ZHAO, X. D., DONG, N. & MA, S. L. 2014. Estrogen receptor-positive breast cancer molecular signatures and therapeutic potentials (Review). *Biomed Rep,* 2**,** 41-52.

ZHANG, Z., KIM, T., BAO, M., FACCHINETTI, V., JUNG, S. Y., GHAFFARI, A. A., QIN, J., CHENG, G. & LIU, Y. J. 2011. DDX1, DDX21, and DHX36 helicases form a complex with the adaptor molecule TRIF to sense dsRNA in dendritic cells. *Immunity,* 34**,** 866-78.

ZHAO, L., MAO, Y., ZHOU, J., ZHAO, Y., CAO, Y. & CHEN, X. 2016. Multifunctional DDX3: dual roles in various cancer development and its related signaling pathways. *Am J Cancer Res,* 6**,** 387-402.